Investigating *Listeria monocytogenes* colonization of the gallbladder

Nicole H. Schwardt

A dissertation
submitted in partial fulfillment of the
requirement for the degree of

Doctor of Philosophy

University of Washington
2024

Reading Committee:
Michelle Reniere, Chair
Patrick Mitchell
Joshua Woodward

Program Authorized to Offer Degree:
Microbiology

University of Washington

Abstract

Investigating *L. monocytogenes* infection of the gallbladder

Nicole H. Schwardt

Chair of Supervisory Committee:
Michelle Reniere
Department of Microbiology

Listeriosis, caused by the bacterium *Listeria monocytogenes*, is the third leading cause of death among foodborne illnesses in the United States. Following oral inoculation of the host, *L. monocytogenes* transverses the intestinal epithelium and rapidly disseminates to the mesenteric lymph nodes, liver, and spleen via the lymph and bloodstream. Bacteria colonizing the liver replicate intracellularly in hepatocytes, and as infected cells lyse some bacteria migrate to the gallbladder via hepatic ducts. Once in the gallbladder, *L. monocytogenes* replicates extracellularly to high bacterial densities. The gallbladder then becomes the primary bacterial reservoir and the source of fecally excreted bacteria. Despite its importance in *L. monocytogenes* pathogenesis, little is known about how *L. monocytogenes* survives and replicates in the gallbladder. The goal of this dissertation is to characterize the gallbladder as an infectious niche for *L. monocytogenes,* which will lead to a more complete understanding of its multi-organ infection cycle and the determinants of intra- vs. extracellular infection. In this work, I investigated both bacterial and host factors that contribute to gallbladder colonization. First, I developed a novel genetic screen using an *ex vivo* primate gallbladder infection model to reveal *L. monocytogenes* genes that are required for replication. Further characterization candidates from the *ex vivo* screen showed that many are also required for intracellular infection and virulence in an oral murine model of listeriosis. Of note, this study identified sugar transport by phosphoenolpyruvate-dependent phosphotransferase systems (PTS) as being important for replication in the gallbladder. These findings represent novel insights into *L. monocytogenes* carbon metabolism during infection and suggests a role for these transporters for infection in extracellular niches. Next, using a *L. monocytogenes* mutant deficient in gallbladder colonization, I found that STING-mediated innate immunity plays a role in gallbladder colonization following oral infection. Finally, I investigated the roles peroxide resistance mechanisms and iron transport systems during intracellular replication, which revealed extensive redundancy in the stress responses employed by *L. monocytogenes* during infection. Overall, my dissertation research highlights the gallbladder as a replicative niche for *L. monocytogenes* and genetic determinants required for *L. monocytogenes* replication, which will lend further insight into the gallbladder's role in its multi-organ pathogenic life cycle.

Table of Contents

List of Tables and Figures

Acknowledgements

I have so many people to acknowledge for their support over the past few years. First, thank you to my advisor, Michelle Reniere, for her support throughout my graduate career. I joined her lab in 2020, which was not an easy time for anyone, and I will always be grateful to her for fostering an inclusive, safe research environment for her trainees. Thank you to all my committee members, Ajai Dandekar, Patrick Mitchell, Joseph Mougous, and Josh Woodward for your feedback and guidance over the years.

Thank you to all members of Reniere lab, past and present. Thank you to Brittany, Rochelle, Monica, and Cortney for introducing me to the lab during my rotation and for welcoming me as a full-time member with open arms. Thank you Rochelle and Monica for being the best elder-graduate student mentors I could ever ask for, and for teaching me so much in and out of the lab. Thank you Cortney for always being encouraging and for being an amazing collaborator. To Lauren, Shania, and Maddy, thank you all for being my rock in my second half of graduate school. And special thank you to Maddy, for learning new techniques just to help with my project, and for being an amazing friend. It has been such an honor to do science with so many amazing women in this lab; thank you for making lab a special place.

Thank you to all members of the Woodward lab who I've crossed paths with. Thank you to Chelsea, Melissa, Lieselotte, Tang, and Susan for being so generous with your time to teach me new techniques and talk through tough science questions. And thank you Moe for being not only a brilliant scientist to bounce even the stupidest questions off of, but also for being a force of encouragement and emotional support. Working with not one, but two amazing labs has been such a joy.

Thank you to Edward, Robin, Jacob, and Ryan for being an amazing cohort. I couldn't have asked for a better group of people to start graduate school with, and it's so exciting to see where we all go next. Thank you to Neel, Lyndsey, Eliot, and Ciara for showing me that serious scientists can also have fun. While we're at it, thank you to each and every UW Microbiology graduate student. The community we've built and maintained in this program is truly special, and it's been such an honor to connect with you all over the years; I will miss you all dearly.

Thank you to all of my non-grad school friends, near and far, for keeping me grounded. Thank you to Rory, Gloria, Ankur, Emma, and Felix for your love and support; I'm so glad that we all ended up in Seattle! Thank you Hana for gracing Seattle with your positive energy so often, despite never living here. Thank you Jen, Dane, and Carlos for always making me laugh and making me feel at home. And thank you to Claire, for being my best friend.

Thank you to my parents, Julie and Jeffrey, for the unconditional support they've shown me for my entire life. Thank you David for always making me laugh and taking my mind off of work when I needed it most. Thank you to my cousins, Jennifer, Katie, Rebecca, and Jon, for being my role models since childhood.

And, finally, thank you Jesse, for everything.

In loving memory of my grandparents:
Susan Kelly, David Schwardt, Jeon Um-Jeon, and Nam Wook

Chapter 1: Introduction

Listeria monocytogenes as a model foodborne pathogen

Listeria monocytogenes is a Gram-positive bacterium known to survive and replicate in a variety of environments, including soil, sludge, and in mammalian hosts where it is the etiologic agent of the severe foodborne illness listeriosis[1]. Most *L. monocytogenes* infections result in self-limiting gastritis that do not require antibiotic treatment or hospitalization. However, in patients with risk factors such as pregnancy, old age, or immunocompromised status, infections spread beyond the GI tract to cause sepsis, meningitis, and pregnancy complications such as pre-term labor or miscarriage. While the incidence of disease is relatively low compared to other foodborne illnesses, the case fatality rate of invasive listeriosis is 15-22%, making *L. monocytogenes* one of the most deadly bacterial pathogens[2,3]. Thus, better understanding the determinants of *L. monocytogenes* replication and pathogenesis remains an important area of investigation for infectious disease and public health researchers.

Humans are exposed to *L. monocytogenes* multiple times per year due to its frequent occurrence in food processing facilities[3]. In addition, it is estimated that 10-12% of healthy adults exhibit asymptomatic fecal shedding of *L. monocytogenes*, emphasizing how prevalent this pathobiont is within the human population[1]. Most exposures do not lead to invasive listeriosis, but *L. monocytogenes* nevertheless causes multiple foodborne outbreaks per year in the United States, with a hospitalization rate of over 90%[4]. Food products are frequently recalled due to *L. monocytogenes* contamination[5]. The high occurrence of contamination with this pathogen is due to the ability of *L. monocytogenes* to grow and form biofilms in high salt, high acid, and in the presence of many disinfectants, which makes it difficult to eliminate from food processing environments[6]. Additionally, *L. monocytogenes* can grow at refrigeration temperatures, which allows it to persist in ready-to-eat foods and further complicates efforts to limit the prevalence of this pathogen in the food supply.

During foodborne infection, *L. monocytogenes* undergoes a multi-organ infection cycle, summarized in **Figure 1**, which involves colonization and replication in both extracellular and intracellular niches. After ingestion of *L. monocytogenes*-contaminated food, the bacteria first colonize the lumen of the gastrointestinal (GI) tract where they replicate extracellularly, primarily in the cecum and colon[7]. In susceptible hosts, a small portion of the *L. monocytogenes* in the GI tract invade intestinal epithelial cells, replicate intracellularly, and spread to neighboring enterocytes via actin-mediated motility[8]. *L. monocytogenes* then cross the mucosal barrier and gain access to the lamina propria, Peyer's patches, and draining mesenteric lymph node (MLN). In the MLN, intracellular replication is required for further dissemination to peripheral organs[9]. Bacteria disseminate from the GI tract indirectly to the spleen through the MLN and lymphatics, and directly to the liver via the portal vein[8,9]. Subsequently, bacteria migrate from the liver through the hepatic ducts to seed the gallbladder, where they replicate extracellularly in the lumen to very high densities[10,11]. After a meal, the gallbladder contracts and delivers a bolus of bile and bacteria into the small intestines, reseeding the GI tract[12]. Thus, the gallbladder becomes the main reservoir of *L. monocytogenes* during infection and the source of bacteria excreted in the feces[10].

Animal models of infection have been crucial for understanding *L. monocytogenes* pathogenesis. Murine infection models are most commonly used because they are conducive to

performing large-scale experiments[13]. Intravenous (i.v.) models of inoculation were found to be more consistent in bacterial colonization and virulence, which led to i.v. models of infection being favored over oral models. Following i.v. infection, bacteria are rapidly filtered from the bloodstream into the liver and spleen[14], where they proliferate to high densities. Typically only livers and spleens were harvested in these studies, and therefore many *L. monocytogenes* virulence factors have been characterized *in vivo* primarily at these systemic sites of infection, but not in other organs relevant to foodborne infection. Taken together, i.v. models of listeriosis have been invaluable to understanding *L. monocytogenes* determinants of infection *in vivo,* but they pose major limitations for studying foodborne listeriosis.

To study the natural foodborne route of *L. monocytogenes* infection, oral inoculation methods have been optimized in recent years and have allowed characterization of the multi-organ pathogenesis. Mice are not natural hosts of *L. monocytogenes* infection, and therefore a very high dose of bacteria is needed to consistently colonize the mouse GI tract via oral inoculation[13]. In addition to determining the proper infectious dose, pre-treating animals with oral antibiotics and fasting immediately before infectious result in more robust colonization of the murine GI tract, which has led to more reproducible experiments[7,15]. With these improvements, oral models of listeriosis have been used to determine the multi-organ route of dissemination (Figure 1)[8,10]. Additionally, oral models of infection have shown that a significant proportion of bacteria are extracellular in the livers, spleens, and MLN[9,16], organs that were previously thought to be predominantly intracellular sites of infection. As oral infection models become more widely used, they will continue to provide insights into both the bacterial and host determinants of *L. monocytogenes* pathogenesis, in particular those required for replication in the GI tract and other infection niches beyond the liver and spleen.

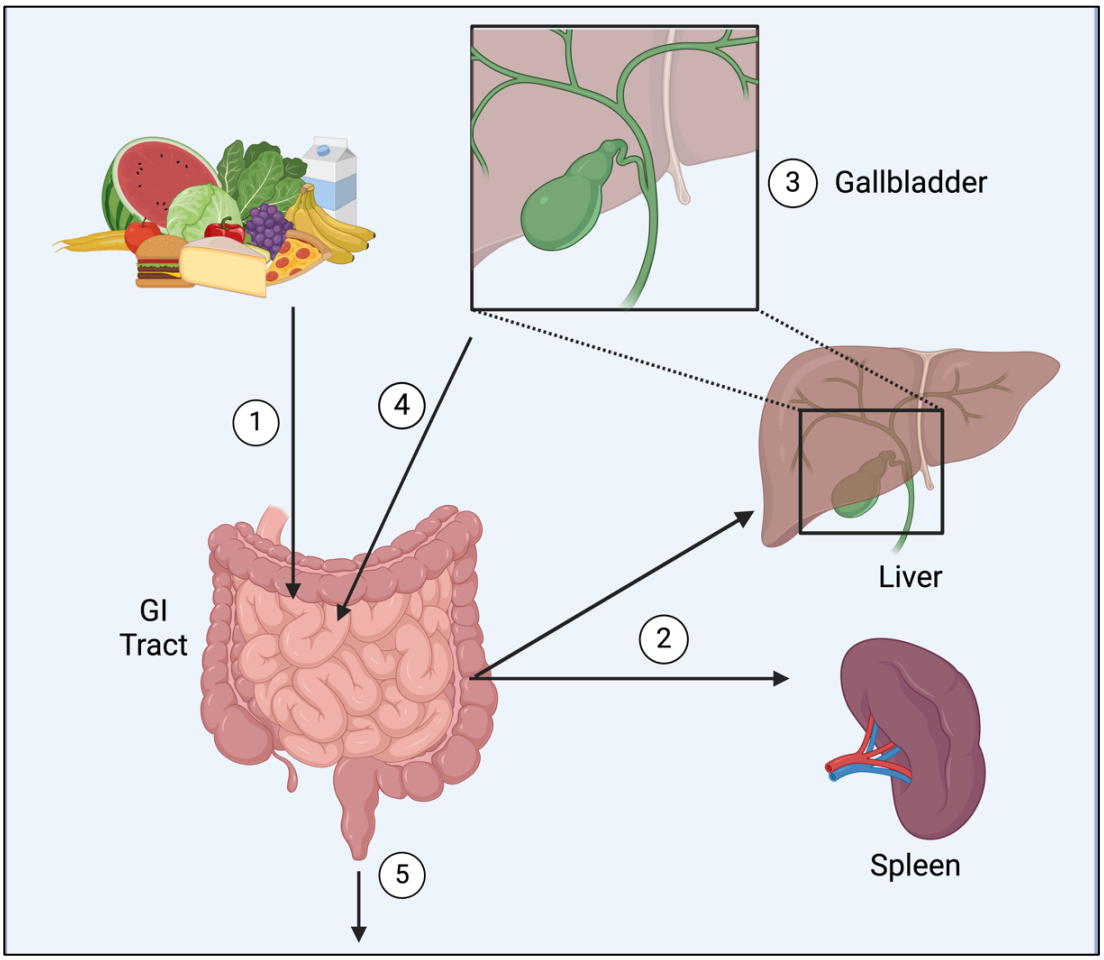

Figure 1. Multi-organ life cycle of *L. monocytogenes.* 1) A susceptible host consumes contaminated food, and *L. monocytogenes* colonizes the intestinal epithelium in the GI tract. 2) *L. monocytogenes* disseminates beyond the GI tract to peripheral organs. 3) After replicating intracellularly in the liver, bacteria descend to the gallbladder via the hepatic ducts. Once in the gallbladder, *L. monocytogenes* replicates extracellularly to extremely high densities. 4) Gallbladder contraction delivers a bolus of bile and bacteria into the small intestines. 5) *L. monocytogenes* is excreted in the feces.

L. monocytogenes infection of the gallbladder

The gallbladder is a sac-like organ in which bile is stored and concentrated. The inner surface of this organ is comprised of a single layer of columnar epithelial cells lining the inner-most surface, a mucus layer lining the epithelial cells, and a lumen filled with bile. Bile is produced in the liver and is composed of bile salts, cholesterol, phospholipids, and the heme degradation products biliverdin and bilirubin, which give bile its characteristic color. Bile stored in the gallbladder lumen is neutral pH, but becomes acidified when it enters the small intestine. Bile acts as an emulsifier, aiding in the digestion of lipids in food and exhibiting antimicrobial activity by damaging membranes, nucleic acids, and proteins[17]. Despite these antimicrobial properties, some bacteria have evolved methods of bile detoxification that render them tolerant to bile and

capable of colonizing the gallbladder, including *L. monocytogenes*, *Salmonella enterica*, and *Campylobacter jejuni*[11,18,19].

The first study characterizing infection of the gallbladder used *in vivo* fluorescent imaging to show that *L. monocytogenes* replicates in murine gallbladders to high densities following both oral and i.v. inoculation, and that replication takes place extracellularly[11]. In a subsequent study, Hardy et al. show that contraction of the gallbladder delivers a bolus of bacteria into the small intestines[12], which reinfects the GI tract and perpetuates the multi-organ cycle of infection. This secretion of bacteria into the intestines supports the hypothesis that *L. monocytogenes* replicates primarily extracellularly in the gallbladder, rather than adhering to the epithelial tissue or mucosal surface. Importantly, the combination of robust replication in the gallbladder and re-seeding of the GI tract following biliary secretion led to the hypothesis that the gallbladder is the primary bacterial reservoir during listeriosis.

L. monocytogenes must colonize the GI tract, disseminate beyond the GI tract, and establish a replication niche in the liver before disseminating to the gallbladder[8,10]. It is therefore important to understand these host barriers to fully characterize the role of the gallbladder in *L. monocytogenes* pathogenesis. To this end, libraries of barcoded strains of *L. monocytogenes* have been used to determine the dissemination pathways from the GI tract to peripheral organs, as well as to quantify the bottlenecks experienced upon reaching those organs[8,10]. After *L. monocytogenes* establishes a replication niche in the liver, 1-5 bacteria further disseminate to the gallbladder and replicate to high densities[10]. This small founding population in the gallbladder represents an incredibly restrictive bottleneck to reach this organ, where in contrast the founding population of the liver is ~200 bacteria following oral infection. Depletion of innate immune cells during infection leads to an increase in founding population size in the gallbladder, which suggests a role of the host immune system in restricting dissemination to this organ[10]. Importantly, the populations recovered from the feces were most genetically to those recovered from the gallbladders, indicating that the gallbladder is the source of fecally shed bacteria during *L. monocytogenes* infection[10].

It is generally accepted that *L. monocytogenes* replicates extracellularly in the gallbladder, which is consistent with most strains of this pathogen readily replicating in the presence of high concentrations of bile[17]. Several *L. monocytogenes* genes have been characterized as required for replication in bile[20–22]. The multidrug resistance transporter MdrT was originally identified to secrete c-di-AMP (CDA)[23,24], and subsequently suggested to be an efflux pump for cholic acid, a component of bile[25]. The bile exclusion system encoded by *bilE* was proposed to be a transporter that protected *L. monocytogenes* from toxicity induced by reconstituted bovine bile[22]. However, BilE was recently renamed EgtU when it was conclusively demonstrated that it specifically binds and transports the low molecular weight thiol ergothioneine[26]. The *bsh* gene encoding bile salt hydrolase was originally described as required for survival in bile *in vitro* and for intestinal persistence in a guinea pig model of infection[20]. SigB is a stress response alternative sigma factor that positively regulates both *bsh* and *bilE*[21,22]. It is now appreciated that *bsh*, *bilE*, and *sigB* confer resistance to acidified bile, as would be found in the small intestine, but are not necessary to detoxify bile at neutral pH, as would be found in the gallbladder lumen[27,28]. Therefore, despite extensive investigations of mechanisms of bile resistance, it remains unclear which *L. monocytogenes* genes are required for replication in the *in vivo* gallbladder environment. A better

understanding of the bacterial factors required for infection of this organ will lead to a more complete model of *L. monocytogenes* pathogenesis.

The innate immune response to *L. monocytogenes* infection

Once *L. monocytogenes* colonizes a host, it must contend with the host immune response. The first line of defense against infection is referred to as the innate immune response, which is not pathogen-specific but is crucial for limiting the growth and dissemination of *L. monocytogenes*. The mammalian innate immune system consists of physical barriers that prevent foreign material entering the body, such as the skin and mucosal surfaces, and innate immune cells, such as monocytes, neutrophils, and macrophages[29], which recognize and eliminate pathogens. These professional immune cells detect the presence of pathogens using proteins known as pattern recognition receptors (PRRs), which sense bacterial ligands and trigger downstream immune activation, such as the release of inflammatory cytokines[29]. Non-immune cells are also involved in the innate immune response. For example, epithelial cells express PRRs and induce recruitment of professional immune cells to an infected tissue. PRRs can be expressed on the host cell surface to sense extracellular pathogens or in the cytosol to sense intracellular pathogens. The extracellular PRRs TLR2 and TLR5 contribute to the early recognition of *L. monocytogenes*, but these PRRs do not significantly contribute to bacterial clearance at systemic sites of infection[29].

Cytosolic sensing of pathogens is critical for combatting intracellular pathogens. *L. monocytogenes* stimulates an immune response during intracellular infection by activating the host protein STING (Stimulator of Interferon Genes), which then induces interferon-b (IFN-β) production. There are two mechanisms by which *L. monocytogenes* can activate STING during intracellular infection[30]. The first mechanism is cGAS-dependent: first, bacteriolysis leads to the release of bacterial DNA into the host cytosol. The host protein cGAS (cyclic-GMP-AMP synthase) then binds the cytosolic DNA and in response produces cyclic-GMP-AMP (cGAMP), which binds and activates STING. The second mechanism is cGAS-independent, where *L. monocytogenes* produces and secretes cyclic-di-AMP (CDA), which also binds and activates STING (Figure 2). Activation of STING by either cGAMP or CDA induces increased expression of IFN-β. In general, innate immune sensors such as STING induce the release of cytokines and recruit additional immune cells to the site of infection[29]. However, the role of IFN-β in mediating *L. monocytogenes* infection remains somewhat elusive. It has been suggested that excess IFN-β signaling can be detrimental to the host, and that the role of IFN-β signaling may differ between intravenous and oral routes of infection[29].

Following activation of the innate immune system by sensors such as STING, the release of cytokines and the recruitment of professional immune cells to the site of infection are induced. The first immune cells to reach the infected tissue following inoculation with *L. monocytogenes* are polymorphonuclear neutrophils (PMNs), which infiltrate infected tissues within 30 minutes of inoculation and contribute to bacterial clearance[29]. Following PMN infiltration, monocytes are recruited the site of infection. While the precise role of monocytes requires further investigation, it is thought that they prevent the spread of *L. monocytogenes* while also preventing PMN-mediated tissue damage. In addition to recruited PMNs and monocytes, tissue resident

macrophages, such as Kupffer cells in the liver, are also involved in mediating killing of *L. monocytogenes* within infected tissues.

The roles of these immune cells in response to *L. monocytogenes* infection were investigated primarily using i.v. murine models of infection, which typically only collect livers and spleens, therefore very little is known about the immune responses to *L. monocytogenes* in the gallbladder. Depletion of circulating PMNs and monocytes results in increased bacterial burdens in the gallbladders of infected mice[10], supporting a role of the host immune system in modulating gallbladder infection. It remains unclear, however, whether recruitment of these immune cells to the gallbladder epithelium directly contributes to bacterial clearance from this organ. Additionally, this effect was demonstrated using an i.v. model of infection, and whether depletion of these cells has a similar effect following oral infection was not tested[10]. During *S. enterica* infection of the gallbladder, both macrophages and PMNs increase in abundance compared to uninfected tissues, showing that immune cell recruitment can play a role during bacterial infection of the gallbladder[31]. Whether these immune cells are present in gallbladders infected with *L. monocytogenes* has not been tested.

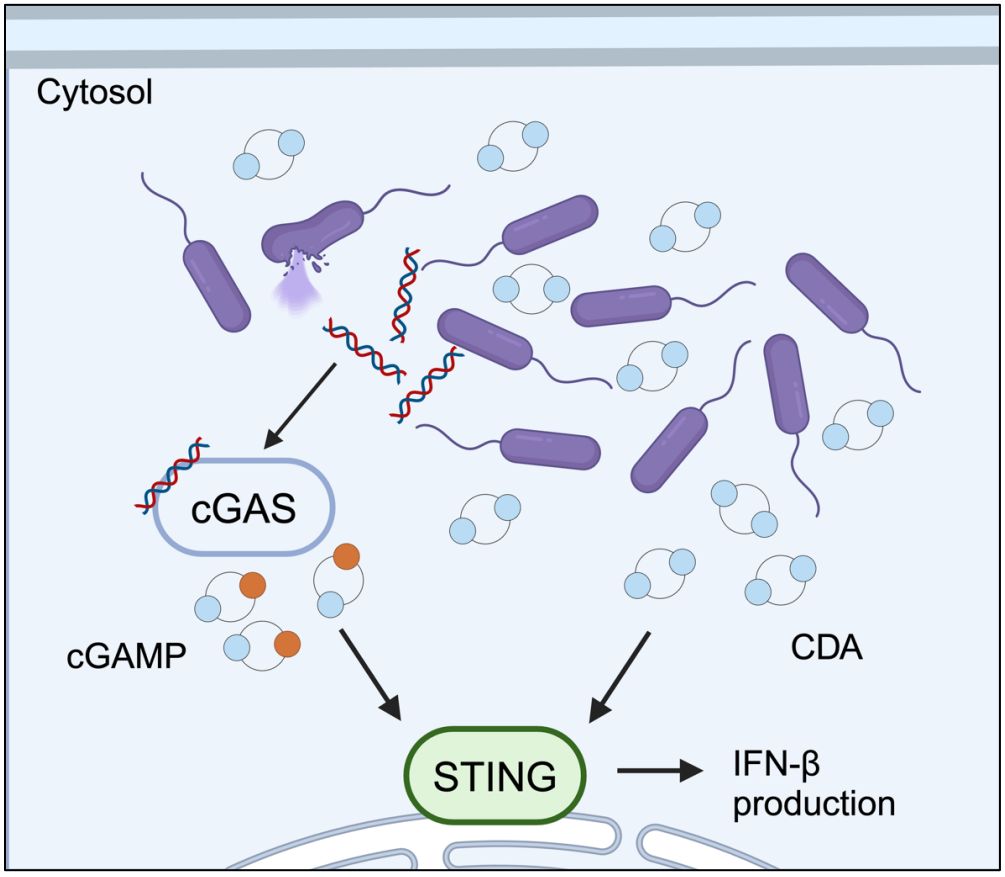

Figure 2: Interferon-β induction by *L. monocytogenes*. (Left) cGAS-dependent activation of STING. Intracellular bacteriolysis leads to release of bacterial DNA into the cytosol. cGAS binds cytosolic DNA, which leads to its production of cGAMP. cGAMP then binds STING, which induces IFN-β production. (Right) cGAS-independent activation of STING. Intracellular *L. monocytogenes* produce and secrete c-d-AMP (CDA). CDA then binds STING, which induces IFN-β production.

L. monocytogenes adaptation to (host)ile environments

L. monocytogenes must rapidly adapt to its environment, and the transcriptional reprogramming to transition from saprophytic to pathogenic lifestyles has been extensively studied[32]. Even within a single host organism, *L. monocytogenes* encounters a variety of different environments, including the GI tract, host cytosol, and gallbladder, all of which present a distinct array of deadly stressors. In the gallbladder those stressors are presumed to be derived from bile acids, but given that most strains of *L. monocytogenes* are resistant to bile stress it is likely that resistance to additional stressors is required for survival in the gallbladder.

One source of stress during infection comes from host-derived reactive oxygen species (ROS), which are a component of the host innate immune system[33]. ROS are produced by bacteria and the host as a byproduct of the incomplete reduction of molecular oxygen during aerobic respiration, and accumulation of ROS leads to DNA damage and mutagenesis and protein damage[34]. Given these deleterious effects that stem from aerobic respiration, it is unsurprising that peroxide detoxification strategies have evolved in all domains of life. Bacteria express many defense many scavenging enzymes to defend themselves against ROS-mediated oxidative stress[35]. Superoxide dismutase detoxifies the highly toxic ROS superoxide (O_2^-), generating molecular oxygen and hydrogen peroxide (H_2O_2). Peroxidase and catalase enzymes then efficiently scavenge and detoxify the resulting hydrogen peroxide. At low concentrations of hydrogen peroxide, peroxidases are the primary scavengers of peroxide, whereas at high concentrations of hydrogen peroxide catalases become the dominant peroxide scavengers[36]. Due to the near-ubiquitous nature of peroxide stress, bacteria typically express multiple functionally redundant enzymes to protect against peroxidases. Given the deleterious effects of ROS, it is unsurprising that the mammalian immune system includes a mechanism known as the phagocytic respiratory burst. During the respiratory burst, increased activity of NADPH oxidase leads to increased oxygen consumption and increased concentrations of ROS, which contributes to eliminating invading pathogens[33].

Another source of stress that bacteria contend with both in the environment and within a host is nutrient scarcity. In addition to carbon sources and other macronutrients, bacteria must scavenge trace micronutrients from their environment. Iron is an essential trace element required by nearly all bacteria, as it serves as a co-factor for enzymes involved in essential metabolic processes such as energy production, DNA replication, and detoxification of reactive oxygen species[37,38]. Despite iron being the most abundant element on Earth, biologically available forms of iron are scarce in most environments and as a result a diverse array of mechanisms of iron acquisition have evolved in bacteria. The two main forms of iron that bacteria can access are molecular iron, which exists in both ferric (Fe^{3+}) and ferrous (Fe^{2+}) forms, and heme, in which an iron molecule rests within a porphyrin ring. Heme is the most abundant source of iron available to bacteria during infection of mammalian hosts, due to both its abundance in the blood in hemoglobin and its function as a co-factor for many essential proteins[39]. Iron in mammalian hosts is also stored in the cytosolic protein ferritin, which can store more than 4,000 iron molecules[38,39].

Iron is an essential trace nutrient and plays a role in the host immune response to infection. Iron-rich tissues, such as the liver, respond to inflammation by inhibiting the secretion of iron, thus limiting the growth of extracellular bacteria in the tissue. Macrophages also limit iron secretion in response to inflammatory cytokines, leading to an increased abundance of intracellular iron in

these cells[40]. While essential to the survival and growth of nearly all bacteria, iron can be toxic to both bacterial and eukaryotic cells. Excess intracellular iron, in the form of heme or molecular iron, can undergo Fenton chemistry, in which iron reacts with ROS and generates more ROS in the process[41]. Cells therefore must employ mechanisms to combat iron toxicity by exporting excess iron back into the environment or sequestering iron in a non-reactive form for later use. Interestingly, the *L. monocytogenes* iron efflux pump FrvA is required for virulence during murine infection[42], highlighting that preventing accumulation of excess iron is necessary for survival in the host.

To maintain optimal levels of iron, *L. monocytogenes* encodes a number of transporters that facilitate uptake and efflux of both heme and molecular iron, which are described in detail in Chapter 5. While the function and regulation of iron homeostasis proteins have been extensively studied in *L. monocytogenes*, the roles of different iron transporters during infection are not well understood. As discussed above, *in vivo* studies have primarily used i.v. murine models of listeriosis, therefore the roles of iron homeostasis genes in the GI tract stage of infection have largely not been investigated. Additionally, the roles of these genes in intracellular vs. extracellular infection have not been studied.

State of the field and open questions

While the pathogenesis of *L. monocytogenes* has been extensively studied for over 40 years, *in vivo* studies of *L. monocytogenes* pathogenesis have historically only characterized infection of the liver and spleen. Moreover, oral infection models that more accurately mimic the natural foodborne route of infection have only recently become widely used[13,29]. Additionally, the gallbladder has only recently been appreciated as the primary reservoir of infection during listeriosis[10], therefore the bacterial determinants of colonization and replication in the gallbladder are not well understood. *L. monocytogenes* is highly tolerant of bile acids *in vitro*[43], therefore bile stress is not thought to be an impediment to *L. monocytogenes* colonization of the gallbladder. Host factors that influence bacterial colonization of the gallbladder, such as availability of metabolites or presence of other anti-microbial factors, are also largely unknown. Identification of the *L. monocytogenes* factors required for colonization of the gallbladder would characterize how it survives and replicates in this organ. Understanding the gallbladder as a replicative niche will also provide insight into the role of extracellular infection sites during listeriosis, such as the GI tract.

The immune responses to *L. monocytogenes* infection of the gallbladder also remain poorly understood, as the role of the host immune system in listeriosis has predominantly been characterized in the liver and spleen. Previous studies have strongly suggested that immune cell infiltration to the gallbladder plays a role in bacterial clearance. Depletion of innate immune cells prior to infection leads to increased bacterial burdens in the gallbladder following i.v. infection[10], but whether these cells play a similar role during oral infection requires further investigation. Further characterizing the host response to infection of the gallbladder, and how bacterial factors modulate this response, will provide important insights into *L. monocytogenes* pathogenesis throughout its multi-organ infection cycle.

Overall, the goal of my thesis is to characterize the stressors encountered during *L. monocytogenes* infection, with a focus on defining the gallbladder as a replicative niche. First, a

genetic screen using an *ex vivo* infection model revealed many *L. monocytogenes* genes that are required for replication in the mammalian gallbladder (Chapter 2). Next, a *L. monocytogenes* mutant deficient in gallbladder colonization was used to investigate the role of STING-mediated innate immunity during gallbladder infection (Chapter 3). Finally, investigating the roles of peroxidases and iron transporters highlighted the diversity of stressors, and stress responses, encountered during infection (Chapters 4 & 5). Together, these studies have identified *L. monocytogenes* genes required for virulence *in vivo* and provided insight into the metabolic requirements and stressors encountered during the multi-organ foodborne infection cycle.

Chapter 2: A genome-wide screen in *ex vivo* gallbladders identifies *Listeria monocytogenes* factors required for virulence *in vivo*

Introduction

Following oral inoculation of a mammalian host, *L. monocytogenes* colonizes the gastrointestinal tract and disseminates to peripheral organs such as the liver, from which *L. monocytogenes* colonizes the gallbladder and replicates to high densities. The gallbladder then becomes the primary bacterial reservoir and the source of fecally excreted bacteria (Figure 1). Despite its importance in *L. monocytogenes* pathogenesis, little is known about how this pathogen survives and replicates in the gallbladder. As mentioned in Chapter 1, *L. monocytogenes* utilizes several bile-resistance mechanisms, such as the bile exclusion system BilE and bile salt hydrolase (Bsh)[20,22]. It is now known that these genes are required for *L. monocytogenes* survival in acidified bile, but are not necessary to detoxify bile at neutral pH[27,28]. Bile stored in the gallbladder lumen is pH neutral, therefore the *L. monocytogenes* genes required for replication in this organ remain largely unknown.

Murine infection models have been crucial for understanding gallbladder colonization of bacterial pathogens, including *L. monocytogenes*, but they pose two major limitations. However, due to the bottleneck in which fewer than five *L. monocytogenes* initially seed the gallbladder following either oral or intravenous infection[10], performing genetic or biochemical screens in mouse models is not feasible. Additionally, murine gallbladders only contain 5 - 15 µL of biofluid[44], which would not yield enough biomass to use infection model for global genetic screens. Purified bile salts and reconstituted powdered bile are frequently used to mimic the gallbladder environment *in vitro*, but it is not clear what concentrations and diluent accurately represent gallbladder biofluid. In fact, studies investigating *L. monocytogenes* requirements for survival in reconstituted porcine bile and *ex vivo* porcine bile identified distinct genes[17,28], supporting the notion that reconstituted bile does not mimic the biofluid encountered *in vivo.*

In this study, we sought to identify *L. monocytogenes* genes required for replication in the mammalian gallbladder using a transposon sequencing (Tn-seq) approach. This technique combines saturating transposon mutagenesis with next-generation sequencing to assess the contribution of every genetic locus in a high-throughput manner[45,46]. Tn-seq has been used to identify essential genes and genes conditionally essential for survival in a host for several pathogenic bacteria, including *Staphylococcus aureus*[47], *Vibrio cholerae*[48], *Streptococcus pneumoniae*[46], and recently *L. monocytogenes*[49]. However, the restrictive bottlenecks in mouse models of listeriosis make the use of global genetic approaches to study gallbladder colonization in vivo unfeasible. Here, we performed Tn-seq on *L. monocytogenes* in *ex vivo* non-human primate gallbladders and identified dozens of genes necessary for survival and replication in this environment and more broadly in the context of a murine model of listeriosis.

This chapter represents collaborative effort by myself, Courtney Halsey, Madison Sanchez, and Michelle Reniere. My contributions to this publication include performing experiments described in Figures 4-8, and the writing and preparation of the final manuscript.

Results

An unbiased approach identifies *L. monocytogenes* genes required for growth and survival in the gallbladder lumen

To identify *Listeria monocytogenes* genes required for gallbladder colonization, we established a novel model of gallbladder colonization using non-human primate (NHP) gallbladders obtained from the Washington National Primate Research Center Tissue Distribution Program. There are several advantages to NHP organs over conventional murine models. First, NHP gallbladders can be inoculated with bacteria via syringe, eliminating bottlenecks to colonization encountered during murine infections. Second, NHP organs are larger and contain ~1,000-fold more biofluid than murine gallbladders, which can support more bacterial biomass or be harvested for *in vitro* assays. Finally, organs were obtained from NHPs at the endpoint of other non-infectious experiments, and therefore no additional animals were sacrificed for this model.

In the development of the gallbladder colonization model, we first assessed whether *ex vivo* gallbladder biofluid (bile) supports growth of *L. monocytogenes.* Bile harvested from three independent NHP gallbladders was determined to be sterile and supported exponential growth of *L. monocytogenes in vitro*. We next injected mid-log *L. monocytogenes* into the lumen of intact *ex vivo* gallbladders and monitored bacterial survival over time by removing luminal contents with a syringe and plating to enumerate colony forming units (CFU). Interestingly, we observed consistent reductions in CFU shortly after inoculation, followed by exponential growth that plateaued between 6 and 12 hours post-injection (data not shown). To minimize host cell death and maintain the integrity of the organs, we limited the incubation time to 6 hours in subsequent experiments.

After establishing growth conditions for *L. monocytogenes* in NHP gallbladders, we used this *ex vivo* organ model to investigate the *L. monocytogenes* genes required for survival and growth in the gallbladder lumen using the unbiased global genetic approach of transposon sequencing (Tn-seq). Four NHP gallbladders were inoculated via syringe with a saturated transposon mutant library of *L. monocytogenes*. To monitor growth of the mutant library in the organs, samples of luminal contents were collected 30 minutes and 6 hours post-injection. As observed previously with wild type (WT) *L. monocytogenes*, an initial reduction in CFU at 30 minutes post-injection was followed by exponential growth through 6 hours, with an average doubling time of 46 minutes (Figure 3A). This doubling time is similar to that observed for *L. monocytogenes* growing in rich medium, demonstrating robust growth in this environment. After 6 hours of incubation in the gallbladders, the entire luminal contents were harvested, diluted in brain heart infusion (BHI) broth, and incubated for 2 hours to increase biomass. Bacterial genomic DNA was then isolated and libraries were prepared for Illumina sequencing of the transposon insertion sites (Figure 3B and Table 1). Using the parameters of a $\log_2$ fold-change less than -1.50 and an adjusted *p*-value of less than 0.05, mutants in 43 genes were significantly depleted after incubation in the gallbladders compared to the input libraries, indicating that these genes are required for growth or survival in the NHP gallbladder lumen.

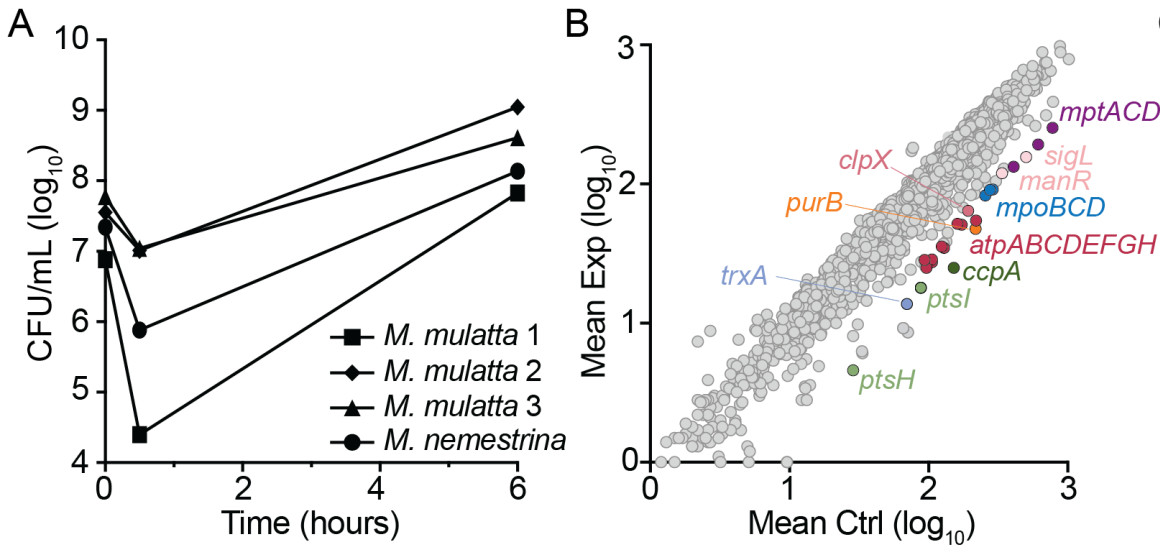

Figure 3. Tn-seq in *ex vivo* NHP gallbladders identifies *L. monocytogenes* genes necessary for growth and survival. (A) Growth of the *L. monocytogenes* transposon library in NHP gallbladders over 6 hours. Bacteria were inoculated via syringe and collected for CFU enumeration 30 minutes and 6 hours post-infection. Gallbladders from three *Macaca mulatta* and one *M. nemestrina* were used. (B) Average read counts of *L. monocytogenes* genes in the gallbladder experimental condition (Exp) compared to the input library (Ctrl).

Genes significantly depleted after incubation in the gallbladder included those involved in stress responses, such as *trxA* encoding thioredoxin and *clpX* encoding a Clp protease ATPase subunit, consistent with the known antimicrobial effects of bile. We also identified the adenylosuccinate lyase encoded by *purB*, consistent with the importance of purine biosynthesis in surviving bile stress[28]. Depleted genes also included those encoding two phosphoenolpyruvate-dependent phosphotransferase system (PTS) permeases known to import both glucose and mannose (*mptACD* and *mpoBCD*)[50]. PTSs are multi-protein complexes utilized by many bacteria to import and phosphorylate defined carbohydrates, with the sugar specificity determined by the Enzyme II (EII) complex proteins[51]. While the *L. monocytogenes* genome encodes 29 complete PTSs[50], our screen identified Mpt and Mpo as the only EIIs required for growth in the gallbladder (Figure 4). In addition to the PTS permeases, genes encoding regulators that activate transcription of the *mpt* and *mpo* operons (*manR* and *sigL*), and for phosphorylation of the PTS sugars (*ptsI* and *ptsH,* encoding EI and HPr, respectively) were also significantly depleted in the gallbladder condition. Identification of multiple PTS-related operons and their regulators, which lie at distinct genetic loci, suggests that *L. monocytogenes* imports glucose and/or mannose via Mpt and Mpo for growth in the gallbladder. The Tn-seq also identified 8 of the 9 genes encoding the F-type ATP synthase as depleted after growth in the gallbladders. The F-type ATP synthase, while not essential for aerobic growth, is required for anaerobic replication in *L. monocytogenes*[52], suggesting that the *ex vivo* gallbladder may be an oxygen-limited environment. Overall, analysis of our screen identified multiple whole operons as depleted after growth in the NHP gallbladder, indicating that the screen was robust. Importantly, many genes identified here have not been previously implicated in the context of infection.

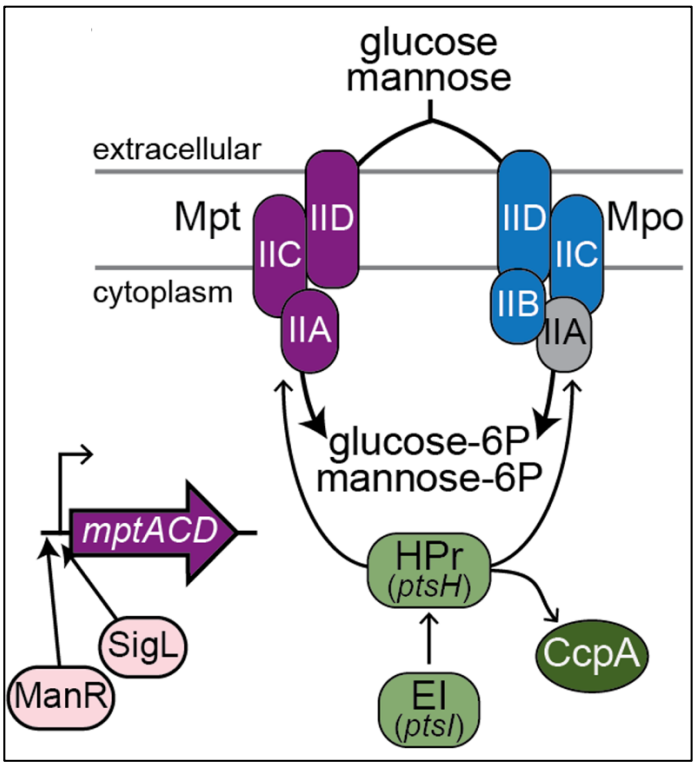

Figure 4: Model depicting the PTSs and their regulators identified by Tn-seq. Color-coded to match Figure 2B. Only Mpo-IIA (gray) was not significantly depleted after incubation in NHP gallbladders.

Table 1. Summary of significant Tn-seq hits. Highlighting indicates genes encoded in operons.
* indicates genes selected for validation

Category:	LMO	Name	Description	log2FC
Protein homeostasis / Redox	1233	*trxA**	Thioredoxin	-2.27
	2219	*prsA2*	Foldase	-1.75
	0964	*yjbH*	Thioredoxin-fold protein	-1.58
	1268	*clpX**	ATP-dependent Clp protease ATPase	-1.57
Nucleotide transport and metabolism	1096	*guaA*	GMP synthase	-2.28
	1773	*purB**	Adenylosuccinate lyase	-2.16
	2538	*upp*	Uracil phosphoribosyltransferase	-1.57
	0055	*purA*	Adenylosuccinate synthetase	-1.53
Carbohydrate metabolism and transport	1571	*pfkA*	6-phosphofructokinase	-2.52
	1002	*ptsH*	PTS system, phosphocarrier protein HPr	-2.42
	1003	*ptsI**	PTS system, enzyme I (EI)	-2.23
	2556	*fbaA*	Fructose-bisphosphate aldolase class II	-2.24
	0097	*mptC**	PTS system, mannose-specific IIC component	-1.66
	0096	*mptA**	PTS system, mannose-specific IIAB component	-1.61
	0098	*mptD**	PTS system, mannose-specific IID component	-1.61

	0781	*mpoD**	PTS system, mannose-specific IID component	-1.65
	0782	*mpoC**	PTS system, mannose-specific IIC component	-1.61
	0783	*mpoB**	PTS system, mannose-specific IIB component	-1.6
Energy production	2530	*atpG**	ATP synthase gamma chain	-1.98
	2534	*atpE**	ATP synthase F0 sector subunit c	-1.91
	2529	*atpD**	ATP synthase beta chain	-1.86
	2528	*atpC**	ATP synthase epsilon chain	-1.85
	2533	*atpF**	ATP synthase F0 sector subunit b	-1.84
	2535	*atpB**	ATP synthase F0 sector subunit a	-1.62
	2532	*atpH**	ATP synthase delta chain	-1.74
	2531	*atpA**	ATP synthase alpha chain	-1.78
	1581	*ackA*	Acetate kinase	-1.65
Regulation	0289	*yycH*	TCS YycFG regulatory protein YycH	-2.72
	0288	*walK*	Two-component sensor histidine kinase	-0.78
	1599	*ccpA**	Catabolite control protein A	-2.56
	1523	*relA*	(p)ppGpp synthetase	-1.76
	2461	*sigL*	RNA polymerase sigma-54 factor RpoN	-1.68
	1891	*recU*	RecU Holliday junction resolvase	-1.51
	1892	*pbpA1*	Bifunctional penicillin-binding protein 1A	-0.92
Coenzyme Metabolism	1901	*panC*	Pantoate--beta-alanine ligase	-2.91
	1902	*panD*	3-methyl-2-oxobutanoate hydroxymethyltransferase	-1.6
	1363	*ispA*	farnesyl diphosphate synthase	-1.58
DNA recombination and repair	1955	*xerD*	Site-specific tyrosine recombinase XerD	-1.82
	1954	*drm*	Phosphopentomutase	-1.47
	2702	*recR*	Recombination protein RecR	-1.66
	1533	*ruvA*	Holliday junction ATP-dependent DNA helicase	-1.62
Amino acid metabolism	1663	*ansB*	Asparagine synthetase	-1.72
	1299	*glnA*	Glutamine synthetase type I	-1.56
Lipid metabolism	1936	*gpsA*	Glycerol-3-phosphate dehydrogenase	-1.71
Hypothetical	-	-	hypothetical protein	-1.92

Genes identified by Tn-seq in the NHP gallbladder contribute to replication in bile *in vitro*

To investigate the roles of the identified genes in *L. monocytogenes* physiology and pathogenesis, we used allelic exchange techniques to generate nine deletion mutants, representative of 19 genes identified in our screen (Table 1). To evaluate the PTS permeases, the

entire *mptACD* (Δ*mpt*) or *mpoABCD* (Δ*mpo*) operons were deleted and a double mutant lacking both operons (Δ*mpt*Δ*mpo*) was generated. To evaluate the F-type ATP synthase, the *atpB* open reading frame was deleted, which eliminates functionality of the entire complex[52]. The mutants were then grown individually either in BHI broth or NHP bile in 96-well plates, and CFU were enumerated after 0.5 and 6 hours of static incubation. Because the oxygen status of the gallbladder lumen is not known, *L. monocytogenes* growth was evaluated in both aerobic and anaerobic conditions. Several mutants exhibited general growth defects and replicated significantly less than WT in rich medium, including Δ*ccpA*, Δ*ptsI*, and Δ*trxA* (Figures 5A and 5B). The Δ*atpB* strain had the most striking phenotype in BHI, displaying a slight ~4-fold reduction in CFU in the presence of oxygen and a complete lack of growth in anaerobic conditions (Figure 5B). This is consistent with a previous report documenting that the F-type ATPase is essential for *L. monocytogenes* anaerobic growth[52]. We additionally measured growth in BHI in shaking flasks to assess growth in maximally aerated conditions in rich medium. Under these growth conditions, the Δ*atpB* mutant exhibited significantly decreased CFU at the earliest time point, while Δ*trxB* was attenuated for growth at 6 and 8 hours post-inoculation (Figures 5C and 5D). Although the relevant oxygen levels during infection are unknown, these data provide a broad view of mutant growth in vitro under varying oxygen levels and reveal that Δ*atpB* and Δ*trxA* are generally impaired for growth in rich medium.

When incubated in bile under anaerobic conditions, all mutants were significantly impaired, with the exception of Δ*ccpA* (Figure 5B). This decrease in CFU at 6 hours was not driven by differences in killing early after inoculation, as all strains exhibited similar reductions in CFU at 30 minutes (Figure 6). Interestingly, some mutants exhibited an oxygen-dependent phenotype. For example, Δ*atpB*, Δ*mpt*, and Δ*mpt*Δ*mpo* grew similarly to WT in bile under aerobic conditions (Figure 5A), but displayed reduced growth under anaerobic conditions (Figure 5B). Together, these results demonstrated that the genes identified by Tn-seq as important during growth in the NHP gallbladder lumen are also required for growth in bile *in vitro*, even in the absence of competing strains.

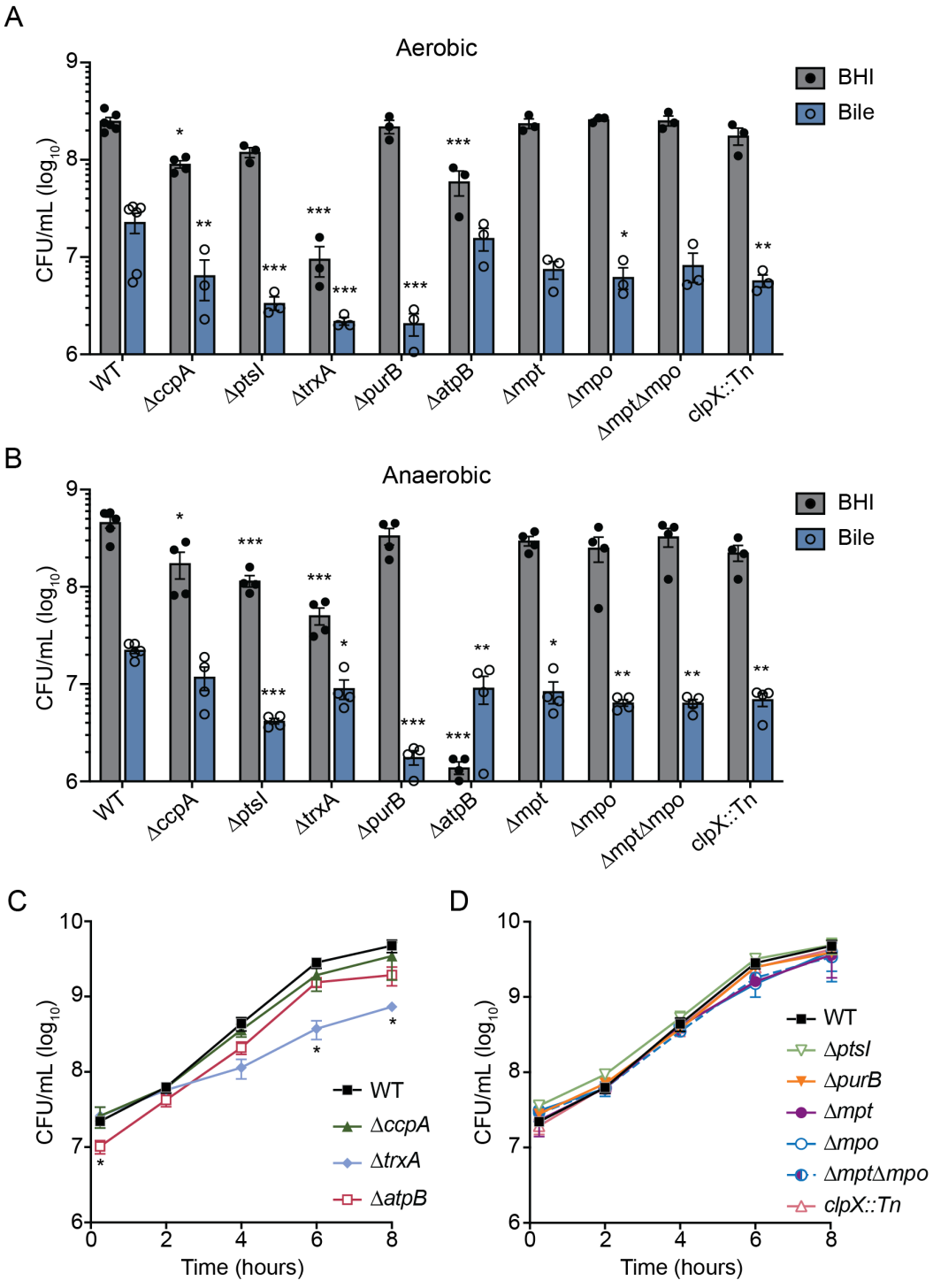

Figure 5. Growth of mutants *in vitro*. (A-B) NHP bile or BHI was inoculated with 10^6 CFU/mL of each *L. monocytogenes* strain, incubated for 6 hours statically in an aerobic incubator (A) or in an anaerobic chamber (B), and then CFU were enumerated. Each circle is an individual data point, while the bars indicate the means and the error bars represent the standard error of the mean (SEM) of at least 3 biological

replicates. (C-D) Flask growth curves in BHI, with shaking. Data in (C) represent the means and SEM of at least 3 biological replicates. Data in (D) represent the means and SEM of at least 2 biological replicates. * $p < 0.05$, ** $p < 0.01$, *** $p < 0.001$, as determined by Dunnett's multiple comparisons test compared to WT in each medium condition and at each time point.

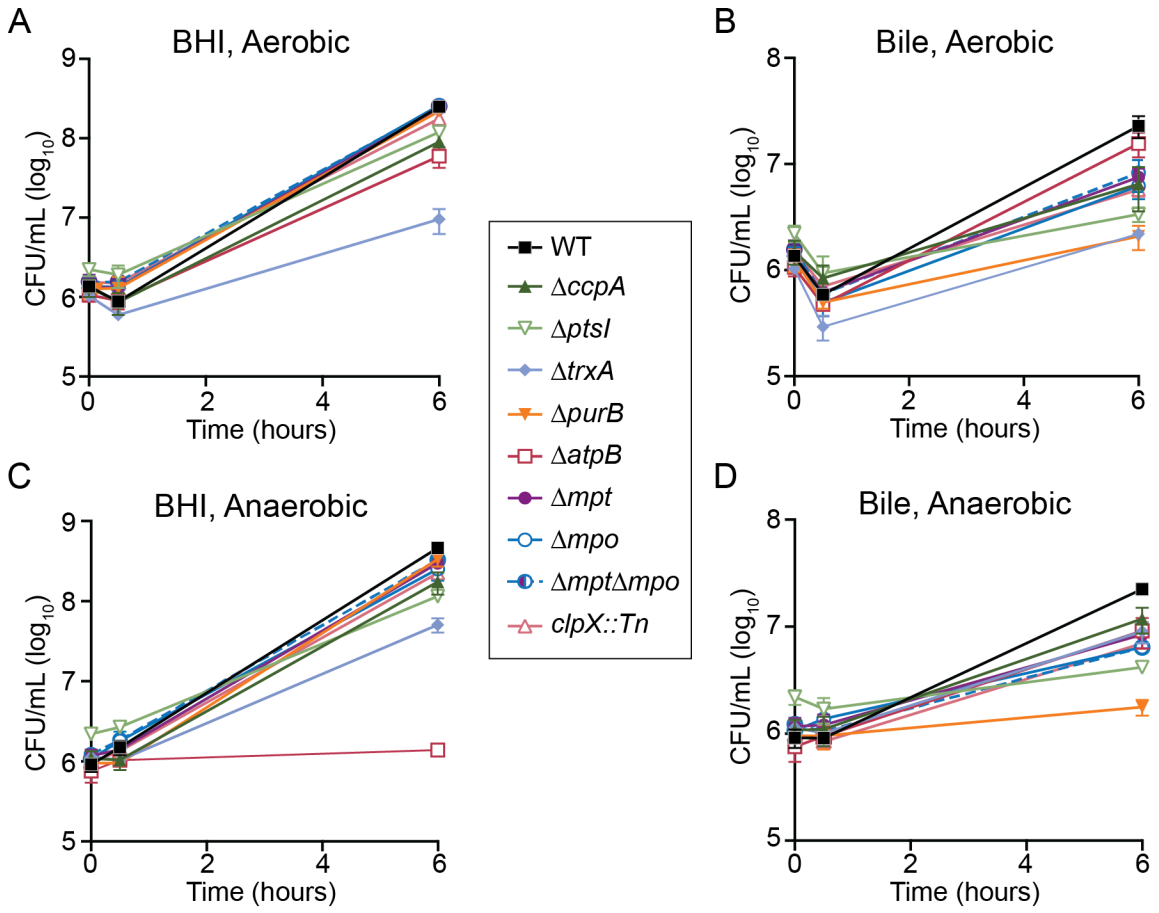

Figure 6. Growth curves of *L. monocytogenes* in BHI or bile *in vitro*. NHP bile or BHI was inoculated with *L. monocytogenes*, incubated statically in an aerobic incubator (A,B) or in an anaerobic chamber (C,D), and CFU were enumerated, as in Figure 2. Data are the means and SEMs of at least three independent experiments. Statistics not shown for clarity.

Genes identified by Tn-seq as critical for survival in the gallbladder lumen also contribute to intracellular fitness

Tn-seq identified *L. monocytogenes* genes required for growth in the gallbladder lumen, which represents one of the extracellular environments that *L. monocytogenes* encounters during infection. While extracellular niches of infection remain largely uncharacterized, the determinants of intracellular infection and their roles in systemic disease have been thoroughly described. The intracellular lifecycle begins with *L. monocytogenes* entering host cells via phagocytosis or receptor-mediated endocytosis, followed by cytosolic replication and intercellular spread to

neighboring cells via actin-dependent motility[53]. To determine if the genes we identified also have important roles in the intracellular lifecycle, we assessed cell-to-cell spread and cytosolic replication of each of the *L. monocytogenes* mutants in cell culture.

The intracellular lifecycle was first evaluated via plaque assay in which a monolayer of cells is infected with *L. monocytogenes* and then immobilized in agarose containing gentamicin to prevent extracellular growth. Three days post-infection, the live cells are stained and the zones of clearance formed by *L. monocytogenes* are measured as an indicator of intracellular growth and intercellular spread. In this assay, most mutants formed significantly smaller plaques than those formed by WT, while mutants lacking the PTS operons *mpt* and *mpo* formed plaques similar in size to WT. (Figure 7A). Notably, infections with Δ*atpB* resulted in no visible plaque formation. We hypothesize this is due to the Δ*atpB* requirement for oxygen, which may be limiting in cells with the agarose overlay. Plaque areas were also measured after infection with the complemented strains, in which each deleted gene was expressed from its native promoter at an ectopic site on the chromosome. With one exception, complementation restored plaque areas to WT levels (Figure 7A). The *ptsI* complemented strain produced even smaller plaque areas than Δ*ptsI,* although this strain did restore other Δ*ptsI* growth defects, as discussed below.

The plaque assay measures both cytosolic replication and cell-to-cell spread. To identify the role of each gene in intracellular growth, we measured replication kinetics in primary bone marrow-derived macrophages (BMDMs) over 8 hours. The Δ*purB* mutant exhibited the most dramatic phenotype as it did not replicate in the host cytosol (Figure 7B). Several additional mutants displayed attenuated intracellular growth, including Δ*ccpA,* Δ*ptsI*, and Δ*trxA* (Figure 7B). Intracellular growth was fully restored in the complemented strains, including Δ*ptsI* + *ptsI* (Figure 7C. Despite defects in plaque formation, both *clpX::Tn* and Δ*atpB* grew similarly to WT in BMDMs, indicating that these mutants are defective specifically in the cell-to-cell spread stage of the intracellular lifecycle. Finally, strains lacking the PTS operons *(*Δ*mpt,* Δ*mpo,* Δ*mpt*Δ*mpo*) displayed no defects in cytosolic growth, consistent with these strains forming WT-sized plaques (Figure 7D). Together, these results indicated that although we identified these genes using the selective pressure of extracellular growth in a mammalian organ, many also contribute to intracellular infection. However, the PTS operons were found to be dispensable during intracellular infection, consistent with prior work[50].

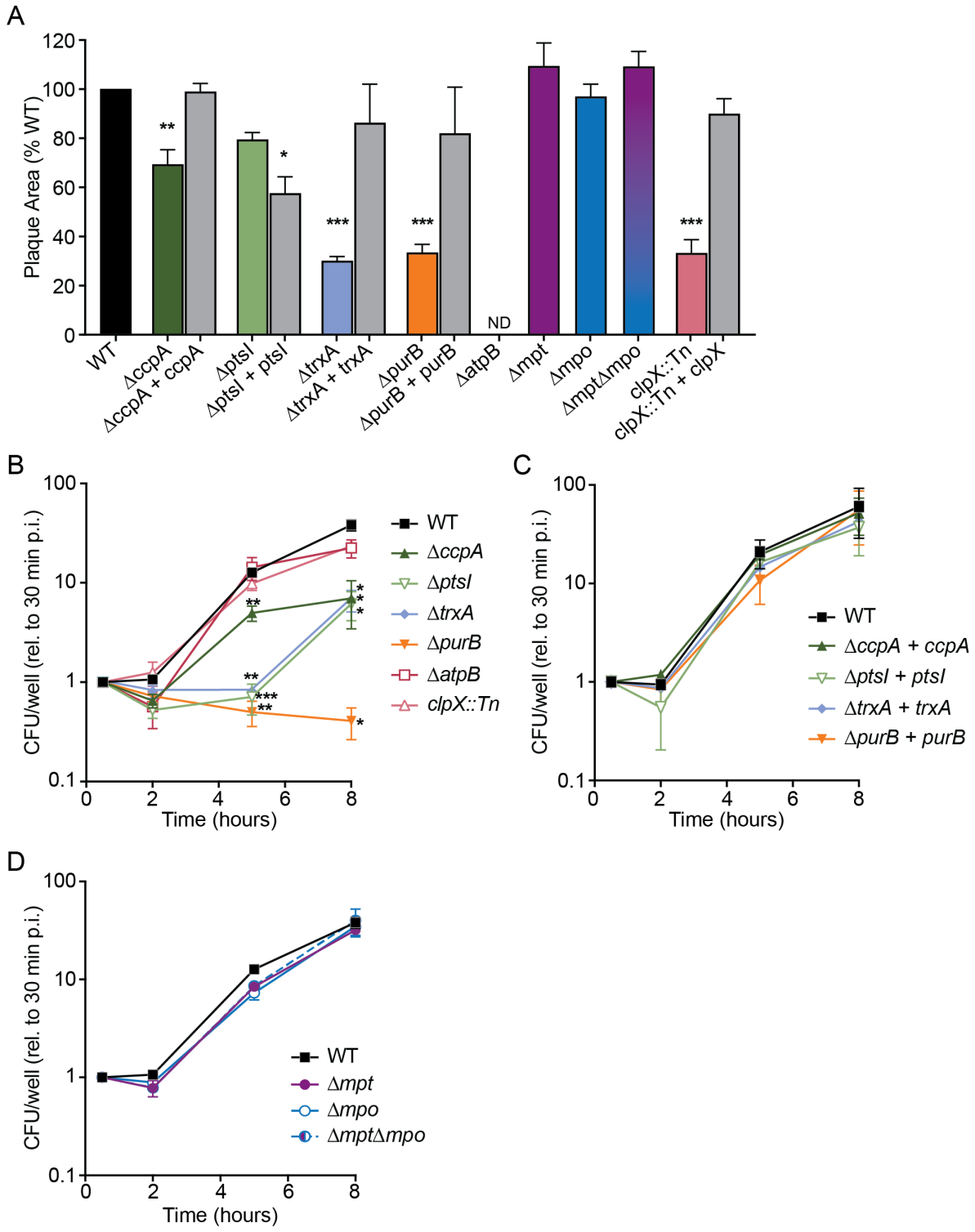

Figure 7. Intracellular replication and intercellular spread. (A) Plaque areas formed in L2 fibroblasts, measured as a percentage of WT *L. monocytogenes*. * $p < 0.05$, ** $p < 0.01$, *** $p < 0.001$, as determined by one-way ANOVA with multiple comparisons to the mean of WT. ND, not detected. (B-D) Intracellular growth of mutants in BMDMs, normalized to CFU at 30 minutes for each strain. * $p < 0.05$, ** $p < 0.01$, *** $p < 0.001$, as determined by Dunnett's multiple comparisons test compared to WT in each condition. Data

in panels A, B, and D are the means and SEMs of at least 3 independent experiments, and data in panel C are the means and SEMs of 2 independent experiments.

L. monocytogenes genes important in the NHP gallbladder are required for oral infection of mice

The Tn-seq screen identified many genes important for extracellular replication in an NHP gallbladder as well as intracellular growth and intercellular spread in murine cells. Thus, we hypothesized that these genes would be important for virulence in a mouse model of oral listeriosis. For these infections, 6-7 week old female BALB/c mice were given streptomycin in their drinking water for 2 days and fasted for 16 hours prior to infection to increase susceptibility to oral infection[7,54]. Mice were then fed 10^8 CFU of each *L. monocytogenes* strain via pipette. Body weights were recorded daily as a measurement of global disease severity. Mice infected with WT lost nearly 20% of their initial body weight throughout the 4 day infection, whereas mice infected with most of the mutant strains exhibited significantly less weight loss (Figures 8A and 8B). Notably, mice infected with Δ*ccpA*, Δ*mpo*, or Δ*mpt*Δ*mpo* lost approximately the same amount of weight as mice infected with WT, suggesting that that these genes may not be required for *L. monocytogenes* pathogenesis *in vivo*. Conversely, mice infected with Δ*ptsI*, Δ*trxA*, and Δ*purB* lost very little weight over the 4 day infection, suggesting that these strains were severely attenuated in their pathogenicity.

To assess bacterial burdens throughout infection, mice were euthanized and CFU were enumerated from organs at both 1 and 4 days post-infection (dpi). After ingestion, *L. monocytogenes* in the GI tract disseminates via the portal vein to the liver and subsequently the gallbladder. At 1 dpi, bacterial burdens in the livers and gallbladders were similar between WT and all mutant strains, indicating that these genes are not required for dissemination from the GI tract to the liver or gallbladder (Figures 8C and 8E). By 4 dpi, 7 of the 9 mutants displayed significantly decreased bacterial burdens in the gallbladder compared to WT (Figure 8D). Bacterial burdens in mice infected with Δ*ptsI*, Δ*purB*, and *clpX::Tn* were decreased by more than 300,000-fold compared to mice infected with WT. In contrast, bacterial loads of mice infected with Δ*trxA*, Δ*mpt*, Δ*mpo*, Δ*mpt*Δ*mpo*, and Δ*atpB* displayed more variability in CFU between animals and were decreased by 174- to over 38,000-fold compared to mice infected with WT. Interestingly, all mutants were significantly attenuated in the livers at 4 dpi, with the exception of Δ*ccpA* (Figure 8F). These data demonstrate that the majority of the *L. monocytogenes* genes identified by Tn-seq as important for colonization of NHP gallbladders *ex vivo* were also required for infection of murine gallbladders *in vivo.*

In addition to disseminating directly to the liver via the portal vein, *L. monocytogenes* disseminates from the GI tract via the lymphatics through the MLN and to the spleen[8]. Most mutants colonized the MLN and displayed similar bacterial burdens as WT at both 1 and 4 dpi, with the exception of Δ*ptsI*, Δ*purB*, and Δ*atpB*, which were significantly attenuated in the MLN compared to WT (Figures 9A and 9B). In the spleens, only Δ*ptsI,* Δ*purB,* Δ*mpt,* and *clpX::Tn* were significantly attenuated at 4 dpi compared to WT (Figure 8F). Bacterial burdens in the feces were also enumerated as a measure of *L. monocytogenes* colonization in the lower GI tract lumen. Bacterial burdens in the feces were similar between most mutants and WT at 1 dpi, whereas the majority of mutants exhibited significantly decreased bacterial loads compared to WT at 4 dpi

(Figures 9E and 9F). The notable exception is Δ*purB*, which was decreased ~150-fold compared to WT in the feces at 1 dpi, but similar to WT by 4 dpi. These data collectively demonstrate that the genes identified in our *ex vivo* screen contribute to infection of multiple organs, including the gallbladder, following oral infection of mice.

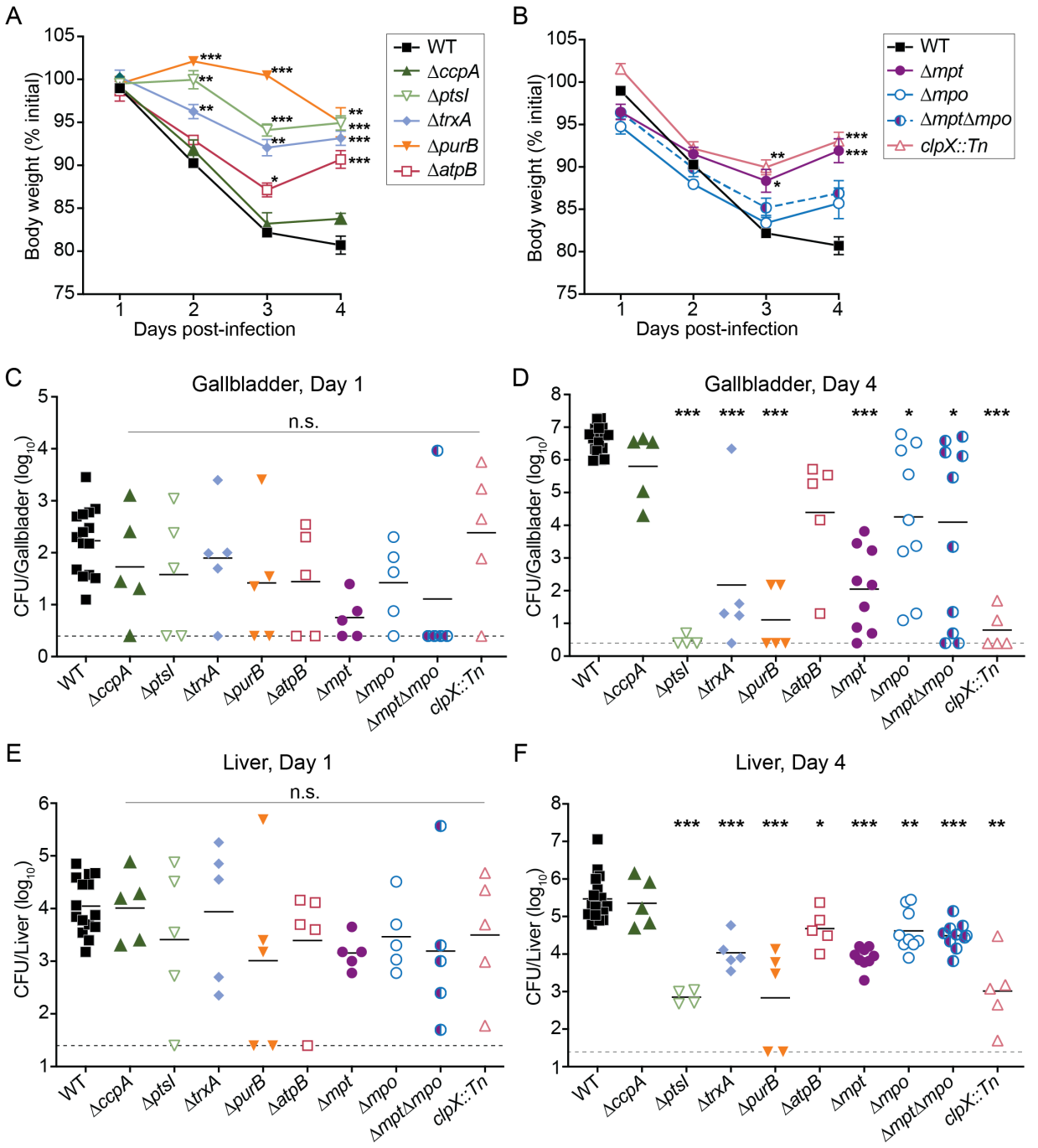

Figure 8. Murine model of oral listeriosis. Mice were orally infected with 10^8 of each *L. monocytogenes* strain. (A-B) Body weights of infected mice over time, reported as a percentage of initial weight before streptomycin treatment. Data are means and SEM of n=4-33. (C-F) CFU were enumerated from tissues at 1 or 4 days post-infection. Each data point represents a single mouse (n=15-18 for WT, n=4-10 for mutants),

horizontal solid lines represent geometric means, and the dotted lines represent the limit of detection. The data are combined from 4 independent experiments. * $p < 0.05$, ** $p < 0.01$, *** $p < 0.001$, as determined by Dunnett's multiple comparisons test compared to WT in each condition.

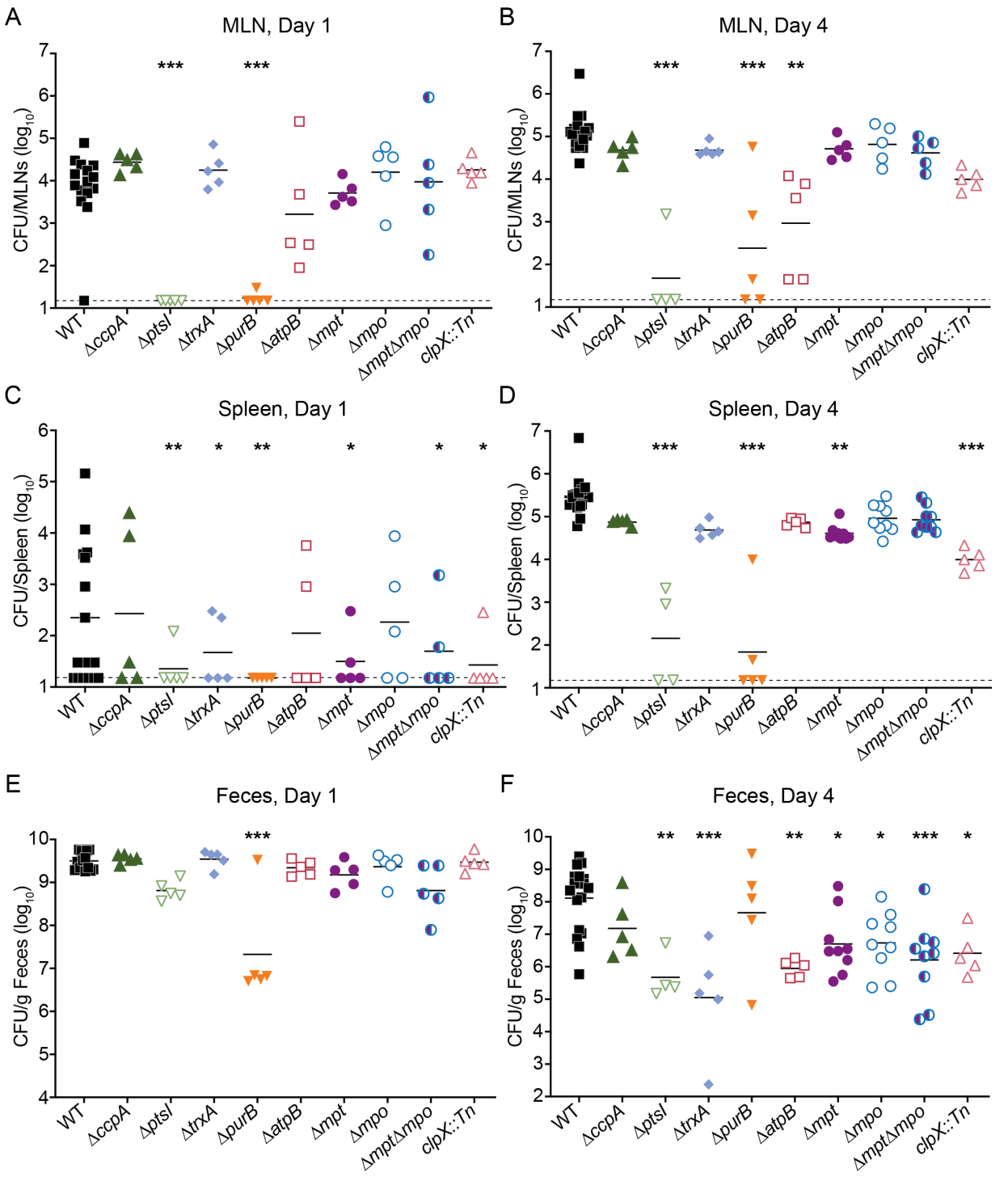

Figure 9. Dissemination after oral listeriosis. Mice were orally infected with 10^8 *Lm* 10403S strains and CFU from tissues were enumerated 1 and 4 days post-infection. Each data point represents a single mouse

(n=15 for WT, n=4-10 for mutants), horizontal solid lines represent geometric means, and the dotted lines represent the limit of detection. The data are combined from 4 independent experiments. * $p < 0.05$, ** $p < 0.01$, *** $p < 0.001$, as determined by Dunnett's multiple comparisons test compared to WT in each condition.

Discussion

In this study we sought to identify *L. monocytogenes* genes important for infection of the mammalian gallbladder. To this end, we developed an *ex vivo* bacterial colonization model of NHP gallbladders and performed Tn-seq to determine the genes necessary for growth and survival in this environment. This unbiased global genetic approach identified mutants in 43 genes that were significantly depleted after growth in the gallbladder condition, including some genes known to be important for virulence and others not previously studied in the context of infection. Several mutants identified by Tn-seq had growth defects in rich medium and most were predictably attenuated for growth in NHP bile *in vitro*. Many mutants also had defects in the intracellular lifecycle, including cytosolic growth and cell-to-cell spread, with the notable exception of the PTS permeases. A murine model of oral *L. monocytogenes* infection revealed that nearly all identified genes are required for full virulence. Together, these data identified genes that are important for *L. monocytogenes* infection of a mammal and, interestingly, not all are required for intracellular replication or intercellular spread.

Animal models have shed light on the importance of gallbladder colonization during *L. monocytogenes* pathogenesis. Murine models of infection demonstrated that *L. monocytogenes* replicates extracellularly in the gallbladder lumen to high bacterial densities and that this population becomes the primary bacterial reservoir and source of fecally shed *L. monocytogenes*[7,10,11]. Further, they revealed the presence of an uncharacterized severe within-host bottleneck in which the founding population of the gallbladder is limited to approximately 3 bacteria[10]. Dowd et al. demonstrated that *L. monocytogenes* readily grows in *ex vivo* porcine gallbladders and the extracted bile[28]. Given the limitations of using murine or porcine infection models for examining bacterial gallbladder colonization, and inspired by Dowd's use of *ex vivo* organs as incubators, we established a new infection model with a less restrictive bottleneck that is also amenable to Tn-seq analysis. While the present study focused on *L. monocytogenes* luminal growth within the organs, the *ex vivo* NHP gallbladder model could be utilized to measure mucosal and epithelial colonization of a variety of gallbladder-tropic pathogens.

Our Tn-seq screen identified mutants in dozens of genes that were significantly depleted after incubation in the NHP gallbladders. These genes include those involved in redox regulation (*trxA, yjbH, rex*), cell wall modifications (*walK*), and protein stability (*clpX*), consistent with the known antimicrobial activities of bile which result in cell envelope stress and protein damage[17]. Purine biosynthesis was previously identified as important for growth in porcine bile and we identified *purB* as essential for replication in the gallbladder[28]. Interestingly, the screen did not identify *mdrT*, *bsh*, *bilE*, or *sigB* as required for growth or survival in the gallbladder[20–22]. MdrT is a multidrug resistance transporter originally identified to secrete c-di-AMP[23,24] and subsequently suggested to be an efflux pump for cholic acid, a component of bile[25]. The *bsh* gene encoding bile salt hydrolase was originally described as required for survival in bile *in vitro* and for intestinal persistence in a guinea pig model of infection[20]. The bile exclusion system encoded by *bilE* was proposed to be a transporter that protected *L. monocytogenes* from toxicity induced by 30%

reconstituted bovine bile[22]. SigB is a stress response alternative sigma factor that positively regulates both *bsh* and *bilE*[21,22]. It is now appreciated that *bsh, bilE*, and *sigB* confer resistance to acidified bile acids, as may be found in the small intestine, but are not necessary to detoxify bile at neutral pH, as would be found in the gallbladder lumen[27,28]. Furthermore, BilE was recently renamed EgtU when it was conclusively demonstrated that it specifically binds and transports the low molecular weight thiol ergothioneine[26].

Some genes we identified by Tn-seq had been previously described as necessary for virulence *in vivo,* while many others had not been studied in the context of infection. The *purB, trxA, yjbH, clpX*, and *rex* genes are known to be required for full virulence, though some of the studies used different mouse strains and different inoculation methods[55–58]. Moreover, *rex* is one of the few *L. monocytogenes* genes specifically required for replication in the murine gallbladder[27]. Conversely, we identified genes encoding all 8 structural components of the F-type ATP synthase, which was not previously examined *in vivo*[52]. We also identified operons encoding two PTS EII complexes (*mpt, mpo*), as well as genes encoding their transcriptional (*sigL, manR*) and post-transcriptional regulators (*ptsH, ptsI*). Mpt and Mpo were previously designated as dispensable for virulence base on tissue culture assays, although were never tested *in vivo*[50].

Most mutants under investigation were deficient for growth in NHP bile *in vitro*, which was unsurprising given the conditions under which the Tn-seq screen was performed. The most attenuated strains after growth in bile were Δ*ptsI*, Δ*trxA*, and Δ*purB*, which also displayed growth defects in rich medium. Additionally, the Δ*atpB* strain was severely attenuated in BHI, which was expected based on the published requirement for the F-type ATP synthase for anaerobic replication[52]. In the aerobic condition, the cultures were incubated statically and we hypothesize that the lack of aeration led to Δ*atpB* growing more slowly than WT in BHI. Surprisingly, Δ*atpB* did replicate in NHP bile under anaerobic conditions. Future research will investigate the role of *atpB* in *L. monocytogenes* growth in bile and *in vivo*. It has been hypothesized that the F-type ATP synthase is required during anaerobic to combat acid stress and generate a proton motive force, not for ATP synthesis[52,59]. It remains unclear, however, if these mechanisms contribute to the role of the F-type ATP synthase during infection.

Tissue culture models of infection have historically been reliable indicators of *L. monocytogenes* pathogenesis *in vivo*, although the correlation was not as strong in this study. Several mutants displayed defects in a plaque assay, which measures both intracellular growth and intercellular spread over three days. Specifically, Δ*ccpA,* Δ*trxA,* Δ*purB*, and *clpX::Tn* formed significantly smaller plaques than WT. Despite this, Δ*ccpA* was surprisingly fully virulent in a murine model of listeriosis. Furthermore, *mpt* and *mpo* were completely dispensable for intracellular growth and intercellular spread in tissue culture, although they were required for infection of mice. Importantly, studies solely using tissue culture models of infection would not have identified these operons as important for pathogenesis *in vivo.*

To assess the validity of the *ex vivo* NHP gallbladder model, we evaluated the roles of genes identified by Tn-seq in an oral murine model of listeriosis. Nearly all mutants tested were significantly attenuated in the gallbladders and livers of infected mice 4 dpi. The notable exception was the strain lacking *ccpA,* the catabolite control protein A that represses transcription of metabolic genes based on the phosphorylation state of HPr and the overall nutrient status of the cell. In the Δ*ccpA* mutant, approximately 100 genes are de-repressed[60], resulting in attenuated *in vitro* growth in rich medium, bile, and BMDMs, yet exhibiting no virulence defect in mice after oral

infection. Interestingly, not all strains were attenuated in the spleens and MLNs of infected mice, suggesting that factors required for colonizing the liver and gallbladder are distinct from those needed to colonize other peripheral organs. For example, Δ*trxA* was attenuated approximately 29,000-fold in the gallbladder, but colonized the spleen and MLN at levels similar to WT, despite a significant growth defect in rich medium *in vitro*. Relatedly, it was recently reported that *L. monocytogenes* folate metabolism is specifically required in the livers but not the spleens of infected mice[49,61,62]. Conversely, Δ*ptsI* and Δ*purB* were significantly attenuated in the MLN at both 1 and 4 dpi, indicating that these genes are necessary for dissemination beyond the gut and/or replication in the MLN. Taken together, oral infections of mice revealed that the genes identified by Tn-seq in the NHP gallbladder have broader roles in disease pathogenesis than simply conferring resistance to bile stress.

Similarly to the gallbladders, most mutants were significantly attenuated in the feces at 4 dpi, supporting the notion that the gallbladder is the main source of fecally excreted bacteria[10]. The two mutants not attenuated in the feces were Δ*ccpA* and Δ*purB.* While Δ*ccpA* was fully virulent in mice, the Δ*purB* mutant was severely attenuated *in vitro* and in all murine organs after infection. These results indicate that purine biosynthesis is required for intracellular infection and virulence, but not for survival in the lumen of the lower GI tract, consistent with previous reports[56,58]. The factors influencing fecal shedding of *L. monocytogenes* are incompletely understood. Zhang et al. used a barcoded library of *L. monocytogenes* to demonstrate that the gallbladder is the source of fecally shed bacteria and that neutrophils and monocytes restrict bacterial dissemination to the gallbladder[10]. A subsequent study using a similar approach determined that the bacterial population in the feces was derived from the inoculum after infection with a severely attenuated strain of *L. monocytogenes*[7]. Thus, multiple factors contribute to fecal shedding during listeriosis, including the level of gallbladder colonization, *L. monocytogenes* virulence capacity, and the host immune response.

In summary, our Tn-seq approach identified dozens of *L. monocytogenes* genes required for replication in *ex vivo* gallbladders, and nearly all genes investigated *in vivo* were required for virulence during oral infection. This study revealed several novel insights into *L. monocytogenes* carbon metabolism during infection. It was previously thought that the glucose and mannose EI PTS proteins encoded by *mpt* and *mpo* were dispensable for virulence[50], but here we show that these operons are required for full virulence in an oral murine model of listeriosis. This study focused on a subset of genes identified in our *ex vivo* Tn-seq screen, and the many other genes identified are likely to reveal novel virulence factors and further our understanding of the *L. monocytogenes* multi-organ infection cycle.

Chapter 3: Investigating the roles of Rex and STING during *Listeria monocytogenes* oral infection

Introduction

The Tn-seq screen described in Chapter 2 identified a number of *L. monocytogenes* genes that are required for both replication in bile and for virulence in an oral murine model of infection. In addition to identifying genes involved in sugar transport and metabolism, the screen identified a number of genes important for combatting redox stress, such as *trxA* encoding thioredoxin, and *rex* encoding a redox-responsive transcriptional repressor. This result was interesting because the lab has previously characterized the role of Rex in *L. monocytogenes*[27]. The absence of Rex repression leads to increased expression of many genes, including those involved in fermentative metabolism. Unexpectedly, expression of virulence genes are also elevated in the Δ*rex* mutant, including bile salt hydrolase (*bsh*) and internalins A and B (*inlAB*)[27]. As expected, Δ*rex* exhibits higher tolerance to bile than WT due to increased *bsh* expression. However, despite being highly resistant to bile stress, the Δ*rex* mutant is attenuated in the gallbladder during oral infection, highlighting that bile resistance alone is not sufficient for full virulence in this organ. In addition, infection with Δ*rex* caused less severe disease than WT as measured by weight loss[27], further emphasizing the importance of gallbladder colonization in systemic virulence. Because Δ*rex* lacks *in vitro* growth defects that could explain its decreased gallbladder colonization and overall attenuation *in vivo,* we hypothesized that the host immune response plays a role in clearing *L. monocytogenes* from the gallbladder, and that lack of transcriptional repression by Rex either exacerbates or renders *L. monocytogenes* unable to evade this response.

L. monocytogenes can stimulate an immune response by activating the host protein STING, which then induces IFN-β expression. There are two mechanisms by which *L. monocytogenes* can activate STING during intracellular infection: 1) bacteriolysis leads to the host protein cGAS binding cytosolic DNA, leading to production of cGAMP, which binds STING, and 2) *L. monocytogenes* produces and secretes CDA, which directly binds STING (Figure 2). The primary mechanism of CDA secretion by *L. monocytogenes* is via the multi-drug resistance transporter, MdrT, a transmembrane protein that exports CDA[23,25]. Expression of *mdrT* is repressed by the regulatory protein TetR, and consequently *L. monocytogenes* mutants lacking *tetR* secrete increased CDA and induce a potent IFN-β response[24].

Repression of *mdrT* transcription by TetR is reportedly alleviated in the presence of cholic acid, a deconjugated bile acid[25]. The Δ*rex* mutant expresses increased transcripts encoding bile salt hydrolase (*bsh*)[27], whose function is converting conjugated bile acids into deconjugated bile acids, such as cholic acid. Based on these known mechanisms, we proposed the following model: The Δ*rex* mutant overexpresses *bsh* compared to WT, even in the absence of bile[27]. Therefore, when Δ*rex* is exposed to bile acids, as in the gallbladder lumen, increased *bsh* expression leads to increased production of deconjugated bile acids, which in turn relieves repression of *mdrT* expression by TetR. Increased production of MdrT leads to an increase in CDA secretion, which, during infection, leads to direct activation of STING (Figures 2 and 10). Finally, the resulting downstream immune activation results in more rapid bacterial clearance.

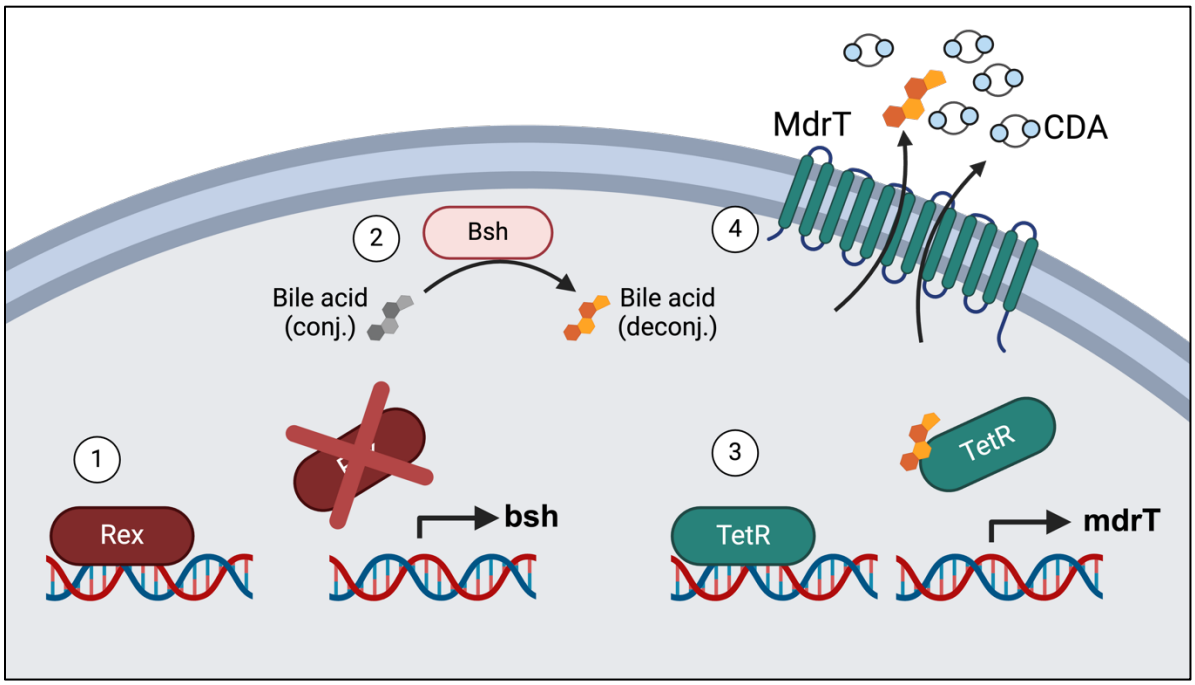

Figure 10. Hypothesized mechanism of immune activation by *L. monocytogenes* Δ*rex* during murine infection. 1) Absence of transcriptional repression by Rex leads to increased expression of *bsh*, encoding bile salt hydrolase. 2) Bsh converts conjugated bile acids to deconjugated bile acids. 3) Deconjugated bile acids, such as cholic acid, bind TetR, leading to release from the *mdrT* promoter and allowing transcription. 4) Increased MdrT production leads to increased secretion of CDA and bile acids. Secreted CDA then activates STING, leading to IFN-β expression (Figure 2).

The goal of experiments presented here is to better understand both bacterial and host factors necessary for survival and replication in the gallbladder. This chapter describes unpublished work investigating the roles of the *L. monocytogenes* transcriptional regulator Rex and the host signaling protein STING during murine oral infection. First, I measured IFN-β expression in response to intracellular infection with Δ*rex* in WT, *cGas*$^{-/-}$, and *Sting*$^{-/-}$ macrophages. To characterize a potential mechanism of this immune activation, transcriptional changes in response to bile and CDA secretion by the Δ*rex* mutant were measured *in vitro.* Finally, I evaluated the role of STING during infection with Δ*rex* using an oral infection model in *Tmem173*$^{-/-}$ mice, which lack STING. While I performed the vast majority of experiments presented here, Dr. Cortney Halsey and Dr. Michelle Reniere conceived of the study, mouse breeding was carried out by Shania Leano, and histology scoring was performed by Dr. Jessica Schneider.

Results

L. monocytogenes mutant Δ*rex* induces an elevated interferon response during intracellular infection

We hypothesized that Δ*rex* induces an elevated type I IFN response due to increased secretion of CDA in the host cytosol (Figure 10). To test this hypothesis, I measured host IFN-β production in WT, *cGas*$^{-/-}$, and *Sting*$^{-/-}$ bone marrow-derived macrophages (BMDMs) in response to *L. monocytogenes* infection. The *L. monocytogenes* strains used in these infections were WT, Δ*rex*, Δ*rex* + *rex*, *tetR::Tn*, Δ*rex tetR::Tn*, and Δ*mdrMTAC*. The *tetR::Tn* strain, which has been shown to induce a robust IFN-β response in macrophages[24] served as a positive control. Conversely, Δ*mdrMTAC* does not secrete any CDA[63], therefore inducing no IFN-β expression, and serves as a negative control. To determine whether the regulators Rex and TetR act synergistically to repress CDA secretion, a Δ*rex tetR::Tn* double mutant was included in these experiments.

The WT, *cGas*$^{-/-}$, and *Sting*$^{-/-}$ BMDMs were inoculated with the 6 *L. monocytogenes* strains for 30 minutes, after which medium containing gentamicin was added to the cells to kill remaining extracellular bacteria. The cells were then incubated for a total of 6 hours, then samples of supernatants were collected from each condition. Supernatants were then applied to ISRE-L929 reporter cells[24], which produce luciferase in response to IFN-β stimulation, and relative luminescence is reported as a proxy measurement of IFN-β protein abundance. WT BMDMs infected with Δ*rex* produced increased IFN-β compared to those infected with WT, indicating that Δ*rex* induces increased IFN-β, and the complement strain Δ*rex* + *rex* induced similar IFN-β production to WT (Figure 11A). As expected, the strains lacking *tetR* induced a potent IFN response compared to WT, and Δ*mdrMTAC* induced little to no IFN-β. Interestingly, the *tetR::Tn* and Δ*rex tetR::Tn* strains induced similar levels of IFN-β, suggesting that TetR and Rex regulate CDA secretion via the same pathway, not separate but synergistic pathways. The IFN-β induced in *cGas*$^{-/-}$ BMDMs was similar to WT BMDMs, which supports the hypothesis that IFN-β production is not induced by *L. monocytogenes* lysing in the cytosol. Infection of *Sting*$^{-/-}$ BMDMs resulted in very little or no IFN-β expression, which supports our hypothesis that Δ*rex* induces increased IFN-β production in a STING-dependent manner.

To further investigate whether the transcriptional regulators TetR and Rex act synergistically to reduce induction of IFN-β, I measured IFN-β transcripts (ifnb) produced by BMDMs following *L. monocytogenes* infection. While the ISRE assay allows for measuring IFN-β protein production in a high throughput manner, one major limitation to this method is that luminescence can have a relatively low upper-limit of detection. In contrast, measuring transcript-level expression by quantitative RT-qPCR is lower throughput, but has a wider range of detection and is thereby more precise. To measure IFN-β transcripts, I infected BMDMs in the same manner as for the ISRE assays described above, and harvested RNA from the BMDMs after 6 hours of infection. Analysis by RT-qPCR revealed that IFN-β expression at the transcript level exhibited similar trends to IFN-β protein production shown by ISRE assay (Figure 11B). RT-qPCR also revealed similar IFN-β transcript abundances in WT and *cGas*$^{-/-}$ BMDMs following infection, but no detectable IFN-β transcripts in the *Sting*$^{-/-}$ BMDMs. RT-qPCR also showed that in all BMDM

genotypes, the *tetR::Tn* and Δ*rex tetR::Tn* strains induced similar levels of IFN-β transcripts. Taken together, these experiments support our hypothesis that intracellular Δ*rex* induces an elevated immune response that is cGAS-independent and STING-dependent.

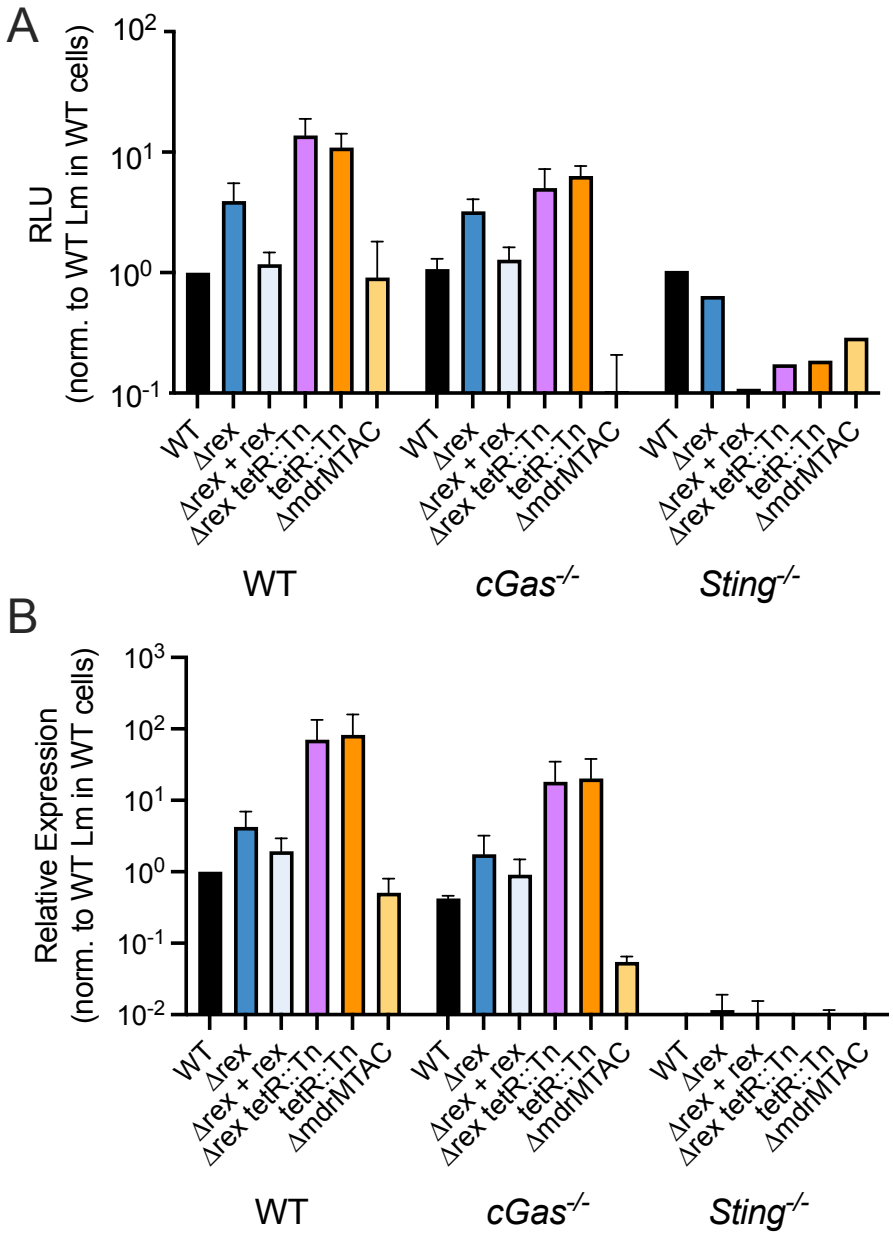

Figure 11. *L. monocytogenes* Δ*rex* induces an IFN-β response in a STING-dependent manner. IFN-b production by BMDMs in response to intracellular infection with *L. monocytogenes* strains as measured by (A) interferon-stimulated response element (ISRE) L929 cells that produce luciferase in response to type-I interferon stimulation; RLU: relative luminescence units (WT and *cGas*$^{-/-}$: n=3; *Sting*$^{-/-}$: n=1), and (B) quantitative RT-qPCR (n=2).

Neither Rex nor Bsh is necessary for bile-induced *mdrT* transcription

I next investigated whether the increased IFN-β production induced by Δ*rex* is related to expression of the CDA export protein MdrT, and whether MdrT expression is further increased upon exposure to bile. To test this, I measured mdrT transcripts produced by Δ*rex* compared to WT in response to bile using RT-qPCR. The *tetR::Tn* and Δ*mdrMTAC* strains were used as positive and negative controls for mdrT transcript production, respectively. We hypothesized that Δ*rex* would express increased mdrT due to increased bile salt hydrolase (Bsh) activity, therefore a Δ*bsh* mutant was also included in these experiments to determine the role of *bsh* in mdrT expression. *L. monocytogenes* strains were grown to mid-log, then incubated with 0.1% reconstituted porcine bile. Samples were collected at baseline (immediately before bile added; 0 min) and 10 and 30 minutes after addition of bile.

Consistent with previous reports[25], WT *L. monocytogenes* expressed increased mdrT transcripts both 10 and 30 minutes after addition of 0.1% porcine bile, resulting in 10- to 20-fold increases in mdrT expression over time (Figure 12A). The *tetR::Tn* strain expressed at least 100-fold more mdrT than WT both before and after bile treatment and the Δ*mdrMTAC* strain expressed no mdrT, as expected. The Δ*rex* mutant produced increased mdrT transcripts following bile treatment, but not to the same magnitude as WT (Figure 12A). The Δ*bsh* mutant expressed similar levels of mdrT as WT, suggesting that Bsh activity is not required for mdrT expression (Figure 12A). These experiments were also performed using 1.1% porcine bile, which resulted in similar transcriptional changes as treatment with 0.1% bile (data not shown). Overall, these data contradict our hypothesis that Δ*rex* expresses increased mdrT compared to WT.

In our model hypothesis we propose that Δ*rex* expresses increased mdrT due to overexpression of bsh (Figure 10). I therefore measured bsh transcripts to determine whether Δ*rex* expresses increased bsh under these conditions. The WT and Δ*rex* strains expressed similar bsh transcripts at baseline and 10 minutes following bile treatment, indicating that lack of transcriptional repression by Rex is insufficient to induce bsh overexpression (Figure 12B). After 30 minutes of bile treatment, Δ*rex* expression of bsh increased 70-fold, while WT expression increased 10-fold compared to baseline. These results suggest that both de-repression by Rex and activation by bile contribute to increased bsh expression (Figure 12B).

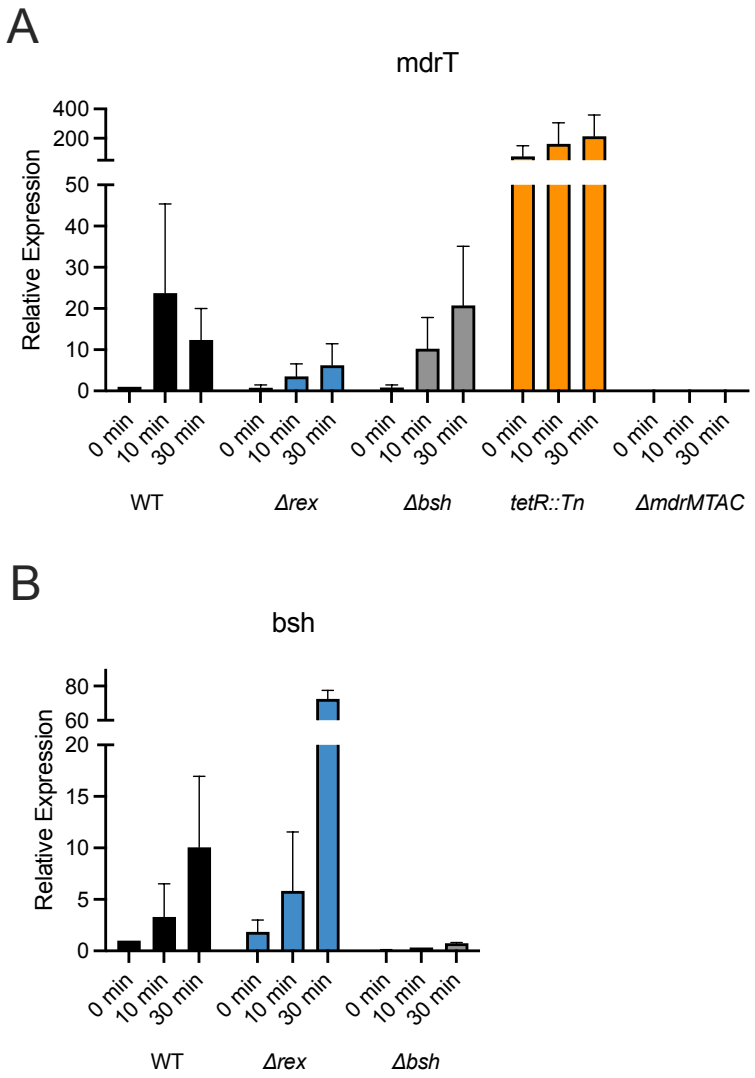

Figure 12. Transcriptional changes by Δ*rex* in response to bile. *L. monocytogenes* strains were grown to mid-log in BHI, then incubated with 0.1% reconstituted porcine bile. Samples were collected immediately before bile was added (0 min), 10 min, and 30 min after addition of bile. Relative expression was measured via RT-qPCR, with rpoB transcripts used as the endogenous control, and normalized to WT expression at 0 min. Bars represent averages of n=2, error bras represent SEMs.

Rex-deletion does not induce increased CDA production in the absence of bile

I have shown that Δ*rex* does not express elevated levels of mdrT transcripts in response to bile treatment. *L. monocytogenes* encodes additional exporters, in addition to MdrT, that contribute to CDA secretion. To directly quantify the CDA produced and secreted by *L. monocytogenes,* I used a luciferase-based detection assay[64]. WT, Δ*rex*, and Δ*rex* + *rex* strains were grown in BHI, samples were collected during exponential and stationary phases of growth, and the samples were then centrifugated to separate the cellular and supernatant fractions. The cellular fraction represents CDA contained within the bacterial cells, while the supernatant fraction represents secreted CDA. Exponential phase cultures of WT and Δ*rex* contained similar levels of

CDA in the cellular fraction, and Δ*rex* cultures contained slightly higher amounts of CDA compared to WT in the supernatants (Figure 13A and 13B). The complement strain Δ*rex* + *rex* contained substantially decreased CDA compared to WT in the cellular fraction, but similar levels of CDA in the supernatant. In the stationary phase cultures, all three strains contained similar amounts of CDA in both cellular and supernatant fractions (Figure 13C and 13D). This result is consistent with Δ*rex* expressing similar levels of mdrT as WT during exponential broth growth in the absence of bile. Taken together, these results do not support our hypothesis that Δ*rex* secretes excess CDA during infection. It remains possible that Δ*rex* secretes excess CDA in the presence of bile or during intracellular infection; CDA production and secretion will be quantified under these conditions in future experiments.

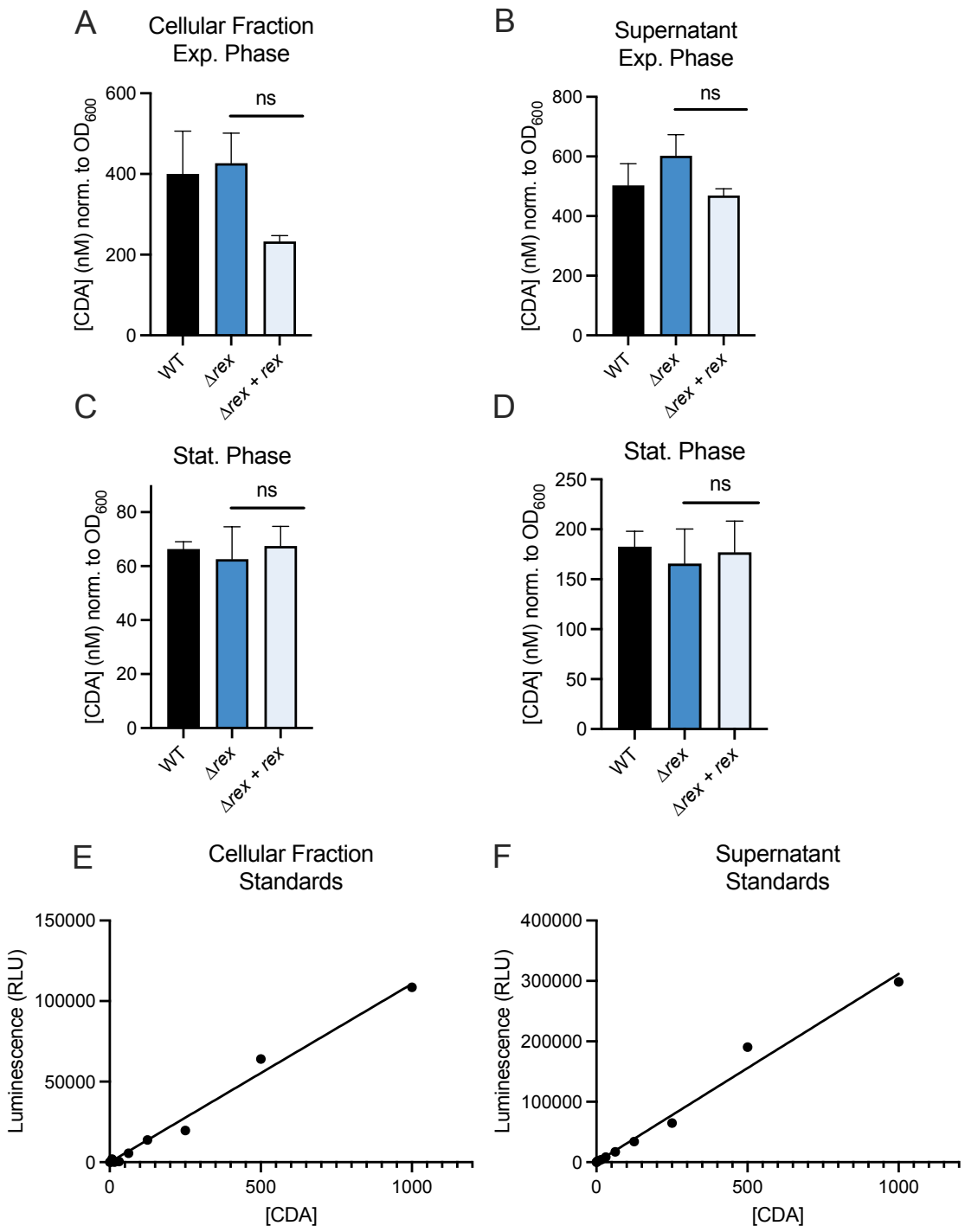

Figure 13. CDA production by Δ*rex* during growth in BHI. (A-D) *L. monocytogenes* strains were grown to either exponential or stationary growth phases. CDA concentrations was measured from cellular (A and C) and supernatant fractions (B and D) using the CDA-Luc assay, and normalized to bacterial density as measured by OD_{600}. Bars represent averages of n=3, error bars represent SEMs. Statistical significance was determined by one-way ANOVA with multiple comparisons to the mean of WT; ns: not significant. (E-F) CDA standards used for calculating sample CDA concentrations. Solid line represents simple linear regression of standards.

Oral infection with *L. monocytogenes* Δ*rex* results in pathology distinct from infection with WT

The experiments presented in this chapter so far have shown that Δ*rex* induces increased IFN-β expression during intracellular infection *in vitro.* We next wanted to determine if Δ*rex* induces an increased immune response *in vivo* following oral infection of mice. More specifically, we wanted to test whether infection with Δ*rex* leads to increased recruitment of immune cells to the gallbladder. To determine if Δ*rex* induces an increased immune response *in vivo*, we collaborated with the UW Histology and Imaging Core (HIC) to visualize the impact of infection with *L. monocytogenes* on immune cell recruitment to the gallbladder and liver. To this end, I orally inoculated BALB/c mice with WT, Δ*rex*, or PBS (uninfected), and harvested livers with gallbladders still attached 4 days post-infection. Harvested tissues were then fixed in 10% formalin, then transferred to the HIC for further processing, slide preparation, and H&E or antibody staining. To maintain structural integrity of the organs, gallbladders remained attached to livers throughout processing, and liver tissue was included in the slide sections. Slides were stained with antibodies raised against F4/80, a macrophage marker, and Ly6B, a surface protein present on most neutrophils and some activated macrophages. Stained slides were de-identified and scored by veterinary pathologist Dr. Jessica Schneider. Scoring categories included inflammation and presence of positive antibody staining, which would indicate recruitment of immune cells to the tissue.

Blinded scoring showed that infection with WT *L. monocytogenes* induced inflammation in both the liver and gallbladder compared to uninfected controls (Figure 14A and 14D). Additionally, livers infected with WT displayed increased F4/80 and Ly6B staining compared to uninfected tissues, indicating increased abundance of macrophages and neutrophils (Figures 14B and 14C). Inflammation and immune cell abundance in the livers of mice infected with Δ*rex* were elevated compared to uninfected controls, but were decreased compared to those infected with WT. The Δ*rex* mutant resulted in pathology more closely resembling uninfected controls in gallbladder inflammation, but more closely resembling WT in gallbladder F4/80 staining (Figure 14E). Positive Ly6B staining was not detected in any gallbladder samples, suggesting that neutrophils were not present in the gallbladder at this time of infection.

Taken together, these data suggest that infection with Δ*rex* results in less inflammation and fewer immune cells recruited to the liver and gallbladder compared to infection with WT, which do not support our model hypothesis that Δ*rex* induces increased inflammation during murine infection. It is possible that Δ*rex* is cleared so rapidly following oral infection that 4 days post-infection is too late to detect evidence of an elevated immune response. Future studies will screen for inflammatory markers earlier during infection, such as 2 days post-infection, to determine the timing of immune responses to the gallbladder following *L. monocytogenes* oral infection.

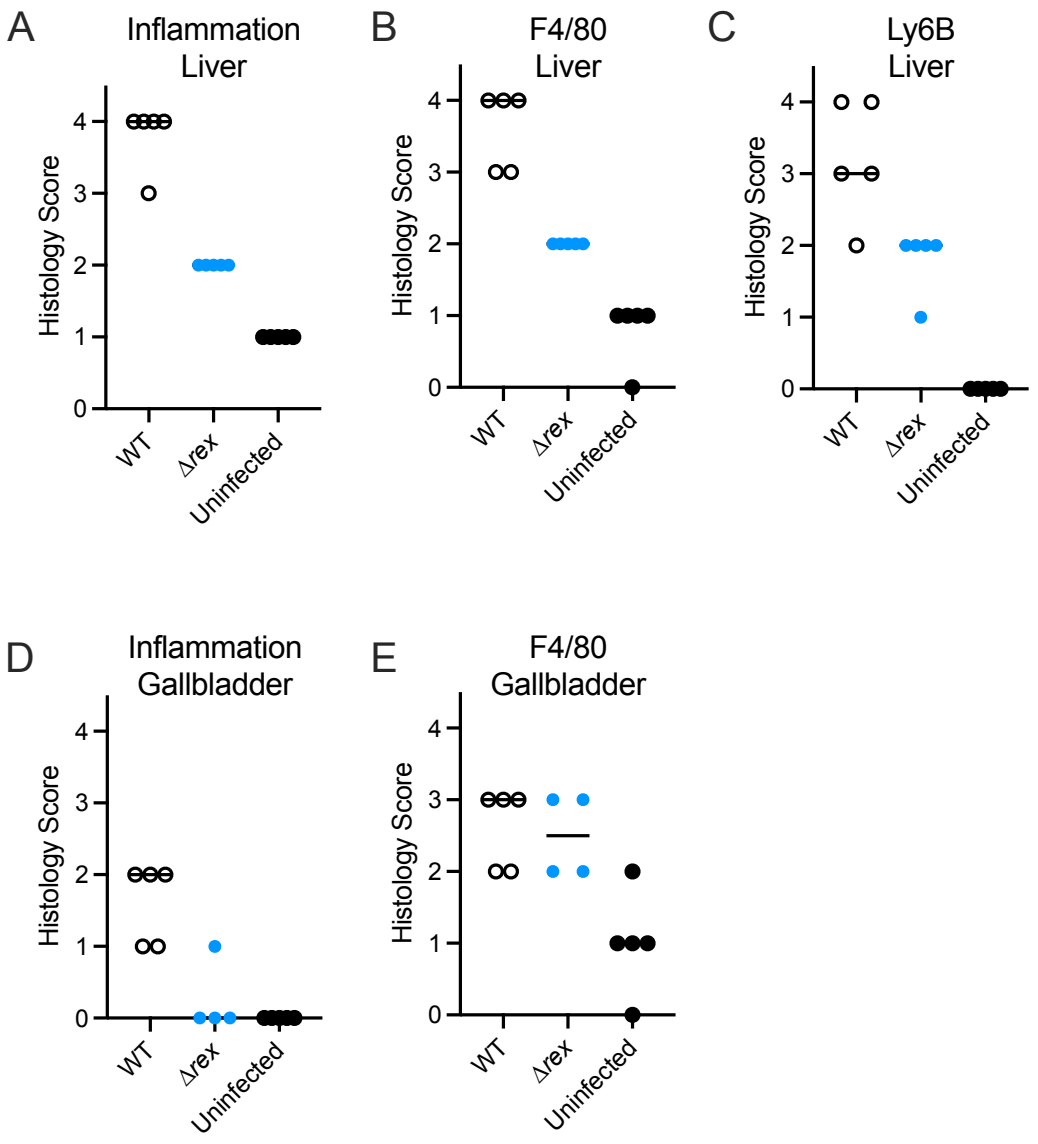

Figure 14. Blinded scoring of tissues following *L. monocytogenes* oral infection. BALB/c mice were orally inoculated with 10^8 of each *L. monocytogenes* strain, or PBS (Uninfected). 4 days post-infection, livers and gallbladders were collected, fixed, stained, and then scored in a single-blinded manner. F4/80, macrophage marker; Ly6B, neutrophil marker.

Attenuation of Δ*rex in vivo* is partially rescued in the absence of STING

I have shown that Δ*rex* induces increased IFN-β during macrophage infection in a STING-dependent manner, but does not express increased mdrT transcripts or secrete increased CDA compared to WT during growth in BHI. However, it remains possible that these transcriptional changes are context dependent, therefore measuring differences in *mdrT* expression during broth growth may not represent changes that occur during replication in the host cytosol. Before measuring transcriptional changes or CDA concentrations during intracellular infection *in vitro*, I

first tested whether STING plays a role during murine infection with Δ*rex in vivo*. To this end, both WT (B6) and *Tmem173*$^{-/-}$ mice were orally inoculated with either *L. monocytogenes* WT or Δ*rex*, and organs were harvested for CFU enumeration 5 days post-infection. Importantly, this was the first infection of B6 mice with Δ*rex* and we predicted similar phenotypes as in the BALB/c mice used previously[27]. I hypothesized that in *Tmem173*$^{-/-}$ mice, bacterial loads would be similar between mice infected with WT and Δ*rex L. monocytogenes*, indicating rescue of Δ*rex* virulence. This result would be consistent with the hypothesis that Δ*rex* induces a more potent, STING-dependent immune response than WT *L. monocytogenes,* leading to more rapid clearance from infected tissues.

Consistent with previous infections of BALB/c mice, B6 mice infected with Δ*rex* lost little to no bodyweight throughout the 5 day infection, whereas B6 mice infected with B6 lost 10-20% of their bodyweight (Figure 15A). This indicates that infection with Δ*rex* leads to significantly less severe disease than infection with WT. In contrast, the *Tmem173*$^{-/-}$ mice did not lose any bodyweight following infection with either *L. monocytogenes* strain, despite these mice harboring substantial bacterial burdens. This result meant that we could not compare overall disease severity of *Tmem173*$^{-/-}$ mice infected with WT vs. Δ*rex*, and suggested that colonization dynamics following oral infection could be different between mouse backgrounds.

Infection of B6 mice with Δ*rex* resulted in significantly decreased bacterial burdens in the spleens, livers, and gallbladders compared to B6 mice infected with WT (Figure 15), consistent with previous work showing that Δ*rex* is attenuated in BALB/c mice[27]. In contrast, we observed no differences in bacterial burdens in the livers, ceca, and feces of *Tmem173*$^{-/-}$ mice infected with WT or Δ*rex*, suggesting that STING is required for the attenuation of Δ*rex* seen in B6 mice (Figure 15B, 15F-G). In the MLN, Δ*rex* had decreased bacterial loads compared to WT, but the magnitude of difference between WT and Δ*rex* was much less pronounced in the *Tmem173*$^{-/-}$ mice than the B6 mice (Figure 15E). Unfortunately, neither WT nor Δ*rex* colonized the gallbladders of the *Tmem173*$^{-/-}$ mice, and therefore gallbladder colonization differences between *L. monocytogenes* strains in this animal model could not be evaluated (Figure 15C).

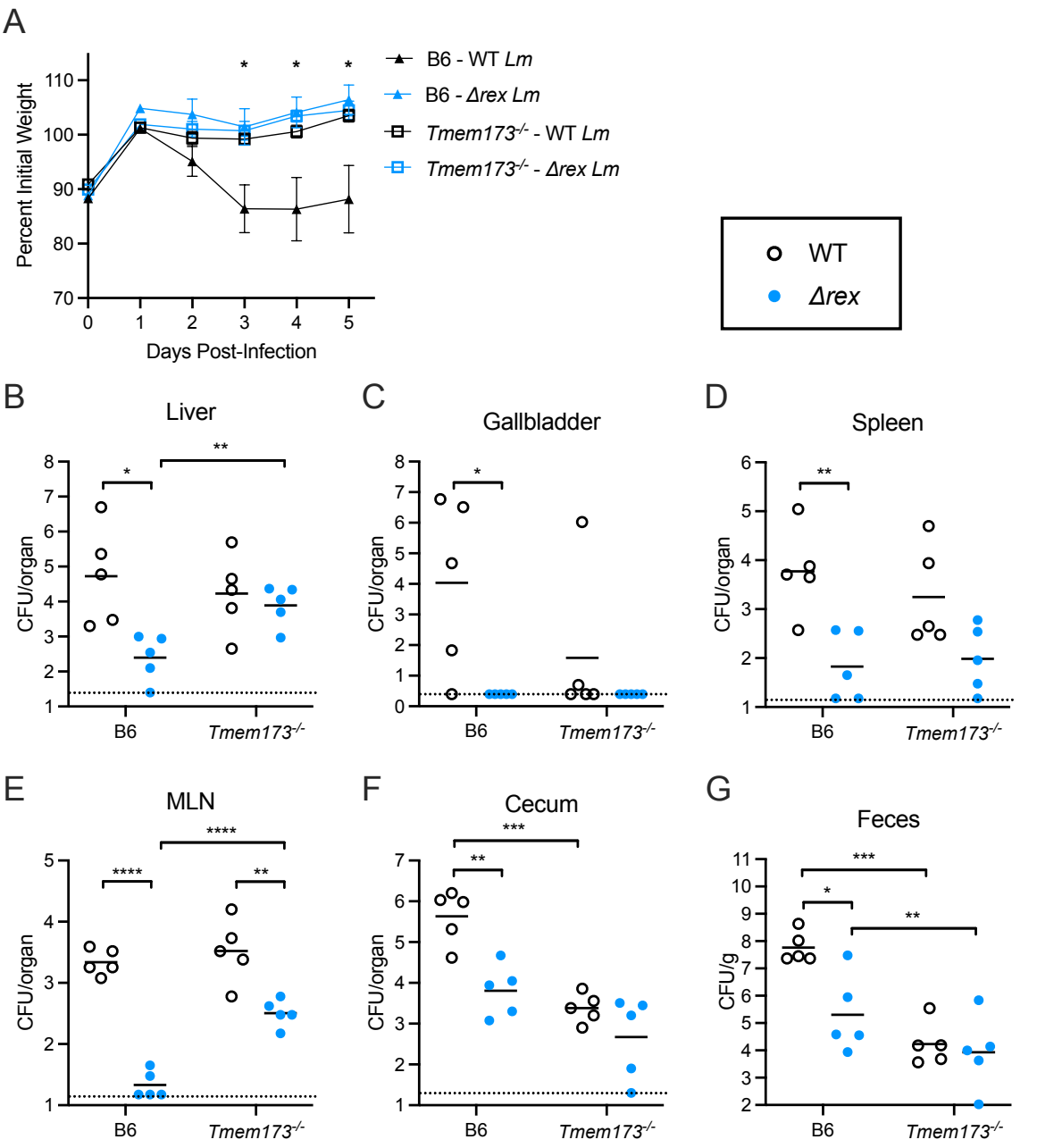

Figure 15. Attenuation of Δ*rex* during oral infection is STING-dependent. B6 and *Tmem173*$^{-/-}$ mice were orally infected with 10^8 of each *L. monocytogenes* strain. (A) Body weights of infected mice over time, reported as a percentage of initial weight before streptomycin treatment. Data are means and SEM of n=5. (B-G) CFU were enumerated from tissues at 5 days post-infection. Each data point represents a single mouse (n=5 per group). Open circles indicate mice infected with WT *L. monocytogenes*; closed blue circles indicate infection with Δ*rex*. Horizontal solid lines represent geometric means. Dashed lines indicate limit of detection. * $p < 0.05$, ** $p < 0.01$, *** $p < 0.001$, as determined by two-tailed t-tests.

Mice lacking STING exhibit distinct colonization dynamics following oral infection

Neither WT nor Δ*rex L. monocytogenes* strains colonized the gallbladders of *Tmem173*$^{-/-}$ mice after oral infection (Figure 14C), which meant that the combined roles of Rex and STING in gallbladder colonization could not be evaluated. Previous studies have shown that a different STING-deficient mouse strain *Sting*$^{Gt/Gt}$ is more susceptible to *L. monocytogenes* oral infection than B6 mice, as evidenced by increased weight loss and increased bacterial loads in the livers, spleens, and MLN compared to B6 mice[65]. It was therefore surprising that our *Tmem173*$^{-/-}$ mice lost no bodyweight and exhibited similar bacterial loads in the livers, spleens, and MLN as WT mice following oral infection (Figure 15). Both the *Tmem173*$^{-/-}$ and *Sting*$^{Gt/Gt}$ mouse strains lack functional STING, but the *Tmem173*$^{-/-}$ mice used in this study were derived via targeted chromosomal deletion[66,67], and the Gt mice via chemical mutagenesis[68].

The data presented in Figure 15 represent the first *L. monocytogenes* oral infections of *Tmem173*$^{-/-}$ mice, therefore it is possible that the timing of colonization and dissemination differs between STING-deficient mouse strains. To establish oral infection dynamics in the *Sting*$^{-/-}$mouse background compared to B6 mice, I orally infected B6 and *Tmem173*$^{-/-}$ mice with WT *L. monocytogenes* and harvested tissues at 1, 3, 5, and 7 dpi. Because B6 mice infected with *L. monocytogenes* typically reach euthanasia criteria after 5 days of infection, only the *Tmem173*$^{-/-}$ mice were taken out to 7 days. As seen previously, *Tmem173*$^{-/-}$ mice did not lose any weight during infection (Figure 16A). In all organs collected from the *Tmem173*$^{-/-}$ mice, bacterial burdens peaked at 5 dpi and decreased between 5 and 7 dpi, suggesting *Tmem173*$^{-/-}$ mice begin to clear the infection after day 5 (Figure 16B-F). Comparing bacterial burdens in B6 and *Tmem173*$^{-/-}$ mice suggests that *L. monocytogenes* does have different colonization phenotypes in the two mouse strains. We observed decreased bacterial burdens in the ceca and feces of *Tmem173*$^{-/-}$ mice compared to WT throughout the 7 day time course (Figure 16E-F), which suggests that STING is involved in *L. monocytogenes* infection of the GI tract. Interestingly, bacterial burdens in the livers, spleens, and MLN were similar between mouse backgrounds throughout the time course, suggesting that STING is not involved in mediating dissemination out of the GI tract (Figure 16B-E). Most importantly, bacterial burdens in the gallbladders of *Tmem173*$^{-/-}$ mice were predominantly below the limit of detection throughout the time course, demonstrating that this animal model is not appropriate for studying gallbladder colonization following oral infection (Figure 16C).

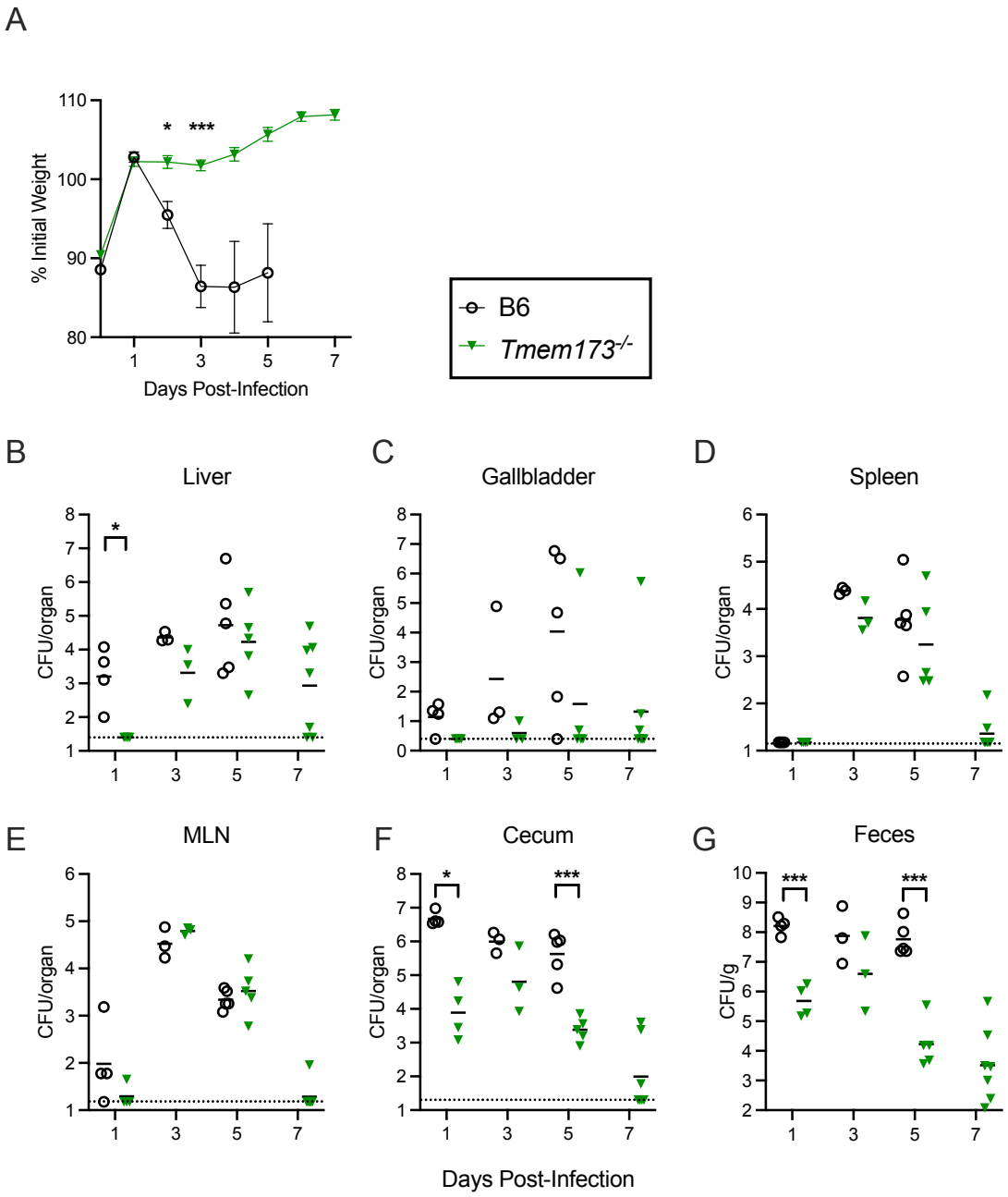

Figure 16. Oral infection dynamics in *Tmem173*$^{-/-}$ mice. B6 and *Tmem173*$^{-/-}$ mice were orally infected with 10^8 of each *L. monocytogenes* strain. (A) Body weights of infected mice over time, reported as a percentage of initial weight before streptomycin treatment. Data are means and SEM of n=5-19. (B-G) CFU were enumerated from tissues. Each data point represents a single mouse (n=3-7), horizontal solid lines represent geometric means, dotted lines represent limit of detection. The data are combined from 3 independent experiments, where Days 1 and 3 were collected in the same experiment, and Day 5 and Day 7 were each collected in separate experiments. Day 5 data is the same as previously shown in Figure 14. B6 mice were infected for max. 5 days, as they reach euthanasia criteria after this time point. * $p < 0.05$, *** $p < 0.001$, as determined by two-tailed t-tests.

Discussion

The *L. monocytogenes* Δ*rex* mutant exhibits increased resistance to bile stress *in vitro*, yet is attenuated for virulence and yielded significantly decreased bacterial loads in the gallbladder following oral infection of mice. In this chapter, I tested a model hypothesis in which Δ*rex* secretes excess CDA in response to bile exposure, leading to an increase in STING-dependent IFN-β expression and more rapid clearance by the host immune response. In support of this hypothesis, I found that Δ*rex* induced IFN-β expression during intracellular infection in a STING-dependent, cGAS-independent manner. However, Δ*rex* did not express elevated mdrT in response to bile and did not secrete increased CDA compared to WT *in vitro*. Histology of livers and gallbladders of infected BALB/c mice showed that *L. monocytogenes* WT and Δ*rex* exhibit varying pathologies during murine oral infection, but there was no evidence that Δ*rex* induced an elevated immune response compared to WT. Finally, oral infections of B6 and *Tmem173*$^{-/-}$ mice with WT and Δ*rex L. monocytogenes* demonstrated that Δ*rex* was less attenuated compared to WT in the absence of host STING. Taken together, these data support the hypothesis that STING is indeed involved in the attenuation of Δ*rex* during oral infection, but the mechanisms underlying this attenuation remain unclear.

L. monocytogenes is well known to induce IFN-β expression via activation of STING during intracellular infection[24,29], and we show here that the Δ*rex* mutant induces a more robust IFN-β response than WT (Figure 10). The Δ*rex* mutant exhibits similar intracellular replication dynamics as WT[27] and induced IFN-β expression in a cGAS-independent manner, therefore we hypothesized that Δ*rex* induces an elevated IFN-β response due to elevated CDA secretion directly activating STING. However, Δ*rex* did not produce increased transcripts of the CDA exporter mdrT compared to WT in the presence or absence of porcine bile *in vitro* (Figure 11). The Δ*rex* mutant also secreted similar amounts of CDA to WT during growth in BHI, but whether this changes with addition of bile still needs testing (Figure 12). Additionally, it is possible that *L. monocytogenes* expresses increased mdrT or secretes elevated CDA in the host cytosol, which will be investigated in future experiments. Even if secreted CDA by Δ*rex* is indeed elevated during intracellular growth, it is still unclear why this would lead to increased bacterial clearance from the gallbladder.

The mechanism by which IFN-β production resulting from intracellular infection leads to clearance of extracellular bacteria remains unclear. *L. monocytogenes* replicates extracellularly in the gallbladder during murine infection[11,12], and recent studies have shown that *L. monocytogenes* colonizes both intra- and extracellular compartments of the liver[9,16]. I hypothesized that increased IFN-β induced during intracellular infection, such as in the liver, leads to recruitment of immune cells to the infected tissue, which then kill extracellular bacteria, such as in the gallbladder, to reduce bacterial loads. To characterize the immune cell types associated with *L. monocytogenes* infection of the gallbladder and to determine whether immune cell recruitment differs between infection with WT and Δ*rex*, we took a histology and immunohistochemistry approach (Figure 13). The resulting pathology scores suggested less inflammation and fewer macrophages in gallbladders infected with Δ*rex* compared to those infected with WT, which does not support our hypothesis that Δ*rex* induces an elevated immune response. In other host tissues, such as the MLN, immune cell recruitment can be measured

using more quantitative methods, such as flow cytometry. I attempted to quantify immune cell recruitment to the gallbladder by flow cytometry and was unsuccessful, as it is technically challenging to apply this method to murine gallbladders due to their small size and cell type composition. It is therefore promising that the blinded histology scoring method distinguished disease pathologies between two strains of *L. monocytogenes* and between infected and uninfected tissues. This histology approach in the gallbladder, in combination with quantitative measurement of immune cells in other tissues, will be used in future studies to characterize the host immune response throughout the body during infection with *L. monocytogenes.*

Oral infections of both B6 and *Tmem173*$^{-/-}$ mice with *L. monocytogenes* WT and Δ*rex* demonstrated that STING is indeed involved in the attenuation of Δ*rex*. Quantification of bacterial loads in infected tissues revealed that in B6 mice, Δ*rex* was significantly attenuated compared to WT *L. monocytogenes* in all organs tested. Of note was that Δ*rex* had significantly decreased CFU in the MLN, as this organ was not harvested in the previous infections[27]. This result introduced the possibility that Δ*rex* disseminates to peripheral organs less efficiently than WT due to poor replication in the MLN, which could explain the decreased bacterial loads of Δ*rex* in the spleens, livers, and gallbladders following oral infection of WT mice. This experiment also revealed differences in infection dynamics between B6 mice, presented in this chapter, and BALB/c mice, which were used in the initial study characterizing Δ*rex*[27]. Infections of BALB/c mice resulted in similar bacterial burdens in the GI tract between WT and Δ*rex*, whereas bacterial burdens were similar between the two strains during infection of B6 mice. It has been previously shown that BALB/c mice are more susceptible to oral infection than B6 mice[15], therefore it was expected for infections of B6 mice in this chapter to yield lower bacterial burdens compared to those reported by Halsey et al[27].

A previous study investigating the role of CDA secretion during *L. monocytogenes* infection found that B6 mice lacking functional STING (*Sting*$^{gt/gt}$) were more susceptible to oral infection than WT B6 mice, as shown by increased weight loss[65]. Additionally, Louie et al. show that bacterial burdens in the liver, spleen, and MLN of *Sting*$^{gt/gt}$ mice were significantly higher than in B6 mice[65]. We were therefore surprised to see the opposite result in our oral infections, where infection with WT *L. monocytogenes* resulted in no weight loss at all in our *Tmem173*$^{-/-}$ mice (Figure 14A), and similar bacterial burdens were observed in the liver, spleen, and MLN of *Tmem173*$^{-/-}$ mice compared to B6 mice (Figure 14B-E). While the *Sting*$^{gt/gt}$ and *Tmem173*$^{-/-}$ mice were assumed to be phenotypically identical, it is clear based on our results that disease severity and bacterial burdens in the two backgrounds are quite different. A 7-day time course of oral infection showed that *Tmem173*$^{-/-}$ mice had decreased bacterial loads to WT mice in the GI tract and similar bacterial loads to WT mice in peripheral organs, and that the *Tmem173*$^{-/-}$ mice did not exhibit any weight loss through 7 days of infection (Figure 15). Importantly, no bacteria were detected in the gallbladders of *Tmem173*$^{-/-}$ mice at any time point tested (Figure 15C). In conclusion, these results support our initial finding that our *Sting*$^{-/-}$ mice are less susceptible to infection than B6 mice, and the *Tmem173*$^{-/-}$ mouse model cannot be used to study gallbladder colonization following *L. monocytogenes* oral infection.

Overall, the work described in this chapter constitutes an effort to characterize the mechanism by which the *L. monocytogenes* Δ*rex* mutant is attenuated during murine infection. I showed *in vitro* that Δ*rex* induces elevated IFN-β expression and that this phenotype is STING-dependent and cGAS-independent. While this work established that the *Tmem173*$^{-/-}$ mouse model

of infection cannot be used to study gallbladder colonization during oral infection, the STING-dependent attenuation of Δ*rex* was observed in multiple organs in addition to the gallbladder. Future studies will investigate the role of STING during *L. monocytogenes* oral infection, with a focus on how STING promotes or restricts dissemination from the GI tract to peripheral organs.

Chapter 4: Investigating the roles of *Listeria monocytogenes* peroxidases in growth and virulence

Adapted from Cesinger et al., DOI: 10.1128/Spectrum.00440-21[69]

Introduction

Reactive oxygen species (ROS), including peroxide, are produced by bacteria and mammalian host cells as a byproduct of aerobic respiration, therefore most organisms have evolved strategies to combat these toxic compounds[35]. During infection, innate immune cells produce a burst of ROS to neutralize invading pathogens[33], making peroxide detoxification strategies particularly important for pathogenic bacteria. While the mechanisms of peroxide detoxification have been studied for decades in the model organisms *E. coli* and *Bacillus subtilis*[35,36,70], the mechanisms by which *Listeria monocytogenes* defends against ROS are less clear. The virulence factors employed by *L. monocytogenes* to successfully infect a host are all transcriptionally regulated by the master virulence regulator PrfA, which is itself redox regulated[71]. In addition to virulence factors, PrfA regulates genes that enhance *L. monocytogenes* resistance to peroxide[72], further indicating that peroxide stress is relevant during infection. We became particularly interested in the peroxide detoxification strategy employed by *L. monocytogenes* during infection when our previous work revealed that the single catalase (encoded by *kat*) produced by the bacterium is required for aerobic growth, but dispensable during infection[73]. These results led to the hypothesis that *L. monocytogenes* produces other redundant peroxidases in order to survive the respiratory burst of the macrophage phagosome. Here, we evaluated the expression and essentiality of all peroxidase-encoding genes during *L. monocytogenes* growth *in vitro* and during infection of murine cells in tissue culture.

We performed *in silico* analysis of the *L. monocytogenes* genome using the RedoxiBase database[74] and identified 9 predicted peroxidases (Table 2). This database includes the peroxidases produced by *Bacillus subtilis*, and each of these was used as a query protein sequence to identify homologous proteins produced by *L. monocytogenes* 10403S[74]. According to the RedoxiBase database, peroxidase proteins belong to two families: heme peroxidases and nonheme peroxidases[74]. Of the heme peroxidases, *L. monocytogenes* encodes a heme-dependent catalase (Kat), a coproheme decarboxylase (ChdC, formerly HemQ), and a DyP-type peroxidase (Lmo0367). Of the nonheme peroxidases, *L. monocytogenes* encodes Lmo0983, AhpA (formerly AhpC or Prx), Tpx, Lmo1609, and OhrA. Finally, Fri is a nonheme bacterial ferritin classified as an oxidoreductase by the RedoxiBase database[74]. Previous work from the lab demonstrated that *L. monocytogenes* requires *kat* to detoxify endogenously produced peroxide during aerobic growth, and that *kat* is dispensable for intracellular growth in macrophages[73]. In order to characterize the roles of the 8 additional peroxidases during infection, each potential peroxidase-encoding gene was deleted by allelic exchange while the strain was growing anaerobically to prevent oxygen-mediated toxicity. Based on the redundant roles of Kat and Ahp in other bacteria[75,76], we also generated a Δ*kat*Δ*ahpA* double mutant to include in our analyses.

The goal of the experiments in this chapter was to test if peroxidases, in addition to catalase, are necessary for intracellular infection. This chapter describes a paper co-authored by Monica Cesinger and myself, in collaboration with Cortney Halsey, Maureen Thomason, and

Michelle Reniere. My contributions to this publication included performing experiments described in Figures 16 and 17 of this chapter, construction of bacterial strains, and preparation of the manuscript.

Table 2. Predicted peroxidases encoded by *L. monocytogenes*

Gene	Name	Predicted Function	Reference(s)
lmo0367	--	Heme-dependent dyp-type peroxidase	--
lmo0943	*fri, dps*	bacterioferritin, oxidoreductase	77,78
lmo0983	--	glutathione peroxidase	--
lmo1583	*tpx*	thiol peroxidase	--
lmo1604	*ahpA*	2-cys peroxiredoxin	79,80
lmo1609	--	thioredoxin	--
lmo2113	*chdC, hemQ*	putative heme peroxidase, involved in heme biosynthesis	81
lmo2199	*ohrA*	organic hydroperoxidase	57
lmo2785	*kat*	heme-dependent catalase	73

Results

Expression of peroxidase-encoding genes in the host cytosol.

To determine whether peroxidase genes are expressed during cytosolic infection, we measured expression of these peroxidase-encoding genes during infection using fluorescent transcriptional reporters. I engineered *L. monocytogenes* strains to express RFP from the native promoter of each peroxidase-encoding gene, and to express GFP from a constitutive promoter. J774 macrophages were infected with each reporter strain for 1 hour before gentamicin was added to the medium to eliminate extracellular bacterial growth. Flow cytometry was performed 6 hours post-infection and infected cells were identified by GFP fluorescence compared to an uninfected, non-fluorescent control. Cells infected with the reporter strains for expression of *fri*, *ahpA*, and *kat* exhibited significantly increased RFP production compared to the background (Figure 17). These results suggested that only *fri*, *ahpA*, and *kat* are significantly expressed during macrophage infection and therefore might have roles in virulence.

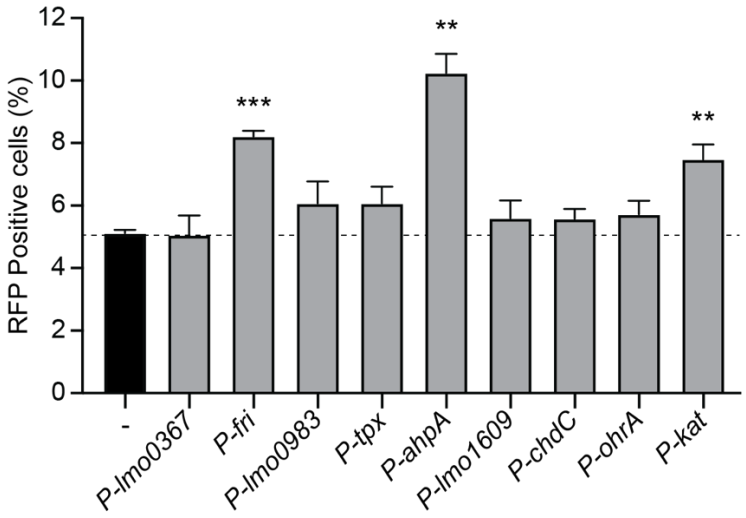

Figure 17. Intracellular expression of peroxidase-encoding genes. J774 macrophages were infected with each reporter strain, which expressed RFP from the indicated promoter and constitutive GFP. Cells were infected for 6 hours and then analyzed by flow cytometry. The dotted line indicates background RFP fluorescence. Data are means and SEM for three biological replicates. *P* values were calculated using a heteroscedastic Student's *t* test comparing each mutant to the wt. **, $p > 0.01$; ***, $p > 0.001$.

Intracellular replication and intercellular spread of peroxidase mutants.

During infection of macrophages, *L. monocytogenes* resides briefly in the phagosome, where it is bombarded by hydrogen peroxide produced by the host respiratory burst[34]. Previous work demonstrated that Kat-mediated peroxide detoxification is not required for intracellular survival or growth in macrophages[73]. To test which peroxidases are important intracellularly, we infected bone marrow-derived macrophages (BMDMs) with each strain and enumerated CFU over time. To ensure a robust innate immune response, BMDMs were pretreated with interferon gamma (IFN-γ) to activate the host respiratory burst[82]. In these experiments, the majority of peroxidase mutants grew similarly to the WT. Surprisingly, the Δ*kat*Δ*ahpA* double mutant exhibited a significant 5- to 8-fold increase in CFU at each time point compared to the WT. In contrast, the Δ*fri* strain was significantly attenuated for intracellular replication, and this defect was genetically complemented by providing *fri in trans*.

One hypothesis to explain the dispensability of the majority of peroxidases for intracellular growth is that the host respiratory burst is ineffective against *L. monocytogenes* because the secreted pore-forming toxin listeriolysin O (LLO) allows rapid escape from the vacuole. To examine which peroxidases may be important specifically in the vacuolar environment, the gene encoding LLO (*hly*) was disrupted in each mutant background, and survival in the vacuole of IFN-γ-activated BMDMs was evaluated over time. In agreement with the intracellular growth curves, the majority of peroxidase mutants survived in the vacuole for 6 hours at rates similar to that of the WT. The exceptions were the Δ*kat*Δ*ahpA* mutant, which survived significantly better than WT, and the Δ*fri* mutant, which exhibited a 1-log decrease in CFU at the earliest time point, although

this was not statistically significant (p = 0.06). Together, these data demonstrate that the only peroxidase important for vacuolar survival and intracellular growth in activated BMDMs is that encoded by *fri*.

We next sought to test the role of each peroxidase in virulence using a plaque assay, which is a measure of intracellular growth and cell-to-cell spread that is highly correlated with virulence in a murine model of infection[57,83]. In this assay, a monolayer of L2 murine fibroblasts is infected and immobilized in agarose containing gentamicin to kill extracellular bacteria. Three days postinfection, the living cells are stained with neutral red and the area of the plaques formed by *L. monocytogenes* are analyzed as a measure of intercellular spread. In this assay, all of the mutant strains formed plaques similar in size to or larger than those formed by the WT (Figure 18A), consistent with most peroxidase-encoding genes being dispensable for vacuolar survival and intracellular replication. Although the Δ*kat*Δ*ahpA* double mutant formed plaques similar in size to those of WT, the mutant exhibited a dramatic advantage at invading host cells. The Δ*kat*Δ*ahpA* mutant formed approximately 5 times more plaques than WT (Figure 18B). This is consistent with the increased bacterial burden observed in IFN-γ-activated BMDMs at the earliest time points and suggests that the Δ*kat*Δ*ahpA* mutant is better able to invade host cells.

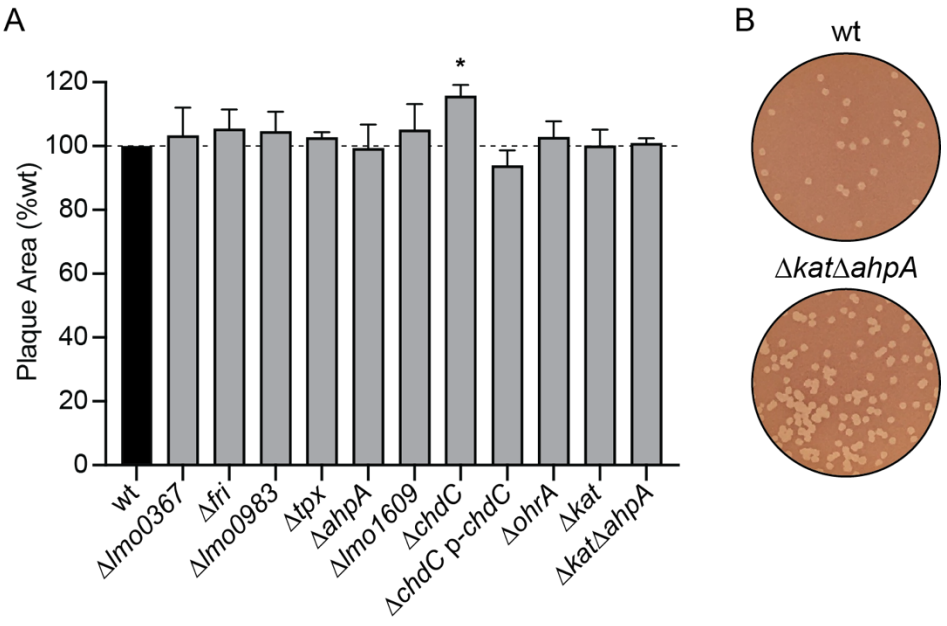

Figure 18. Intercellular spread of peroxidase mutants. (A) Plaque areas formed in L2 fibroblasts, measured as a percentage of WT *L. monocytogenes*. Data are means and SEM of n=3. (B) Representative images of plaques demonstrating the greater number of plaques formed by the Δ*kat*Δ*ahpA* mutant than the WT.

Discussion

Bacterial pathogens must detoxify endogenously produced ROS and exogenous sources of oxidative stress during infection. Hydrogen peroxide is particularly dangerous, as it is an uncharged molecule that can penetrate membranes[35]. In this study, we performed the first comparison of the expression and essentiality of all proteins with predicted peroxidase activity in *L. monocytogenes* during intracellular infection. I showed using fluorescent reporter strains that most peroxidases are not expressed during cytosolic growth, with the exceptions of *kat, ahpA,* and *fri.* I next showed that *L. monocytogenes* peroxidase mutants all formed WT-sized plaques, indicating that no single peroxidase gene is required for cytosolic replication or cell-to-cell spread. Considering that the host respiratory burst assaults invading bacteria with up to 100 mM peroxide in the phagosome[75], our results suggest a high degree of redundancy in the *L. monocytogenes* peroxide stress response.

Lmo1604 is annotated as an alkyl hydroperoxide reductase (Ahp) based on similarity to other enzymes. The classical Ahp system is composed of two components: the peroxiredoxin (AhpC) and a dedicated reductase (AhpF) that reduces and recycles AhpC and is typically encoded by a sequence adjacent to *ahpC*[84]. Many organisms encode multiple Ahp proteins; however, *L. monocytogenes* encodes only Lmo1604, and there is no adjacent reductase. We found that *ahpA* is expressed during intracellular replication but is not required for growth in IFN-γ-activated macrophages or prolonged survival in the vacuole. These results are consistent with published work showing that the Δ*ahpA* mutant had no defect in macrophages or during infection of mice[80].

The most dramatic aerobic growth defect was seen in the *L. monocytogenes* mutant lacking *chdC*, encoding a putative heme-dependent peroxidase[81]. This severe growth defect resembled that of *L. monocytogenes* Δ*hemEH*, which also cannot produce heme[73]. As our data attribute the Δ*chdC* growth defect to the heme deficiency, it is unlikely that ChdC peroxidase activity plays a primary role in endogenous peroxide detoxification. However, our results raise an interesting question: why is heme biosynthesis required for *L. monocytogenes* aerobic growth? Heme is an essential cofactor for cytochrome oxidases of the electron transport chain, and therefore, *S. aureus hem* mutants are impaired for growth due to a lack of aerobic respiration[85,86]. However, *L. monocytogenes* lacking one or both terminal cytochrome oxidases are only moderately impaired for aerobic growth, compared to the complete lack of replication observed for Δ*chdC* and Δ*hemEH* mutants[73,87]. Interestingly, *S. aureus* requires heme biosynthesis for virulence in murine models of acute infection[41]. In contrast, *L. monocytogenes* mutants lacking *hemEH* or *chdC* are not defective for intracellular replication and, in fact, exhibit increased intercellular spread compared to WT[73] (unpublished observations). These results suggest either that heme biosynthesis is dispensable for *L. monocytogenes* pathogenesis or that exogenous host-derived heme can support growth of the Δ*chdC* mutant during infection. Ongoing research aims to determine the role of heme in *L. monocytogenes* aerobic growth and virulence.

Hydrogen peroxide toxicity and iron are inextricably linked due to the Fenton reaction, in which ferrous iron reacts with hydrogen peroxide to generate hydroxyl radicals that damage DNA[75]. One method used by bacteria to mitigate the danger of free iron and the Fenton reaction is to sequester iron within bacterial ferritin proteins, which are multimeric protein shells that can store up to 4,500 iron atoms[39]. The amino acid sequence of *L. monocytogenes* Fri is identical to

that of the *Listeria innocua* Dps protein, which has been biochemically characterized as a bacterial ferritin. *L. innocua* Dps has a smaller internal diameter than typical ferritins and therefore can store only ~400 iron atoms per shell[38]. The protection afforded by *L. innocua* Dps is due to the hydrogen peroxide-mediated iron oxidation, which occurs rapidly and in a manner that prevents Fenton chemistry[88,89]. Based on the identity of the proteins, we predict that *L. monocytogenes* Fri has a similar function and uses peroxide to oxidize and store iron. It is therefore not possible to distinguish between the importance of the peroxidase activity of Fri and its role in iron homeostasis in the cell. The role of Fri in *L. monocytogenes* has been investigated previously by several groups, and in fact, the protein encoded by *lmo0943* has been given multiple different names, including Flp (ferritin-like protein)[90], Frm (ferritin-like protein from *L. monocytogenes*)[91], and Frl (ferritin-like protein in *Listeria* species)[92]. Here, we kept the more common name Fri[77,78,93]. Our results are consistent with the literature showing that *fri* expression increases 8-fold upon entry into stationary phase and a Δ*fri* mutant is more sensitive to peroxide stress when treated in log phase[77,93]. We also determined that *fri* expression is increased during intracellular growth and accordingly, *fri* is required for growth in activated BMDMs.

In our assays, we did not observe phenotypes for *L. monocytogenes* lacking *lmo0367, lmo0983, tpx, lmo1609,* or *ohrA*, and little is known about their functions. Lmo0367 shares 52% amino acid identity with the *B. subtilis* YwbN/EfeB protein, a DyP-type peroxidase that is transported as a folded protein across the cytoplasmic membrane via the twin-arginine translocation (Tat) pathway[94,95]. While the protein localization and function of *L. monocytogenes* Lmo0367 have not been examined, the corresponding gene was found to be regulated by the ferric uptake regulator Fur and expression was consequently decreased in response to heme stress[96,97]. Additionally, *lmo0367* is co-transcribed with genes *fepCA*, which encode a ferrous iron transport complex[38,98], which further emphasizes the intricate link between iron and peroxide toxicity.

Taken together, the experiments presented in this chapter characterized the roles of peroxidase-encoding genes on *L. monocytogenes* intracellular infection. Our results support the notion that hydrogen peroxide toxicity and iron are intimately linked, which is evident by several of the putative peroxidases also being involved in maintaining iron homeostasis, including the heme-dependent peroxidase Lmo0367, the bacterial ferritin Fri, the terminal heme biosynthesis enzyme ChdC, and the heme-dependent catalase Kat. Additional studies are necessary to assess the roles of these enzymes in iron influx, oxidation, and storage in response to oxidative stress.

Chapter 5: Investigating the iron sources consumed by *Listeria monocytogenes* during intracellular infection

Introduction

When transitioning from one replication niche to another, such as from soil to a host organism, bacteria must adapt to the nutrients available in that environment. One essential nutrient that is often scarce is iron, and bacteria have evolved to utilize a diverse array of iron acquisition mechanisms. *L. monocytogenes* encodes a number of transport proteins that import either molecular iron or heme[38] (Figure 19). Two complexes transport ferrous iron into the cell: the transporter encoded by *feoAB* (*lmo2104-5*) imports ferrous iron into the cell[99], and the Fep complex encoded by *fepCAB* (*lmo0365-0367*) first converts iron from a ferric to ferrous state, and then imports the ferrous iron into the cell[38,100]. *L. monocytogenes* utilizes two mechanisms to facilitate uptake of heme from the environment. The first takes place in conditions where heme is abundant, and the transport complex encoded by *hupDGC* (*lmo2429-31*) facilitates uptake of heme[101]. The second mechanism occurs when heme is scarce; the proteins Hbp1 and Hbp2 are anchored to the cell wall and bind heme at high affinity. Once heme is bound, it is transferred to HupDGC and transported into the cytoplasm[101]. As mentioned in Chapter 4, iron is essential to the survival and growth of nearly all bacteria, but it can also be toxic to both bacterial and eukaryotic cells. Excess intracellular iron, in the form of heme or elemental iron, can undergo Fenton chemistry, in which the iron reacts with reactive oxygen species (ROS) and generates more ROS in the process[41]. Cells therefore must employ mechanisms to combat iron toxicity by exporting excess iron back into the environment and sequestering iron in a non-reactive form for later use. *L. monocytogenes* encodes the protein FvrA, an iron/heme exporter which transports excess iron out of the cell[42,102], and Fri, a non-heme-containing iron storage protein, to prevent accumulation of free iron in the bacterial cytosol. Interestingly, *fvrA* is required for virulence during murine infection[42], highlighting that preventing accumulation of excess iron is necessary for survival in the host. In mammalian host cells, iron is either associated with proteins as a co-factor, usually as heme, or stored by ferritins in the cytosol[38].

Heme is the most abundant source of iron available to bacteria during infection of mammalian hosts[39], so it is unsurprising that both the Hup complex and proteins Hbp1 and 2 have both been shown to be required for virulence *in vivo* using an intravenous murine model of infection[101,103,104]. These studies strongly suggest that *L. monocytogenes* utilizes heme as an iron source during mammalian infection. The roles of molecular iron transporters during *L. monocytogenes* infection, however, require further investigation. The transporter encoded by *feoAB,* which imports ferrous iron into the cell, was found to be dispensable *in vivo*[99]. Conversely, previous studies suggest that the *fep* operon is required for virulence during murine infection[42]. While some of these iron transporters have been shown to be required for virulence *in vivo*, the roles of these transporters during intracellular infection have not been thoroughly investigated.

In this chapter, I present data collected towards the goal of identifying the source of iron used by *L. monocytogenes* during intracellular infection and the corresponding bacterial transporters. The project was terminated when we discovered a second site mutation in the Δ*hbp1,2* mutant, which had significant effects on a key phenotype. Despite this caveat, most

experiments presented in this chapter served to optimize media conditions to grow *L. monocytogenes* on different iron sources, which could be of use to future researchers. While I performed the majority of experiments in this chapter, Mauna Edrozo and Michelle Reniere constructed mutant strains and performed preliminary experiments (Figure 20A and Table 3).

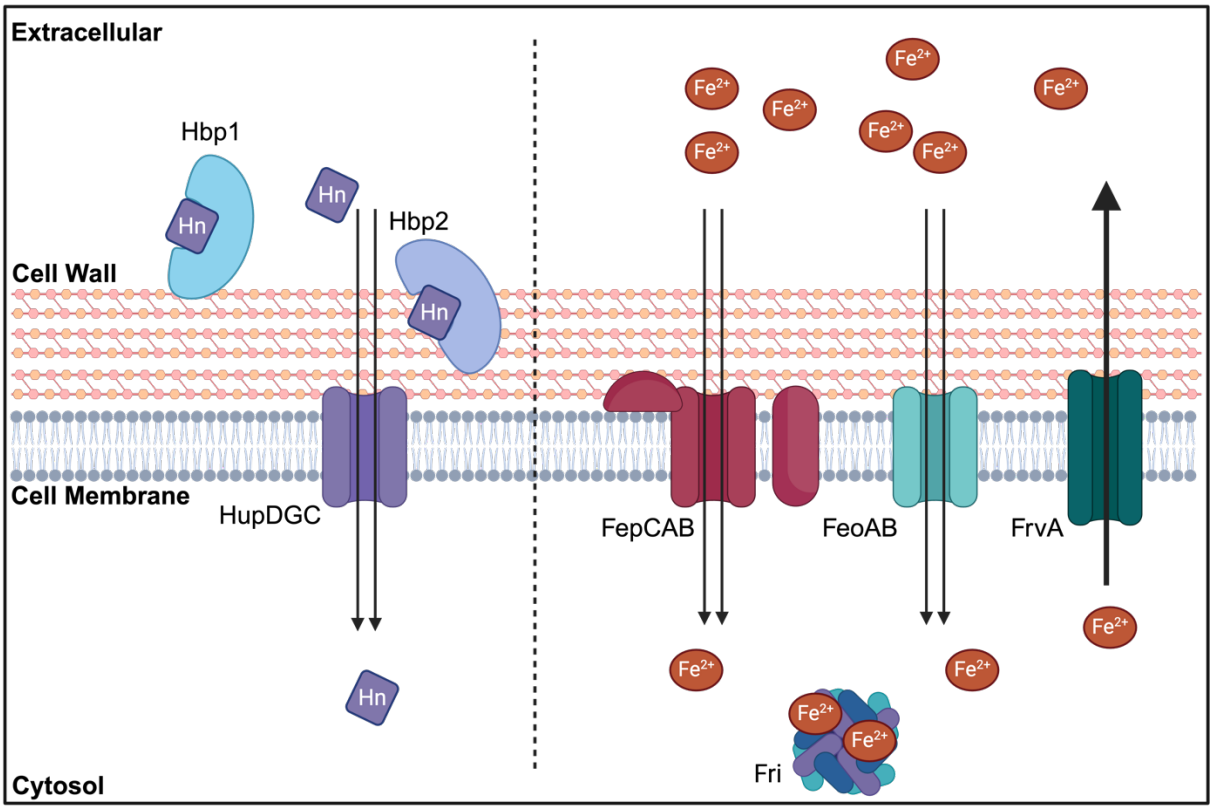

Figure 19: Iron uptake systems in *Listeria monocytogenes.* (Left) Heme acquisition. In heme-replete conditions, HupDGC complex imports heme into the cytosol. In low heme conditions (<50 nM), cell-wall anchored proteins Hbp1 and Hbp2 bind heme at high affinity, and deliver the heme to HupDGC for import into the cytosol. (Right) Ferrous iron transport mechanisms. The protein complexes FepCAB and FeoAB transport ferrous iron into the cytosol. The bactoferritin Fri then stores cytosolic iron. The efflux pump FrvA exports molecular iron out of the cell.

Results

Transcriptomics of *L. monocytogenes* replicating in the macrophage cytosol

To determine what *L. monocytogenes* genes are expressed during cytosolic replication, the lab utilized a non-biased approach and performed RNA-seq comparing transcript abundance after replication in rich BHI broth and in the cytosol of J774 macrophages. Surprisingly, many genes involved in iron homeostasis were significantly depleted in the cytosol (Table 3), including those involved in heme uptake (*hbp1,2, hupDCG*) and ferrous iron uptake (*fepCA, feoAB*). In contrast, *frvA,* which encodes an iron efflux pump, had increased transcript abundance in the host

cytosol, suggesting that *L. monocytogenes* encounters iron in excess during intracellular infection. Transcripts encoding the iron storage protein Fri were not differentially expressed, suggesting that iron storage is not differentially regulated during intracellular infection compared to growth in broth. The combination of iron acquisition genes being downregulated and iron efflux being upregulated led me to hypothesize that *L. monocytogenes* is iron-replete while replicating in the host cytosol, and therefore iron acquisition genes are dispensable for intracellular growth, which is inconsistent with the notion that there is very little iron available in the cytosol[41].

Table 3. RNA-seq comparing *L. monocytogenes* transcripts after growth in BHI vs. macrophage cytosol. Genes related to iron homeostasis that were differentially expressed during intracellular replication in J774 macrophage-like cells. Shading indicates genes transcribed in operons.

Lmo	Name	Function	Fold change
lmo0641	*frvA*	Fe(II) efflux P1B4-type ATPase	+46.28
lmo2186	*hbp1*	Cell wall anchored heme uptake protein IsdC	-35.26
lmo2185	*hbp2*	Cell surface protein IsdA, transfers heme from hemoglobin to apo-IsdC	-22.63
lmo2184	*isdE*	Heme ABC transporter, heme-binding protein IsdE	-10.54
lmo2183	*isdF*	Heme ABC transporter, permease component IsdF	-8.91
lmo2182	*isdD*	Heme transporter analogous to IsdDEF, ATP-binding protein	-5.98
lmo2181	*srtB*	Sortase B	-4.52
lmo0484	*isdG*	heme-degrading monooxygenase	-10.19
lmo1957	*fhuG*	Ferrichrome transport system permease protein	-4.78
lmo1958	*fhuB*	Ferrichrome transport system permease protein	-4.35
lmo1959	*fhuD*	Ferrichrome-binding periplasmic protein precursor	-2.71
lmo0366	*fepA*	Ferrous iron transport periplasmic protein	-4.41
lmo0365	*fepC*	Ferrous iron transport permease	-3.72
lmo0367	*fepB*	tat-translocated enzyme	-2.39
lmo2105	*feoB*	ferrous iron transporter B	-3.77
lmo2104	*feoA*	Ferrous iron transport protein A	-2.68
lmo1960	*fhuC*	Ferrichrome transport ATP-binding protein	-3.72
lmo1961		ferredoxin-NADP reductase 1	-2.97
lmo2429	*hupC*	Ferrichrome transport ATP-binding protein	-2.74
lmo2430	*hupG*	Ferrichrome transport system permease protein	-2.11
lmo2431	*hupD*	Ferrichrome-binding periplasmic protein precursor	-2.06

Heme-binding proteins are required for cell-to-cell spread, but not replication

To evaluate the roles of iron transporters during *L. monocytogenes* infection, mutants lacking the ferrous iron transporter Fep (Δ*fepCA*) and heme-binding proteins 1 and 2 (Δ*hbp1,2*) were generated via allelic exchange. To determine whether these genes contribute to intracellular infection, plaque assays were performed in L2 fibroblasts. The Δ*fepCA* mutant formed plaques similar in size to WT and the Δ*hbp1,2* mutant formed plaques 40% the size of WT (Figure 20A), suggesting that uptake of heme, but not ferrous iron, is required for intracellular infection. Plaque

assays are a measurement of both cytosolic replication and cell-to-cell spread. To evaluate whether these mutants also exhibit decreased intracellular replication compared to WT, I measured replication kinetics in both bone marrow-derived macrophages (BMDMs) and TIB73 hepatocytes over 8 hours and found that both Δ*fepCA* and Δ*hbp1,2* replicated to similar bacterial densities as WT in both cell types (Figures 20C and 20D). Together these results indicate that neither Fep nor Hbp is required for cytosolic replication, but Hbp1 and Hbp2 are required for cell-to-cell spread during intracellular infection. Additionally, the two mutants grew similarly to WT in BHI broth (Figure 20B), further supporting that these iron transporters are not required for *L. monocytogenes* replication.

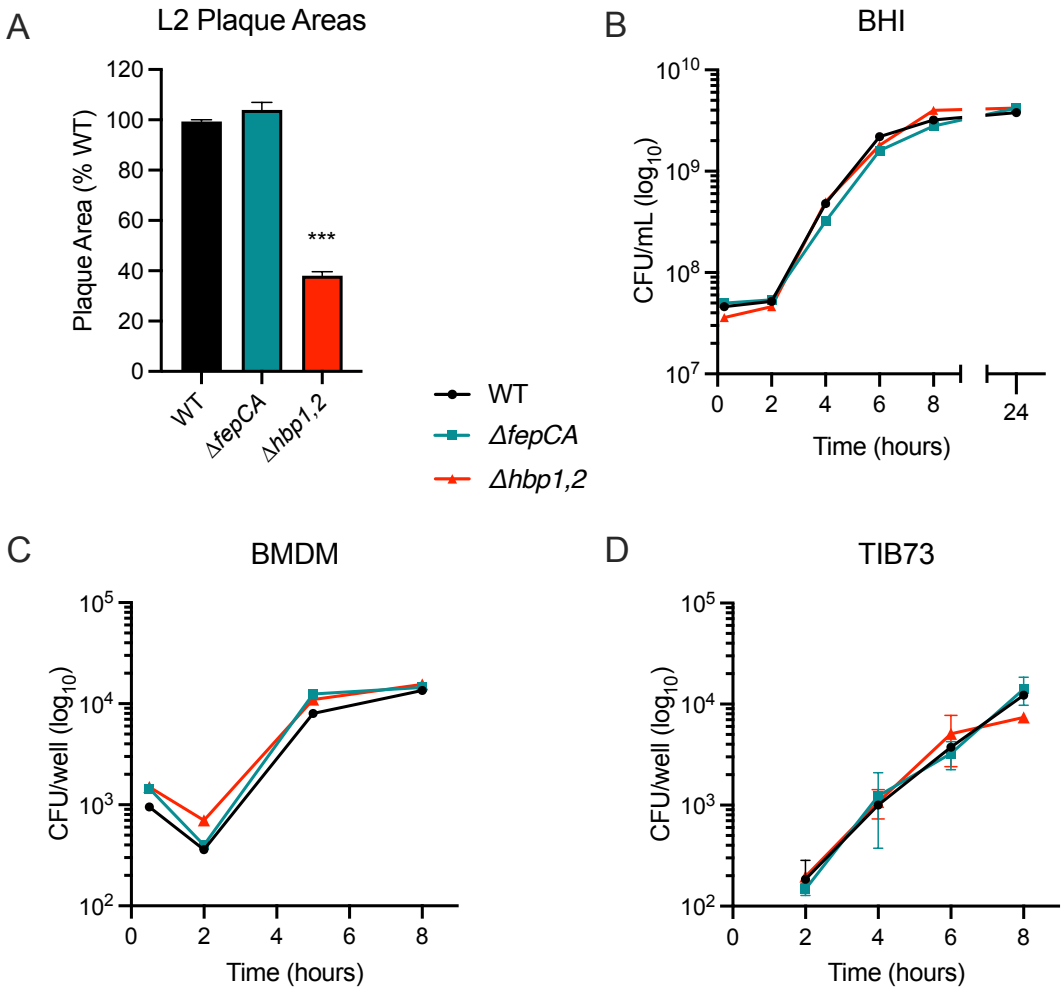

Figure 20. Heme binding proteins 1 and 2 are required for cell-to-cell spread. (A) Plaque areas formed in L2 fibroblasts, measured as a percentage of WT *L. monocytogenes*. Data are means and SEM of n=3. *** $p < 0.001$, as determined by one-way ANOVA with multiple comparisons to the mean of WT. (B) Growth kinetics in BHI. (C) Intracellular growth of mutants in BMDMs. (D) Intracellular growth of mutants in TIB73 cells. Data are means and SEM of n=2.

Serial passaging in iron-free media

The goal of this project was to determine the impact of iron acquisition systems on *L. monocytogenes* intracellular infection. I therefore sought to determine culture conditions in which *L. monocytogenes* becomes iron-starved, so that in later experiments I could infect host cells with iron-starved bacteria. To establish how long *L. monocytogenes* can grow before depleting all iron, I grew WT and mutant strains of *L. monocytogenes* in *Listeria*-synthetic medium (LSM)[105] containing no exogenous iron source, and then serially passaged these strains into fresh iron-free LSM once per day. The Δ*fri* strain was included in this experiment to assess the role of iron storage on iron starvation, as this mutant lacks the only iron storage protein encoded by *L. monocytogenes*[38]. Surprisingly, most strains continued to grow in iron-free LSM for 12 days of passaging, at which point the experiment was terminated (Figure 21). The only mutant that did not replicate in the iron-free LSM was Δ*fepCA*, which suggests that Fep alone is sufficient for *L. monocytogenes* to survive and replicate in low-iron conditions. Additionally, the Δ*fri* mutant continued to grow in iron-free LSM similarly to WT, which indicates that even in very low iron conditions storage of iron does not confer a fitness advantage.

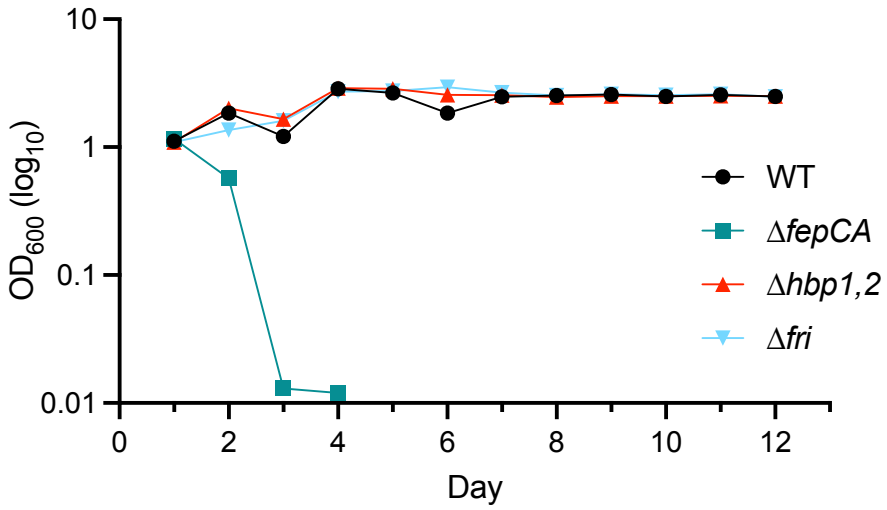

Figure 21. Serial passaging in iron-free medium. *L. monocytogenes* strains were grown in *Listeria*-synthetic medium lacking any iron source, and serially passaged into fresh iron-free medium every 24 hours for 12 days. Data are bacterial densities as measured by OD_{600} 24 hours post-inoculation.

Determining optimal concentrations of exogenous iron in *Listeria*-defined medium for growth and starvation

It was immediately clear that passaging in iron-free medium was not an efficient method of starving *L. monocytogenes*, as depletion of iron should result in an inability to replicate. Another method of starving bacteria of iron is to add chelators to the growth media, which sequester iron and render it biologically unavailable. However, before determining concentrations of chelator necessary to starve bacteria of iron, the concentrations of ferrous iron and heme in LSM needed to be optimized. To this end, I grew cultures of WT *L. monocytogenes* in LSM containing $FeCl_2$

ranging from 0 to 500 μM, or heme ranging from 0 to 50 μM for 48 hours. The goal was to determine a concentration high enough to support robust growth, but not so high to become toxic. Based on the growth dynamics in the concentrations tested, 20 μM $FeCl_2$ and 5 μM heme (Figure 22A and 22B) were used in subsequent experiments.

Once these concentrations were determined, the growth dynamics of iron transport mutants were evaluated (Figure 22C and 22D). First, *L. monocytogenes* strains were grown in either 0 μM (no exogenous iron source) or 20 μM $FeCl_2$. The Δ*hbp1,2*, Δ*fri*, and Δ*hbp1,2*Δ*fri* mutants all grew similarly to WT in both 0 and 20 μM $FeCl_2$. The mutants lacking Fep *(*Δ*fepCA* and Δ*fepCA*Δ*fri*) did not replicate in either condition, consistent with this transporter being required for uptake of ferrous iron (Figure 22D). Next, mutants were grown in either 0 μM or 5 μM heme as the sole exogenous iron source. All mutants grew similarly to WT in 5 μM heme, including those lacking heme binding proteins 1 and 2, suggesting that these secreted proteins are not required for growth on this concentration of heme as a sole iron source. Additionally, 5 μM heme restored the growth of strains lacking *fepCA* to WT levels, indicating that transport of ferrous iron is dispensable when heme is present (Figure 22E).

After confirming that these concentrations of ferrous iron and heme support robust growth of both WT and most mutant strains, I next established culture conditions in which iron is biologically unavailable, thereby starving the bacteria of iron. To this end, I grew WT *L. monocytogenes* in LSM containing no iron source and increasing concentrations of bipyridyl (BP), a metal chelator that binds iron and other metal ions. The goal of this first titration experiment was to determine a concentration of BP that restricts bacterial growth without killing. Of the concentrations tested in the first experiment, both 250 μM and 500 μM BP led to no replication over 12 hours, with 500 μM leading to a decrease in bacterial densities over time (Figure 23A). Iron bound to heme cannot be chelated by BP, therefore addition of heme should restore growth even in the presence of BP. The goal of this second titration was, therefore, to determine a concentration of BP that restricts growth, but this growth restriction should be restored by addition of heme. This experiment determined that 250 μM BP is sufficient to restrict growth of WT *L. monocytogenes*, but growth was fully restored in LSM containing heme, indicating that this concentration of BP was not overly toxic to the bacteria (Figure 23B and 23C). Finally, I measured the growth dynamics of mutants Δ*fepCA,* Δ*hbp1,2*, and Δ*fri* in LSM containing BP and heme, and confirmed that growth of all the mutants was restricted with BP alone, and restored with the addition of heme (Figure 23D). Future studies will use these conditions to starve *L. monocytogenes* of iron, and then these iron-starved bacteria can aid in our understanding of how these pathogens acquire iron during intracellular infection.

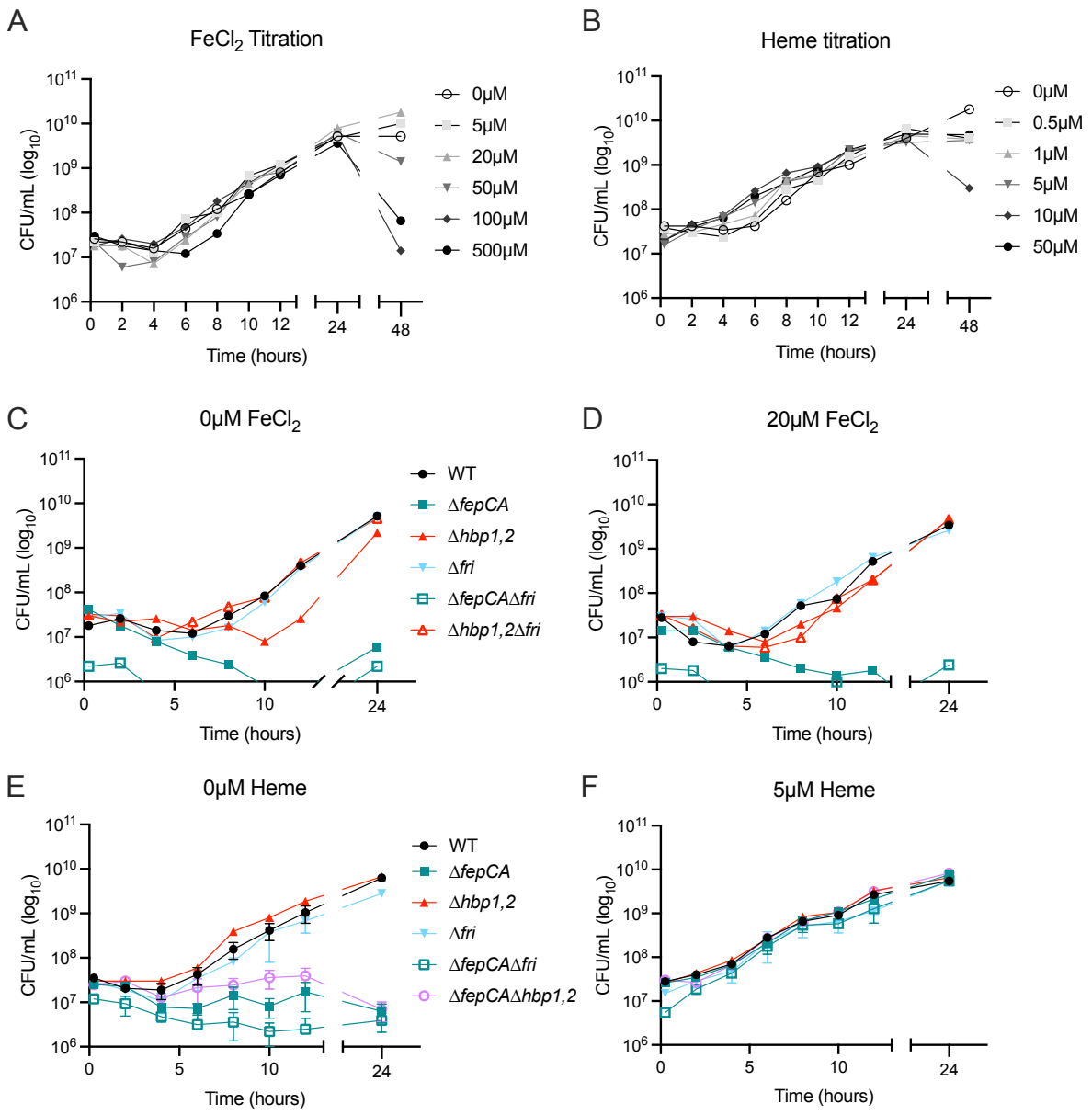

Figure 22. Determining optimal concentrations of exogenous iron for replication in *Listeria* defined medium. WT *L. monocytogenes* was grown in LSM containing increasing concentrations of FeCl2 (A) or heme (B) as the sole iron source. A panel of *L. monocytogenes* strains was cultured in LSM containing either 0 μM or 20 μM FeCl2 (C-D) and 0 μM or 5 μM heme (E-F). In all conditions, cultures were inoculated with $5x10^7$ CFU/mL of *L. monocytogenes* culture grown overnight in LSM. E-F: data are means and SEM of n=3; all other panels n=1.

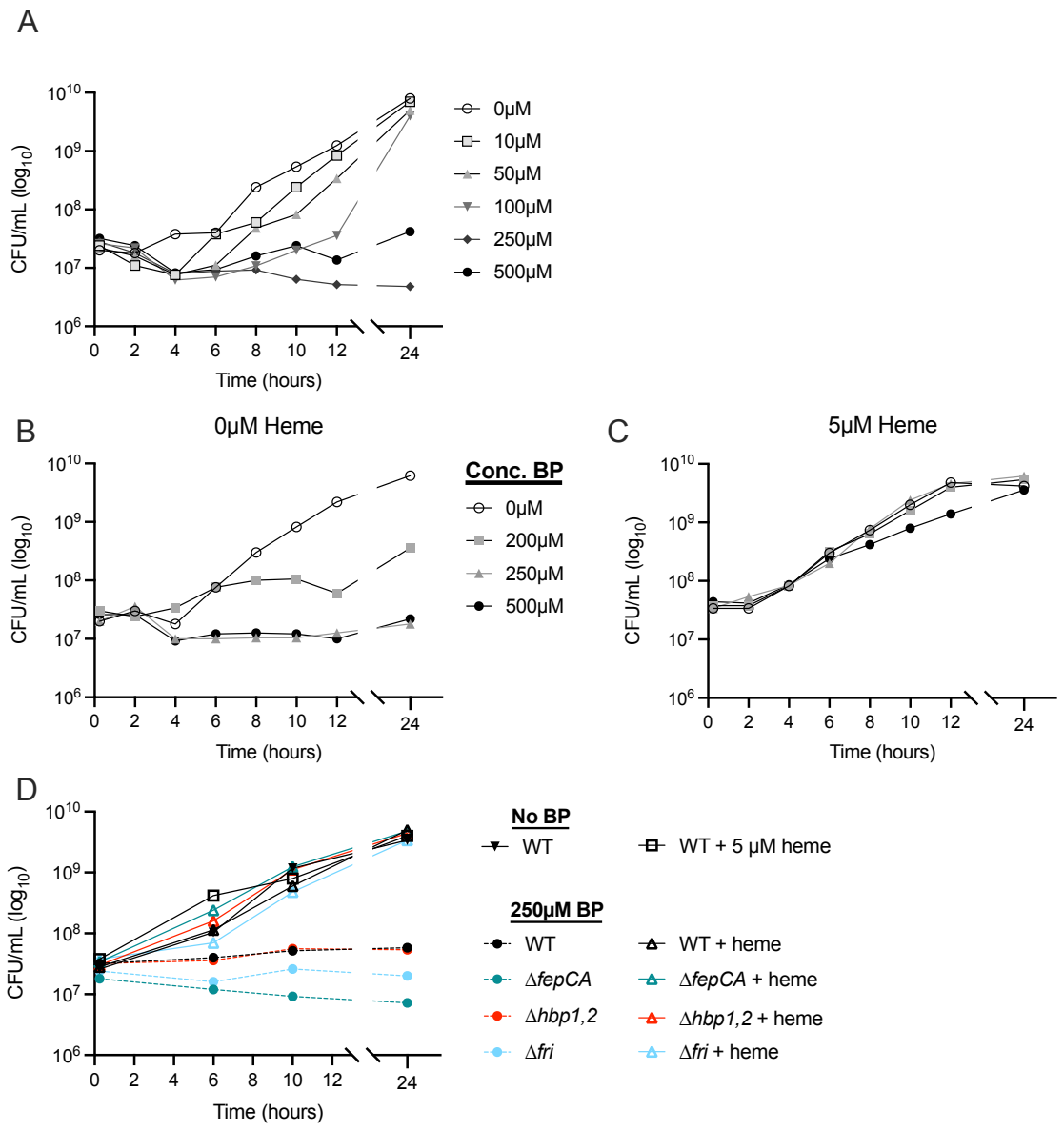

Figure 23. Determining optimal concentration of bipyridyl to restrict bacterial replication in *Listeria* synthetic medium. (A) WT *L. monocytogenes* grown in LSM containing increasing concentrations of bipyridyl (BP). WT was then cultured in LSM containing a different panel of increasing concentrations of BP and either 0 μM (B) or 5 μM heme (C). (D) A panel of mutants was cultured in LSM containing 0 μM or 5 μM heme and 250 μM BP.

Quantifying iron-regulated genes in tissue culture

To investigate the role of iron acquisition by *L. monocytogenes* during intracellular infection, I aimed to deplete iron from both the bacteria and host cells prior to infection. In this section, I describe two experiments in which I attempted to deplete host cells of iron in tissue culture and to quantify the iron starvation state of the cells.

I first incubated cells in tissue culture in L2 media containing reduced amounts of fetal bovine serum (FBS). Most of the iron in this medium comes from FBS, therefore reducing the amount of FBS in media also reduces the total iron. TIB73 hepatocytes were seeded in media containing 0.3%, 1%, or 10% FBS (standard media conditions = 10% FBS) and incubated overnight. Additionally, cells were seeded in 10% FBS and 100 μM bipyridyl (BP). After 12-16 hours of incubation overnight, I harvested RNA from the cells and performed RT-qPCR to measure expression of iron uptake and storage genes. Transcripts measured encode transferrin receptor (TfR), the iron import protein Dmt1, and the iron storage protein ferritin (ferritin-h, heavy chain). It has been shown that treatment with BP leads to increases in TfR and Dmt1 expression, and a decrease in ferritin expression[106], and I hypothesized that incubation with low FBS would result in the same transcriptional changes. I found that dmt1 expression correlated well with FBS concentration, but TfR expression did not, as 0.3% and 1% FBS resulted in decreased TfR transcripts compared to the standard 10% FBS (Figure 24A). Cells incubated with less FBS exhibited increased ferritin expression, which is the opposite of what was expected. Additionally, cells incubated with BP overnight did not exhibit different transcript levels of any of these host iron genes. Overall, the results of this experiment suggested that these overnight incubation conditions do not result in a quantifiable iron starvation state.

One major caveat to incubating cells overnight with very little FBS is that FBS contains many nutrients and growth factors necessary for keeping cells alive and healthy. While I was able to harvest enough RNA from the first experiment to perform RT-qPCR, the cells incubated with less FBS and the cells incubated with BP, were visibly less healthy and less confluent the next morning (not shown). To starve host cells of iron without depriving them of serum, I seeded cells in 10% FBS overnight, and the next morning treated the cells with 100 μM BP for 30 or 60 minutes before performing RT-qPCR to quantify expression of iron-regulated genes. Expression of TfR, Dmt1, and ferritin was compared to that of cells that received no BP treatment. Under these conditions, both TfR and dmt1 transcript levels increased following 30 and 60 minutes of BP treatment compared to untreated (Figure 24B). Ferritin transcript abundance was similar between untreated and BP-treated cells. Taken together, acute treatment with BP led to transcript-level differences in expression of iron-regulated genes. Future experiments will determine whether longer BP treatment results in a stronger “iron-starvation” signature, while maintaining cell viability. Ultimately, these conditions will be used to evaluate the role of iron within the host on *L. monocytogenes* survival and replication.

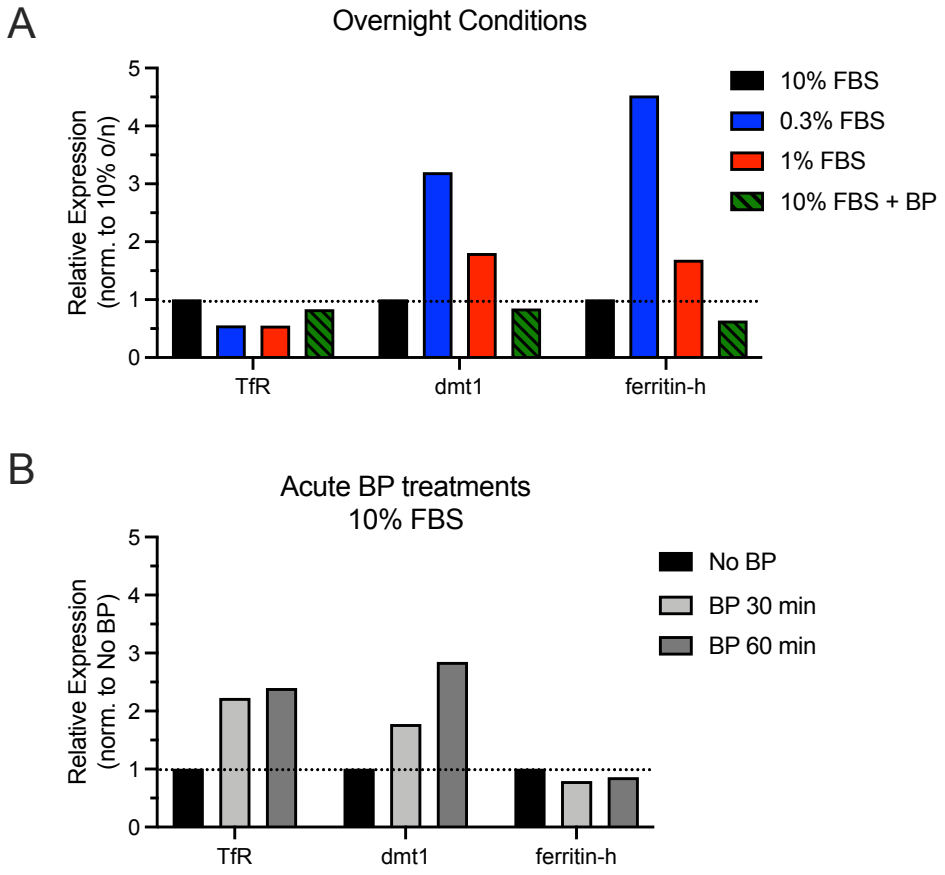

Figure 24. Quantifying iron-regulated gene expression in tissue culture. (A) TIB73 hepatocytes were seeded overnight in media containing varying concentrations of FBS. (B) TIB73 hepatocytes were seeded overnight in medium containing 10% FBS, then cells were treated with 100 μM BP or vehicle for the indicated time. Transcript abundances of TfR, Dmt1, and ferritin-h were measured via RT-qPCR, with hprt as the endogenous control. Expression in (A) was normalized to that of 10% FBS (standard media conditions), and expression in (B) was normalized to that of cells that did not receive BP treatment. Dotted lines: relative expression = 1.

Whole-genome sequencing revealed unforeseen mutations

While optimizing conditions for depriving both bacteria and host cells of iron, I performed plaque assays in TIB73 cells to ensure that the plaque phenotypes seen in L2 cells were consistent in hepatocytes, which are more relevant to *in vivo* infection. As expected, Δ*fepCA* formed plaques similar in size to WT, and Δ*hbp1,2* formed plaques 40% the size of WT, which is nearly identical to what we have previously observed in L2 cells (Figures 20A and 25A). I also generated complement strains in which genes *hbp1,2* were expressed from their native promoter at an ectopic site on the chromosome. Surprisingly, the complemented strain also formed plaques 40% the size of WT, which suggested that the defect in plaque formation of Δ*hbp1,2* is not due to the gene deletion alone (Figure 25A). To investigate this, we performed whole-genome sequencing on the Δ*hbp1,2* mutant, and found that this strain also harbored a mutation in *pdhA*

(P143S), which is most likely the explanation for this mutant strain forming smaller plaques. To confirm this, I re-generated the Δ*hbp1,2* in a clean background, and evaluated plaque formation in L2 cells. L2 cells were used in this last experiment to replicate the conditions in which these mutants were first studied (Figure 20A). The new deletion mutant formed plaques similar in size to WT, while the old mutant formed smaller plaques as seen previously, confirming that the "Old" mutant was not attenuated due to deletion of *hbp1,2* (Figure 25B).

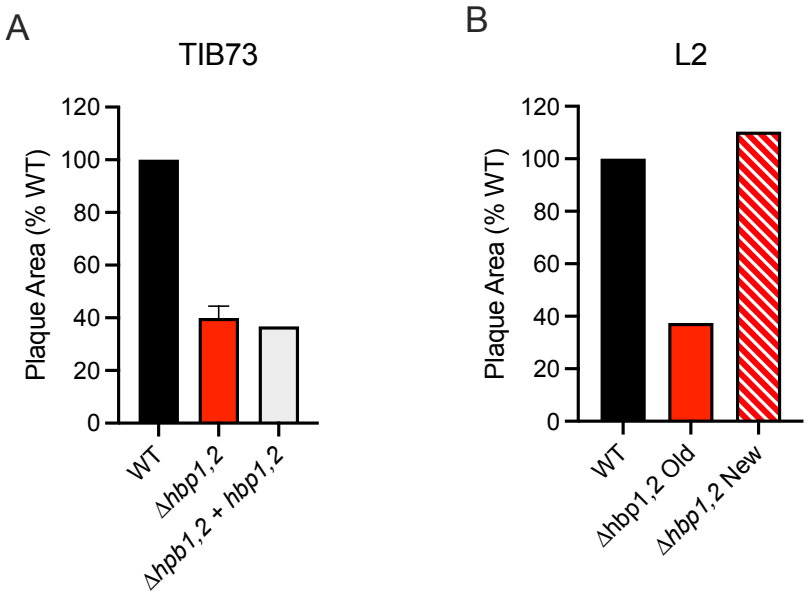

Figure 25. Heme binding proteins 1 and 2 are not required for plaque formation. Plaque areas formed in (A) TIB73 hepatocytes and (B) L2 fibroblasts, measured as a percentage of WT *L. monocytogenes*. Where error bars are present, data are means and SEM of n=2, all other bars represent mean plaque area of n=1.

Discussion

Iron is an essential nutrient and therefore bacterial pathogens must employ appropriate mechanisms to acquire it during infection. We found that the *L. monocytogenes* mutant Δ*hbp1,2* had a plaque-forming defect in L2 fibroblasts and TIB73 hepatocytes, despite replicating similarly to WT intracellularly and in rich broth. Conversely, the mutant Δ*fepCA* exhibited no defects in plaque formation nor intracellular growth. These results suggested that heme uptake is required for intracellular infection, while uptake of ferrous iron is dispensable, and that heme is the main host-derived source of iron used by *L. monocytogenes* during infection. To further investigate this, I determined concentrations of ferrous iron, heme, and BP that would starve bacteria of iron during growth in LSM. I also began determining conditions that would starve host cells of iron in tissue culture. Finally, I found via complementation and whole-genome sequencing that the plaque-forming defect seen in the Δ*hbp1,2* mutant was not due to deletion of *hbp1,2*. Generating a deletion mutant in a clean background confirmed that *hbp1,2* is dispensable for intracellular infection in tissue culture.

The most striking over-arching finding from these experiments is that it is challenging to starve *L. monocytogenes* of iron, even after serial passaging in LSM containing no exogenous

iron source for 12 days. The only *L. monocytogenes* strain that did not grow for the full-length passaging experiment was Δ*fepCA*, which lacks the main ferrous iron transporter. Even the Δ*fri* mutant, which lacks the sole iron storage encoded by *L. monocytogenes,* continued to grow after 12 passages. These results strongly suggested that uptake of trace amounts of ferrous iron in the medium, most likely found in the water, was sufficient for bacterial growth, even when iron storage mechanisms are absent. Because serial passaging proved an inefficient method of starving *L. monocytogenes* of iron, I next used the metal chelator BP to restrict metal availability in the medium. I determined a concentration of BP that halted growth of *L. monocytogenes* without being bactericidal. In optimizing these conditions, I also determined concentrations of $FeCl_2$ and heme to support bacterial growth in LSM. These growth conditions could be used in future research investigating the source of iron used during infection or the regulation of iron uptake systems.

In addition to establishing bacterial growth conditions that restrict iron, I began optimizing tissue culture conditions that would starve host cells of iron, using levels of iron-regulated transcripts as a measure of starvation. I found that culturing cells in low amounts of FBS did indeed lead to an iron starvation state in host cells, but it also caused the cells to grow more sparsely and become round in morphology. To maintain the health of the host cells, I next acutely treated cells cultured in standard medium with BP, which led to increases in transcripts associated with iron starvation. These conditions require further optimization, as this concentration of BP was determined for treatment of a different cell type[106].

L. monocytogenes encodes multiple iron acquisition systems that import ferrous iron. In addition to FepCA, a transport channel encoded by *feoAB* imports ferrous iron from the environment[38,100]. While both FepCA and FeoAB in *L. monocytogenes* are predicted to be regulated by Fur[96,99,100], I observed that deletion of *fepCA* alone was sufficient to render *L. monocytogenes* unable to grow on $FeCl_2$ as a sole exogenous iron source, suggesting that FeoAB is either not expressed or not active in these conditions. Future experiments measuring transcript-level expression of the operons encoding these two transporters will determine the mechanism behind this discrepancy.

We determined that heme binding proteins encoded by *hbp1,2* were not required for *L. monocytogenes* growth in rich broth, LSM, or during intracellular infection. Proteins Hbp1 and Hbp2 function in conjunction with the heme transporter encoded by *hupDGC.* In low-heme conditions, proteins Hbp1 and Hbp2 are secreted and anchored to the cell wall, where they bind exogenous heme or hemoglobin at high affinity[101]. The Hbps then deliver heme to the HupDCG transport system, which transports the heme into the bacterial cytosol. In conditions where heme is abundant (>50 nM), the Hbps are dispensable and the HupDCG system alone imports heme[101]. It is therefore likely that deletion of *hupDCG* will be necessary to render bacteria unable to take up heme.

The overall conclusion of this study is that the ferrous iron transporter FepCA and heme binding proteins Hbp1 and Hbp2 are all dispensable for growth in rich medium and for intracellular infection, and that the cell-to-cell spread defect observed in the original Δ*hbp1,2* strain was caused by an off-target mutation. However, it is still unclear why *L. monocytogenes* iron uptake genes are all downregulated in the host cytosol, as typically the host cytosol is thought to be a nutrient-scarce environment[41]. Future studies will use the experimental conditions determined in this work to investigate the role of iron acquisition during infection.

Chapter 6: Future Directions

Introduction

In this thesis, the bacterial and host determinants of *L. monocytogenes* infection of the gallbladder were investigated. Using a Tn-seq approach, I identified many genes that were required for both replication in the gallbladder lumen. In validating the screen, I found that most genes identified as depleted in the *ex vivo* gallbladder lumen were also required for full virulence in an oral murine model of infection. In characterizing the host determinants of infection, I found that the innate immune sensor STING contributes to the attenuation of *L. monocytogenes* Δ*rex* during murine oral infection, but the molecular mechanism driving this phenotype remains unknown. Both of these studies have opened up new areas of investigation in *L. monocytogenes* infection of the gallbladder, as well as *L. monocytogenes* oral infection in general.

Characterizing the role of PTS-mediated sugar transport during *L. monocytogenes* infection

Despite the gallbladder being an important component of the *L. monocytogenes* multi-organ foodborne infection cycle, the bacterial determinants of replicating in this organ are poorly understood. To address this gap in knowledge, we performed a genome-wide Tn-seq screen in *ex vivo* non-human primate (NHP) gallbladders and identified dozens of genes that are required for replication in the gallbladder lumen, as described in Chapter 2. Genes significantly depleted in the gallbladder condition included two operons encoding mannose/glucose PTS permeases (*mpt, mpo*), as well as their transcriptional (*sigL, manR*) and post-transcriptional regulators (*ptsH, ptsI*). These PTS permeases were previously designated as dispensable for virulence, although were never tested *in vivo*[50].

Identification of PTS sugar transporters as required for replication in the gallbladder reveals novel insights into *L. monocytogenes* carbon metabolism during infection. It is well-accepted that the primary carbon sources consumed by *L. monocytogenes* in the cytosol are host-derived glycerol and hexose-phosphates and thus, the permeases that import these sugars are required for intracellular replication and virulence[107–109]. Conversely, *L. monocytogenes* encodes 84 genes that assemble into 29 complete PTSs, which were previously thought to be dispensable for virulence[50]. Indeed, the main glucose and mannose PTSs, encoded by the *mpt* and *mpo* operons, are not required for intracellular growth or intercellular spread[50,110]. However, we found that strains lacking *mpt* or *mpo* are significantly attenuated in a murine model of listeriosis. These results suggest that glucose and mannose are important nutrients for *L. monocytogenes* replicating in extracellular sites *in vivo*, such as the gallbladder and, to a lesser extent, the liver. Moreover, all PTSs are activated by a phosphorelay between enzyme I (encoded by *ptsI*) and HPr (encoded by *ptsH*). It is then perhaps not surprising that the Δ*ptsI* mutant, which functionally lacks all 29 PTSs, is deficient for intracellular replication and dramatically attenuated *in vivo*. Ongoing studies are aimed at characterizing the intra- vs. extracellular bacterial loads during murine infection with PTS mutants, as well as identifying additional PTSs that are required for full virulence.

Of note, infection with Δ*mpt* resulted in reduced bacterial burdens compared to Δ*mpo*, suggesting that the two seemingly redundant operons play distinct roles during infection. The differences in bacterial burdens between Δ*mpt* and Δ*mpo* were also reflected in the body weights of mice; mice infected with Δ*mpt* lost significantly less weight than WT, whereas those infected with Δ*mpo* lost similar amounts of weight to WT. Previous studies investigating these operons *in vitro* determined that deletion of *mpt* results in increased mpo transcripts, and deletion of *mpo* strongly inhibits mpt expression[50,110]. Based on these *in vitro* transcription data, one would expect Δ*mpt* to be more virulent than Δ*mpo*, and for the double mutant to phenocopy Δ*mpo*. While the double mutant did indeed phenocopy Δ*mpo in vivo*, it remains unclear why Δ*mpt* was significantly less virulent than both Δ*mpo* and Δ*mpt*Δ*mpo*. In addition to *mpt* and *mpo*, *L. monocytogenes* encodes 2 additional glucose/mannose PTSs[50] and I have found in preliminary experiments that the Δ*mpt*Δ*mpo* mutant expresses increased levels of these 2 additional PTSs compared to WT (data not shown). Future studies will continue investigating the expression regulation of PTSs *in vivo*, with a particular focus on SigL and ManR, the transcriptional activators of *mpt* and *mpo* that were also identified in our Tn-seq analysis as important for gallbladder survival.

The roles of Rex and STING during *L. monocytogenes* gallbladder infection remain unclear

While the study presented in Chapter 2 identified bacterial determinants of gallbladder infection, the experiments in Chapter 3 sought to characterize how *L. monocytogenes* interacts with the host innate immune response, and how those interactions influence colonization and replication in the gallbladder. Previous studies have strongly suggested that the innate immune system plays a role in bacterial clearance from the gallbladder[10], but whether these cells are recruited to the gallbladder to promote clearance had not been investigated. Further characterizing the host response to infection of the gallbladder will provide a deeper understanding into the multi-organ infection cycle of *L. monocytogenes*.

In this chapter, I tested the hypothesis that the *L. monocytogenes* mutant Δ*rex* secretes excess CDA in response to bile exposure in the gallbladder, leading to an increase in STING-dependent IFN-β expression and more rapid clearance by the host immune response. Measuring transcripts encoding the CDA exporter MdrT suggested that Δ*rex* does not secrete increased CDA compared to WT during replication in rich broth, both in the presence and absence of bile. These experiments were performed using reconstituted porcine bile, and we wanted develop a method to measure bacterial transcription during *in vivo* murine infection. To this end, I engineered *L. monocytogenes* strains to express RFP from the native promoter of *mdrT*, such that RFP fluorescence could be measured as a proxy for *mdrT* transcription. Preliminary attempts to orally infect mice with these fluorescent strains and quantify bacterial fluorescence by flow cytometry were unsuccessful. I found that fluorescence from samples harvested from uninfected mice was indistinguishable from infected mice, which could be due to either autofluorescence of bile or insufficient bacterial loads in the gallbladders of infected mice. These preliminary experiments were performed using B6 mice, which are relatively resistant to *L. monocytogenes* oral infection and gallbladder colonization[15]. These pilot experiments will therefore be repeated in the more

susceptible BALB/c mouse strain to determine whether RFP fluorescence can be used to indirectly quantify transcription in murine gallbladders.

Oral infection results demonstrated that STING is indeed involved in the attenuation of Δ*rex*, as evidenced by Δrex exhibiting less attenuation in *Tmem173*$^{-/-}$ mice than B6. However, the lack of gallbladder colonization in the *Tmem173*$^{-/-}$ mice by either *L. monocytogenes* strain meant that we could not use this model to evaluate the role of STING specifically in the gallbladder. Interestingly, Δ*rex* was significantly attenuated in the mesenteric lymph nodes (MLN) following oral infection of B6 mice, and this attenuation was partially rescued in the *Tmem173*$^{-/-}$ background. This result supports our hypothesis that Δ*rex* induces an innate immune response leading to its clearance, and me to hypothesize that Δ*rex* disseminates to peripheral organs less efficiently than WT. Poor replication in the MLN could therefore explain the decreased bacterial loads of Δ*rex* in the spleens, livers, and gallbladders of B6 mice. I also hypothesize that Δ*rex* induction of a STING-dependent immune response leads to increased recruitment of immune cells to the MLN. To test these hypotheses, future studies will quantify immune cell infiltration to the MLN in both WT and *Tmem173*$^{-/-}$ mice infected with *L. monocytogenes* WT or Δ*rex* using flow cytometry. Together, characterizing the innate immune responses in the gallbladder via histology and in the MLN via flow cytometry will lead to a more complete understanding of the host responses to *L. monocytogenes* infection.

Concluding Remarks

The work presented in this thesis has shed light on the *L. monocytogenes* and host determinants of colonizing and replicating in the gallbladder following foodborne infection. Many open questions remain, but the experiments reported here have established multiple new areas of investigation into *L. monocytogenes* pathogenesis. Given that listeriosis remains a significant public health concern, especially in immunocompromised groups, deepening our understanding of how this bacterium causes disease and how the host immune system contributes to its pathogenesis is crucial to identifying therapeutic targets.

Chapter 7: Materials and Methods

Bacterial strains and culture conditions

The bacterial strains used in this study are listed in S2 Table. *L. monocytogenes* was cultured in brain heart infusion (BHI) and *E. coli* was cultured in Luria-Bertani (LB) broth at 37°C, with shaking (220 rpm), unless otherwise specified. Antibiotics (purchased from Sigma Aldrich) were used at the following concentrations: streptomycin, 200 μg/mL; chloramphenicol, 10 μg/mL (*E. coli*) and 7.5 μg/mL (*L. monocytogenes*); and carbenicillin, 100 μg/mL. *L. monocytogenes* mutants were derived from wild type strain 10403S[111,112]. Plasmids were introduced to *E. coli* via chemical competence and heat shock and introduced into *L. monocytogenes* via trans-conjugation from *E. coli* SM10[113]. All strains used in this work are listed in Tables 4 and 5.

Murine cells

L2 fibroblasts, TIB73 hepatocytes, and ISRE reporter cells were incubated at 37°C in 5% CO2 in Dulbecco's modified Eagle's medium (DMEM) with 10% heat-inactivated fetal bovine serum (FBS) (Cytiva) and supplemented with sodium pyruvate (1 mM) and L-glutamine (1 mM) (L2 Medium). For passaging, cells were maintained in Pen-Strep (100 U/ml) but were plated in antibiotic-free media for infections.

Bone marrow-derived macrophages (BMDMs) were routinely incubated in DMEM supplemented with 20% heat-inactivated FBS, 1 mM sodium pyruvate, 1 mM L-glutamine, 10% supernatant from M-CSF-producing 3T3 cells, and 55 μM β-mercaptoethanol (BMDM medium). BMDMs were isolated as previously described[114]. Briefly, femurs and tibias from C57BL/6 mice were crushed with a mortar and pestle in 20 mL BMDM medium and strained through 70-μm cell strainers. Cells were plated in 150-mm untreated culture dishes, supplemented with fresh BMDM medium at day 3, and then harvested by resuspending cells in cold PBS at day 7. BMDMs were aliquoted in 80% BMDM medium, 10% FBS, and 10% DMSO and stored in liquid nitrogen.

Mice

This study was carried out in strict accordance with the recommendations in the Guide for the Care and Use of Laboratory Animals of the National Institutes of Health. All protocols were reviewed and approved by the Animal Care and Use Committee at the University of Washington (Protocol 4410–01). All animals were group-housed in University of Washington Department of Comparative Medicine facilities under specific pathogen-free conditions. Female BALB/c WT mice (#000651) were purchased from The Jackson Laboratory at 5 weeks of age and used in experiments when they were 6–7 weeks old. WT and *Tmem157*$^{-/-}$ (StingKO) C57B6/6J were bred in-house using breeders gifted from the Woodward lab.

Vector construction and cloning

To construct deletion mutants in *L. monocytogenes*, ~700 bp regions up- and downstream of the gene of interest were PCR amplified using *L. monocytogenes* 10403S genomic DNA as a template. PCR products were digested and ligated into pLIM (gift from Arne Rietsche, Case Western). pLIM plasmids were then transformed into *E. coli* and sequences confirmed via Sanger sequencing (Azenta). Plasmids harboring mutant alleles were then introduced into *L. monocytogenes* via trans-conjugation and integrated into the chromosome as previously described[115,116].

Complemented strains of *L. monocytogenes* were generated using the pPL2 integration plasmid[117]. Genes were PCR amplified with their respective native promoters using *L. monocytogenes* 10403S genomic DNA as a template, and sequences were confirmed by Sanger sequencing. The constructed pPL2 plasmids were then introduced into *L. monocytogenes* by trans-conjugation and integration into the *L. monocytogenes* chromosome was confirmed by antibiotic resistance.

Fluorescent transcriptional reporters were engineered to express GFP constitutively from the HyPer promoter using the integrative plasmid pPL1[57,117]. This was integrated into the chromosome of a phage-cured WT *L. monocytogenes* strain DP-L4056[117]. Next, the promoter regions of peroxidase genes were amplified and ligated to mTAG-RFP via NEBuilder HiFi DNA assembly. The mTAG-RFP was amplified from DP-L6508[57]. The promoter-rfp fusions were ligated into pPL2t and confirmed via PCR and Sanger sequencing. *E. coli* SM10 harboring the pPL2t.Promoter-rfp constructs were mated with MLR-L850 (pPL1.pHyper-gfp) to generate the two-color transcriptional reporter strains. Integration was confirmed by antibiotic resistance and PCR.

Growth curves in NHP bile

NHP bile aliquots were plated to evaluate sterility and stored at -80°C. Before an experiment, aliquots were thawed overnight at 4°C and warmed to room temperature immediately before the inoculation into a 96-well plate. Overnight *L. monocytogenes* cultures were washed twice, resuspended in PBS, and 10^5 CFU were inoculated into either NHP bile or BHI, in a total volume of 100 µL per well. Bacterial growth was measured by collecting samples of the cultures, serially diluting in PBS, and plating for CFU. For experiments performed anaerobically, NHP bile aliquots were thawed overnight in GasPak EZ Anaerobe gas-generating pouches (Becton Dickinson), and BHI and the 96-well plate were degassed overnight in a closed-system anaerobic chamber (Don Whitley Scientific A35 anaerobic work station). After washing and resuspending aerobically-grown overnight *L. monocytogenes* cultures in PBS, the *L. monocytogenes* suspensions and bile aliquots were transferred into the anaerobic chamber and the plate was inoculated and incubated within the chamber. Bacterial growth was measured by collecting samples of the cultures, serially diluting in PBS, and plating for CFU.

L. monocytogenes transposon library in NHP gallbladders

The *L. monocytogenes* transposon library[49] was inoculated directly from the -80°C stock into BHI broth and incubated at 37°C for 2 hours, with shaking. The library was then washed twice and resuspended in PBS to a density of 10^8 CFU per 2 kg of NHP body weight. The inoculum size was determined to maintain 1,000-fold coverage of the library. Gallbladders were injected via syringe with 100 µL of inoculum, the injection site was sealed with liquid bandage (3M), and incubated in a 15 cm petri dish at 37°C and 5% CO_2. After 30 minutes, 200 µL of bile was removed from the gallbladder via syringe, serially diluted, and plated to enumerate CFU. 6 hours post-injection, bile was extracted from the organ via syringe and the remaining luminal contents collected via cell scraper after resection. The gallbladder contents were diluted into 50 mL BHI broth and incubated at 37°C for 2 hours, with shaking. The cultures were pelleted, washed twice with PBS, and stored at -80°C.

Tn-seq library preparation, sequencing, and analysis

Genomic DNA was extracted using a Quick-DNA Fungal/Bacterial MiniPrep Kit (Zymo Research). DNA was diluted to 3 µg/130 µL in microTUBES (Covaris) and sheared in duplicate on a Covaris LE220 Focused-Ultrasonicator using the following settings: duty cycle 10%; peak intensity 450; cycles per burst 100; duration 100 sec. Sheared DNA was then end-repaired with NEBNext End Repair (NEB), and purified with Ampure SPRIselect beads (Beckman Coulter). Poly-C tails were added to 1 µg of end-repaired DNA with Terminal Transferase (Promega), then purified with Ampure SPRIselect beads. Transposon junctions were PCR amplified with primers olj376 and pJZ_RND1 (Sx Table) using 500 ng DNA and KAPA HiFi Hotstart Mix (Kapa Biosystems). PCR reactions were stopped once the inflection point of amplification was reached (6-14 cycles), and amplified transposon junctions were purified with Ampure SPRIselect beads. Barcoded adaptors were added using KAPA HiFi Hotstart Mix, and primers pJZ_RND2 and one TdT_Index per sample. DNA was purified and size-selected with Ampure SPRIselect beads for 250-450 bp fragments. Samples were pooled and sequenced as single end 50 bp reads on a NextSeq MO150 sequencer with a 7% PhiX spike in and primer pJZTnSq_SeqPrimer.

Trimmed reads were mapped to the *L. monocytogenes* 10403S NC_17544 reference genome in PATRIC (now https://www.bv-brc.org/) and assessed for essentiality using TRANSIT software [Wattam 2014; Wattam 2017; DeJesus 2015]. Genes were considered required for survival or growth in *ex vivo* NHP gallbladders if they met the following criteria: 5 or more insertion sites in the input libraries, a *p* value less than 0.05, and a 1.5-fold or greater depletion after incubation in the gallbladder.

Intracellular growth curves

To measure intracellular growth kinetics in macrophages, BMDMs were plated in TC-treated 24-well plates at a density of 6 x 10^5 cells per well in BMDM medium. *L. monocytogenes* cultures were grown overnight at 30°C, stationary. The next day, *L. monocytogenes* cultures were washed twice, resuspended in PBS, and added to BMDMs at an MOI of 0.1. After 30 minutes,

cells were washed twice with PBS and BMDM medium containing gentamicin (50 μg/mL) was added to kill extracellular bacteria. At various time points post-infection, cells were washed twice with PBS and lysed in 250 μL cold 0.1% Triton-X in PBS. Lysates were then serially diluted and plated to enumerate intracellular CFU. To measure growth kinetics in hepatocytes, TIB73 cells were plated in TC-treated 24-well plates at a density of 2 x 10^5 cells per well in L2 medium, then infected with *L. monocytogenes* cultures the following day at an MOI of 50. After 1 hour, cells were washed twice with PBS and BMDM medium containing gentamicin (50 μg/mL) was added to kill extracellular bacteria. At various time points post-infection, cells were washed twice with PBS and lysed in 250 μL cold 0.1% Triton-X in PBS. Lysates were then serially diluted and plated to enumerate intracellular CFU.

Plaque assays

Plaque assays were performed as previously described[57,83]. In brief, 1.2 x 10^6 L2 fibroblasts were plated in TC-treated 6-well plates overnight in L2 medium. *L. monocytogenes* cultures were grown overnight at 30°C stationary. The next day, *L. monocytogenes* cultures were diluted 1:10 in PBS and 5 μL of diluted bacteria was added to cell monolayers. To measure intercellular spread in hepatocytes, TIB73 cells were seeded at a density of 1.5 x 10^6 cells per well in TC-treated 6-well plates overnight in L2 medium. Overnight bacterial cultures grown statically at 30°C were diluted 1:20 in PBS and 5 μL of diluted bacteria was added to the monolayers. After 1 hour of infection in either L2 and TIB73 cells, monolayers were washed twice with PBS, then overlaid with 3 mL of molten agarose solution (1:1 mixture of 2X DMEM and 1.4% SuperPure Agarose (U.S. Biotech Sources, LLC), containing 10 μg/mL gentamicin). After 3 days of incubation, 2 mL of molten agarose solution containing Neutral Red was added to wells to visualize plaques. After 12-24 hours, plates were scanned, plaque areas quantified using ImageJ software[118] and normalized to WT plaque areas.

Measuring interferon expression with ISRE-Luc

The ISRE-Luc bioassay was performed as previously described[24]. In brief, WT, *cGas*$^{-/-}$, and *Sting*$^{-/-}$ BMDMs were seeded at a density of 6 x 10^5 cells per well in TC-treated 24-well plates overnight in BMDM medium. *L. monocytogenes* cultures were grown overnight at 30°C stationary. The next day, *L. monocytogenes* cultures were washed twice, resuspended in PBS, and added to BMDMs at an MOI = 10. After 30 minutes, cells were washed twice with PBS and BMDM medium containing gentamicin (50 μg/mL) was added to kill extracellular bacteria. After a total infection time of 6 hours, BMDM supernatants were harvested and stored at -80°C. The remaining supernatant was then aspirated, cells were washed twice with PBS, and then cells were lysed in 250 μL cold 0.1% Triton-X in PBS. Lysates were then serially diluted and plated to enumerate intracellular CFU.

ISRE-L929 BMMs were seeded at a density of 5 x 10^4 cells per well in TC-treated 96-well plates overnight in L2 medium. The next day, media was aspirated from the BMMs, and 30 μL of fresh L2 medium was added to each well. BMDM supernatants were then thawed to room temperature, and 20 μL of each supernatant was added to the cells. BMMs were then incubated

for 4 hours, then the culture medium was aspirated and 50 µL of TNT lysis buffer (20 mM Tris; 200 mM NaCl; 1% Triton-X) was added to each well. 40 µL of lysate was transferred to a white, opaque 96-well plate, and 40 µL of luciferase substrate solution (20 mM Tricine, 2.67 mM $MgSO_4 7H_2O$, 0.1 mM EDTA, 33.3 mM DTT, 530 µM ATP, 270 µM acetyl CoA lithium salt, 470 µM luciferin, 5 mM NaOH, 265 µM magnesium carbonate hydroxide) was added to each well. Luminescence was quantified using a Synergy HT microplate reader (BioTek).

Measuring transcription in murine cells

WT, *cGas*$^{-/-}$, and *Sting*$^{-/-}$ BMDMs were seeded at a density of 1 x 10^6 cells per well in TC-treated 12-well plates in BMDM medium, then infected with *L. monocytogenes* cultures at an MOI of 10, as described above. After 6 hours of incubation, cells were washed twice with PBS and 500 µL of Trizol reagent (Invitrogen) was added to each well to lyse the cells. RNA was isolated from the Trizol-lysates, followed by treatment with TURBO Dnase per manufacturer's specification (Invitrogen). cDNA was then synthesized using iScript cDNA synthesis Kit (Bio-Rad) according to the manufacturers' instructions and qPCR was then performed using the iTaq universal SYBR green supermix (Bio-Rad) and primers in Table 6.

Measuring bacterial transcription following porcine bile exposure

To measure bacterial transcription, overnight *L. monocytogenes* cultures were normalized to an OD_{600} of 0.02 in 27 mL BHI in 250-mL flasks and incubated at 37°C with shaking. After 4 hours, porcine bile (Sigma Aldrich) was added at concentrations of 0.1% and 1.1%, and then flasks were incubated at 37°C with shaking. Samples of cultures were removed for downstream processing 0 min (just before addition of porcine bile), 10 minutes, and 30 minutes following addition of porcine bile. RNA was then isolated from bacteria as previously described[71]. Briefly, bacterial cultures were mixed 1:1 with ice-cold methanol, pelleted, and stored at -80°C. Bacteria were lysed in acidified phenol:chloroform containing 1% SDS by bead beating with 0.1 mm diameter silica/zirconium beads. Nucleic acids were precipitated from the aqueous fraction for 1 hour at -80°C in ethanol containing sodium acetate (150 mM, pH 5.2). Precipitated nucleic acids were washed with ethanol and treated with TURBO DNase per manufacturer's specification (Invitrogen). cDNA was then synthesized using iScript cDNA synthesis Kit (Bio-Rad) according to the manufacturers' instructions and qPCR was then performed using the iTaq universal SYBR green supermix (Bio-Rad) and primers in Table 6.

CDA-Luc Bioassay

To measure CDA abundance in *L. monocytogenes* cultures, overnight bacterial cultures were normalized to an OD600 of 0.02 in 5 mL BHI and incubated at 37°C with shaking. After 4 and 8 hours, the OD600 of each culture was measured, 1.5 mL (4 hours) or 1 mL (8 hours) was pelleted, and supernatants transferred to new tubes. The bacterial pellets were resuspended in cold pull-down buffer (100 mM Tris pH 7.5, 20 mM MgCl2, 50 mM NaCl), then sonicated to lyse

bacterial cells. CDA in the supernatant and bacterial fractions was then quantified using the CDA-Luc bioassay as described previously[64].

Oral murine infections

Infections were performed as previously described[7,27]. Streptomycin (5 mg/mL) was added to drinking water 48 hours prior to infection and food and water were removed 16 hours before infection. *L. monocytogenes* cultures were grown overnight at 30°C, stationary. Overnight cultures were diluted 1:10 in 5 mL fresh BHI and incubated at 37°C for 2 hours, with shaking. Bacteria were then washed twice and diluted in PBS. Mice were fed 10^8 bacteria in 20 µL of PBS and food and water were returned immediately after infection. Inocula were serially diluted and plated. Body weights were recorded daily and mice were humanely euthanized for tissue collection. Tissues were homogenized in the following volumes of 0.1% Igepal CA-630 (Sigma): MLN, 3 mL; cecum (contents removed and tissues rinsed with PBS), 4 mL; liver, 5 mL; spleen, 3 mL. Feces were homogenized in 1 mL of 0.1% Igepal with a sterile stick, and gallbladders were ruptured and crushed in 500 µL of 0.1% Igepal with a sterile stick. All samples were serially diluted in PBS and plated to enumerate CFU.

Histology and Immunohistochemistry

Female 6-week-old BALB/c mice were orally infected with *L. monocytogenes* as described above. A group of uninfected mice was included, which received streptomycin in the drinking water and were fasted before infection, but these mice were fed PBS alone. Four days post-infection, mice were humanely euthanized and livers were harvested with the gallbladders still attached and intact. The organs were left whole and fixed in 10% formalin for 3 days with gentle rocking. Fixed organs were then de-identified and transferred to the UW Histology and Imaging Core for slide preparation and staining, and slides were scored for inflammation and positive antibody staining by Dr. Jessica Schneider.

J7 infections with fluorescent reporters

J774 cells were plated in 12-well TC-treated dishes at 10^6 cells per well. *L. monocytogenes* transcriptional reporter strains were grown to mid-log phase at 37°C with shaking. After being washed twice and resuspended in phosphate-buffered saline (PBS), bacterial suspensions were added to the cells at an MOI of 10. At 1 hour postinfection, cells were washed twice with PBS, and medium containing gentamicin (50mg/ml) was added to each well. At 6 hours postinfection, the cells were washed twice with PBS, treated with 0.25% trypsin (Gibco), and resuspended in an equal volume of medium. The cells were then fixed with 2% formaldehyde, washed twice with flow buffer (PBS containing 5% FBS), and resuspended in 300 µl flow buffer. Flow cytometry was performed on an LSR II flow cytometer (BD) and analyzed using FlowJo (FlowJo, LLC). Cells were discriminated from debris by forward scatter area (FSC-A) and side scatter area (SSC-A). Single cells were gated using FSC-A and forward scatter height (FSC-H). The GFP gate was set to include 5% of the uninfected sample; this gate represents infected cells

and is referred to as GFP positive. Within the infected-cell population, the RFP gate was set to include 5% of cells infected with pH-gfp; this gate is referred to as RFP positive. Reported values represent percent RFP-positive cells within GFP-positive cells of a given sample.

Growth curves in rich broth

To evaluate aerobic growth in rich medium, *L. monocytogenes* overnight cultures were normalized to an OD600 of 0.02 in 25 mL BHI in 250-mL flasks at 37˚C with shaking. At each time point, bacteria were serially diluted and plated on BHI agar to enumerate CFU.

Serial passaging in *Listeria* synthetic medium

Cultures of *L. monocytogenes* strains were grown overnight in tryptic soy broth (TSB). The following day, bacteria were washed twice with PBS then normalized to OD_{600} = 0.02 in *Listeria* synthetic medium (LSM) with or without an exogenous iron source, and incubated at 37°C with shaking. Every 24 hours, OD_{600} was measured and each culture was back-diluted into fresh LSM (with or without iron) such that the OD_{600} = 0.02. This was repeated every day for 12 days.

Growth curves in *Listeria* synthetic medium

L. monocytogenes strains were grown overnight in media meant to pre-condition the bacteria for the next day's growth curve conditions, because transitioning from conditions with no iron to higher concentrations of iron can be toxic to the bacteria. If the bacteria were used for growth curves in LSM containing $FeCl_2$, then the overnight cultures were grown in LSM containing 2.5 μM $FeCl_2$. Similarly, if the bacteria were used for growth curves in LSM containing heme, then the overnight cultures were grown in LSM containing 1 μM heme. The next day, cultures were washed twice with PBS then normalized to OD_{600} = 0.05 in LSM containing increasing concentrations of $FeCl_2$ or heme. In experiments with bipyridyl (BP) treatment, 2,2'-bipyridyl (Sigma) resuspended in ethanol was added to cultures.

Iron starvation of host cells

To measure the iron starvation state of host cells in tissue culture, TIB73 hepatocytes were seeded at a density of 1.5 x 10^6 cells/well in TC-treated 6-well plates. The following day, cells were washed twice with PBS and then lysed with 750 μL Trizol reagent. RNA isolation, RT-PCR, and qPCR were then performed as described above (see "Measuring Transcription in Murine Cells").

Table 4. *E. coli* strains used in this study.

Strain	Description	Reference or Source
XL1	for strain construction	Stratagene
SM10	for trans-conjugation	[113]
MLR-E893	pLIM1	Gift from A. Rietsch
MLR-E1156	pLIM.ccpA-KO	This study
MLR-E1157	pLIM.ptsI-KO	
MLR-E1158	pLIM.trxA-KO	
MLR-E1159	pLIM.purB-KO	
MLR-E1160	pLIM.atpB-KO	
MLR-E1161	pLIM.mpt-KO	
MLR-E1162	pLIM.mpo-KO	
MLR-E006	pPL2	[117]
MLR-E1171	pPL2.Pnat-ccpA	This study
MLR-E1172	pPL2.Pnat-ptsI	
MLR-E1173	pPL2.Pnat-trxA	
MLR-E1174	pPL2.purB-comp	
MLR-E1175	pPL2.atpB-comp	
MLR-E1176	pPL2.mpt-comp	
MLR-E1177	pPL2.mpo-comp	
MLR-E873	pKSV7.ahpA-KO	[69]
MLR-E947	pLIM.lmo0367-KO	
MLR-E949	pLIM.lmo1609-KO	
MLR-E950	pLIM.tpx-KO	
MLR-E951	pLIM.fri-KO	
MLR-E952	pLIM.lmo0983-KO	
MLR-E972	pPL2t.P-kat-rfp	
MLR-E973	pPL2t.P-chdC-rfp	
MLR-E974	pPL2t.P-ahpA-rfp	
MLR-E975	pPL2t.P-lmo0367-rfp	
MLR-E976	pPL2t.P-lmo0983-rfp	
MLR-E977	pPL2t.P-tpx-rfp	
MLR-E978	pPL2t.P-fri-rfp	
MLR-E979	pPL2t.P-lmo1609-rfp	
MLR-E980	pPL2t.P-ohrA-rfp	
MLR-E868	pPL2t.pH-rfp	
MLR-E738	pKSV7.fepCA-KO	This study (Mauna Edrozo)
MLR-E739	pKSV7.hbp1,2-KO	
MLR-E1189	pPL2.hbp1,2	This study

Table 5. *L. monocytogenes* strains used in this study.

Strain	Description	Reference / Source
MLR-L001	WT 10403S	[119]
MLR-L1148	ΔccpA	This study
MLR-L1149	ΔptsI	
MLR-L1150	ΔtrxA	
MLR-L1151	ΔpurB	
MLR-L1152	ΔatpB	
MLR-L1153	Δmpt	
MLR-L1154	Δmpo	
MLR-L1155	Δmpt Δmpo	
MLR-L449	clpX::himar1	[55]
MLR-L1163	ΔccpA p-ccpA	This study
MLR-L1164	ΔptsI p-ptsI	
MLR-L1165	ΔtrxA p-trxA	
MLR-L1166	ΔpurB p-purB	
MLR-L1167	ΔatpB p-atpB	
MLR-L1170	clpX::himar1 p-clpX	
MLR-L752	Δrex	[27]
MLR-L957	Δrex + rex	
MLR-L955	Δbsh	
JW516	ΔmdrMTAC	[63]
JW33	tetR::Tn	[24]
MLR-L1085	Δrex tetR::Tn	This work
MLR-L828	Δkat (lmo2785)	[73]
MLR-L174	ΔohrA (lmo2199)	[57]
MLR-L879	ΔahpA (lmo1604)	[69]
MLR-L880	ΔkatΔahpA	
MLR-L944	ΔchdC (lmo2213)	
MLR-L948	Δlmo0367	
MLR-L953	Δlmo1609	
MLR-L954	Δlmo0983	
MLR-L959	Δtpx (lmo1583)	
MLR-L960	Δfri (lmo0943)	
MLR-L981	pH-gfp P-kat-rfp	
MLR-L982	pH-gfp P-chdC-rfp	
MLR-L983	pH-gfp P-ahpA-rfp	
MLR-L984	pH-gfp pH-rfp	
MLR-L985	pH-gfp P-lmo0367-rfp	

MLR-L986	pH-gfp P-fri-rfp	
MLR-L987	pH-gfp P-lmo0983-rfp	
MLR-L988	pH-gfp P-tpx-rfp	
MLR-L989	pH-gfp P-lmo1609-rfp	
MLR-L990	pH-gfp P-ohrA-rfp	

Table 6. qPCR primers used in this study.

Name	Sequence	Citation
tfrc F	gcagcattggtcaaaacatgg	120
tfrc R	gctttgggcatttgcaacc	
ferritin-h F	gctgaatgcaatggagtgtgca	
ferritin-h R	ggcacccatcttgcgtaagttg	
dmt1 F	ggagtactcttgttttagctttcgtaaa	106
dmt1 R	ccagactgcaaatcagattcg	
mdrT F	ccccaaccatcattacccgctgaactaaatccgtatag	25
mdrT R	ggttggattgtggattcgtatgattggcgcg	
mdrM F	ggtattttgattgttatgcttatgg	
mdrM R	ttgtaaatcgttcaattaaaaaggc	
rpoB F	gcggatgaagaggataattacg	23
rpoB R	ggaatccattgatggaccgtta	
hprt F	atcattatgccgaggatttgg	From Melissa Locke
hprt R	gcaaagaacttatagccccc	
ifnb F	ctggagcagctgaatggaaag	82
ifnb R	cttgaagtccgccctgtaggt	

References:

1. Hafner L, Pichon M, Burucoa C, et al. Listeria monocytogenes faecal carriage is common and depends on the gut microbiota. *Nat Commun*. 2021;12(1):6826. doi:10.1038/s41467-021-27069-y

2. McCollum JT, Cronquist AB, Silk BJ, et al. Multistate Outbreak of Listeriosis Associated with Cantaloupe. *N Engl J Med*. 2013;369(10):944-953. doi:10.1056/NEJMoa1215837

3. EFSA Panel on Biological Hazards (BIOHAZ), Ricci A, Allende A, et al. Listeria monocytogenes contamination of ready-to-eat foods and the risk for human health in the EU. *EFS2*. 2018;16(1). doi:10.2903/j.efsa.2018.5134

4. CDC. Listeria Outbreaks. Listeria Infection (Listeriosis). September 19, 2024. Accessed November 8, 2024. https://www.cdc.gov/listeria/outbreaks/index.html

5. Investigations O of I and. Recalls, Market Withdrawals, & Safety Alerts. FDA. October 1, 2024. Accessed November 8, 2024. https://www.fda.gov/safety/recalls-market-withdrawals-safety-alerts

6. Camargo, Anderson C, Woodward, Joshua J, Call, Douglas R, Nero, Luis A. Listeria monocytogenes in Food-Processing Facilities, Food Contamination, and Human Listeriosis: The Brazilian Scenario. *Foodborne Pathogens and Disease*. 2017;14:623-636.

7. Louie A, Zhang T, Becattini S, Waldor MK, Portnoy DA. A Multiorgan Trafficking Circuit Provides Purifying Selection of Listeria monocytogenes Virulence Genes. Miller SI, ed. *mBio*. 2019;10(6). doi:10.1128/mBio.02948-19

8. Melton-Witt JA, Rafelski SM, Portnoy DA, Bakardjiev AI. Oral Infection with Signature-Tagged Listeria monocytogenes Reveals Organ-Specific Growth and Dissemination Routes in Guinea Pigs. Camilli A, ed. *Infect Immun*. 2012;80(2):720-732. doi:10.1128/IAI.05958-11

9. Tucker JS, Cho J, Albrecht TM, Ferrell JL, D'Orazio SEF. Egress of Listeria monocytogenes from Mesenteric Lymph Nodes Depends on Intracellular Replication and Cell-to-Cell Spread. Bäumler AJ, ed. *Infect Immun*. Published online March 14, 2023:e00064-23. doi:10.1128/iai.00064-23

10. Zhang T, Abel S, Abel zur Wiesch P, et al. Deciphering the landscape of host barriers to *Listeria monocytogenes* infection. *Proc Natl Acad Sci USA*. 2017;114(24):6334-6339. doi:10.1073/pnas.1702077114

11. Hardy J, Francis KP, DeBoer M, Chu P, Gibbs K, Contag CH. Extracellular Replication of *Listeria monocytogenes* in the Murine Gall Bladder. *Science*. 2004;303(5659):851-853. doi:10.1126/science.1092712

12. Hardy J, Margolis JJ, Contag CH. Induced Biliary Excretion of *Listeria monocytogenes*. *Infect Immun*. 2006;74(3):1819-1827. doi:10.1128/IAI.74.3.1819-1827.2006

13. D'Orazio SEF. Animal models for oral transmission of Listeria monocytogenes. *Front Cell Infect Microbiol*. 2014;4. doi:10.3389/fcimb.2014.00015

14. Gregory SH, Sagnimeni AJ, Wing EJ. Bacteria in the bloodstream are trapped in the liver and killed by immigrating neutrophils. *The Journal of Immunology*. 1996;157(6):2514-2520. doi:10.4049/jimmunol.157.6.2514

15. Bou Ghanem EN, Jones GS, Myers-Morales T, Patil PD, Hidayatullah AN, D'Orazio SEF. InlA Promotes Dissemination of Listeria monocytogenes to the Mesenteric Lymph Nodes during Food Borne Infection of Mice. O'Riordan M, ed. *PLoS Pathog*. 2012;8(11):e1003015. doi:10.1371/journal.ppat.1003015

16. Jones GS, Bussell KM, Myers-Morales T, Fieldhouse AM, Bou Ghanem EN, D'Orazio SEF. Intracellular Listeria monocytogenes Comprises a Minimal but Vital Fraction of the Intestinal Burden following Foodborne Infection. Roy CR, ed. *Infect Immun*. 2015;83(8):3146-3156. doi:10.1128/IAI.00503-15

17. Begley M, Gahan CGM, Hill C. The interaction between bacteria and bile. *FEMS Microbiol Rev*. 2005;29(4):625-651. doi:10.1016/j.femsre.2004.09.003

18. Gunn JS, Marshall JM, Baker S, Dongol S, Charles RC, Ryan ET. Salmonella chronic carriage: epidemiology, diagnosis, and gallbladder persistence. *Trends in Microbiology*. 2014;22(11):648-655. doi:10.1016/j.tim.2014.06.007

19. Kreuder AJ, Schleining JA, Yaeger M, Zhang Q, Plummer PJ. RNAseq Reveals Complex Response of Campylobacter jejuni to Ovine Bile and In vivo Gallbladder Environment. *Front Microbiol*. 2017;8:940. doi:10.3389/fmicb.2017.00940

20. Dussurget O, Cabanes D, Dehoux P, et al. Listeria monocytogenes bile salt hydrolase is a PrfA-regulated virulence factor involved in the intestinal and hepatic phases of listeriosis. *Mol Microbiol*. 2002;45(4):1095-1106. doi:10.1046/j.1365-2958.2002.03080.x

21. Begley M, Hill C, Gahan CGM. Identification and disruption of *btlA* , a locus involved in bile tolerance and general stress resistance in *Listeria monocytogenes*. *FEMS Microbiology Letters*. 2003;218(1):31-38. doi:10.1111/j.1574-6968.2003.tb11494.x

22. Sleator RD, Wemekamp-Kamphuis HH, Gahan CGM, Abee T, Hill C. A PrfA-regulated bile exclusion system (BilE) is a novel virulence factor in *Listeria monocytogenes*. *Molecular Microbiology*. 2005;55(4):1183-1195. doi:10.1111/j.1365-2958.2004.04454.x

23. Crimmins GT, Herskovits AA, Rehder K, et al. *Listeria monocytogenes* multidrug resistance transporters activate a cytosolic surveillance pathway of innate immunity. *Proc Natl Acad Sci USA*. 2008;105(29):10191-10196. doi:10.1073/pnas.0804170105

24. Woodward JJ, Iavarone AT, Portnoy DA. c-di-AMP Secreted by Intracellular *Listeria monocytogenes* Activates a Host Type I Interferon Response. *Science*. 2010;328(5986):1703-1705. doi:10.1126/science.1189801

25. Quillin SJ, Schwartz KT, Leber JH. The novel *Listeria monocytogenes* bile sensor BrtA controls expression of the cholic acid efflux pump MdrT. *Molecular Microbiology*. 2011;81(1):129-142. doi:10.1111/j.1365-2958.2011.07683.x

26. Zhang Y, Gonzalez-Gutierrez G, Legg KA, et al. Discovery and structure of a widespread bacterial ABC transporter specific for ergothioneine. *Nat Commun*. 2022;13(1):7586. doi:10.1038/s41467-022-35277-3

27. Halsey CR, Glover RC, Thomason MK, Reniere ML. The redox-responsive transcriptional regulator Rex represses fermentative metabolism and is required for Listeria monocytogenes pathogenesis. O'Riordan M, ed. *PLoS Pathog*. 2021;17(8):e1009379. doi:10.1371/journal.ppat.1009379

28. Dowd GC, Joyce SA, Hill C, Gahan CGM. Investigation of the Mechanisms by Which *Listeria monocytogenes* Grows in Porcine Gallbladder Bile. Flynn JL, ed. *Infect Immun*. 2011;79(1):369-379. doi:10.1128/IAI.00330-10

29. D'Orazio, Sarah EF. Innate and Adaptive Immune Responses during Listeria monocytogenes Infection. *Microbiol Spectr*. 2019;7(3):GPP3-0065-2019. doi:doi:10.1128/microbiolspec

30. Zaver SA, Woodward JJ. Cyclic dinucleotides at the forefront of innate immunity. *Current Opinion in Cell Biology*. 2020;63:49-56. doi:10.1016/j.ceb.2019.12.004

31. Gonzalez-Escobedo G, Gunn JS. Gallbladder Epithelium as a Niche for Chronic Salmonella Carriage. McCormick BA, ed. *Infect Immun*. 2013;81(8):2920-2930. doi:10.1128/IAI.00258-13

32. Radoshevich L, Cossart P. Listeria monocytogenes: towards a complete picture of its physiology and pathogenesis. *Nat Rev Microbiol*. 2018;16(1):32-46. doi:10.1038/nrmicro.2017.126

33. Nauseef, William M, Clark, Robert A. Intersecting stories of the phagocyte NADPH oxidase and chronic granulomatous disease. In: Knaus, Ulla G, Leto, Thomas L, eds. *NADPH Oxidases: Methods and Protocols*. Vol 1982. Springer; 2019:3-16.

34. Reniere ML. Reduce, Induce, Thrive: Bacterial Redox Sensing during Pathogenesis. *J Bacteriol*. 2018;200(17). doi:10.1128/JB.00128-18

35. Imlay JA. Cellular Defenses against Superoxide and Hydrogen Peroxide. *Annu Rev Biochem*. 2008;77(1):755-776. doi:10.1146/annurev.biochem.77.061606.161055

36. Mishra S, Imlay J. Why do bacteria use so many enzymes to scavenge hydrogen peroxide? *Archives of Biochemistry and Biophysics*. 2012;525(2):145-160. doi:10.1016/j.abb.2012.04.014

37. Klebba PE, Charbit A, Xiao Q, Jiang X, Newton SM. Mechanisms of iron and haem transport by *Listeria monocytogenes*. *Molecular Membrane Biology*. 2012;29(3-4):69-86. doi:10.3109/09687688.2012.694485

38. Lechowicz J, Krawczyk-Balska A. An update on the transport and metabolism of iron in Listeria monocytogenes: the role of proteins involved in pathogenicity. *Biometals*. 2015;28(4):587-603. doi:10.1007/s10534-015-9849-5

39. Cassat JE, Skaar EP. Iron in Infection and Immunity. *Cell Host & Microbe*. 2013;13(5):509-519. doi:10.1016/j.chom.2013.04.010

40. Monteith AJ, Skaar EP. The impact of metal availability on immune function during infection. *Trends in Endocrinology & Metabolism*. 2021;32(11):916-928. doi:10.1016/j.tem.2021.08.004

41. Choby JE, Skaar EP. Heme Synthesis and Acquisition in Bacterial Pathogens. *Journal of Molecular Biology*. 2016;428(17):3408-3428. doi:10.1016/j.jmb.2016.03.018

42. McLaughlin HP, Xiao Q, Rea RB, et al. A Putative P-Type ATPase Required for Virulence and Resistance to Haem Toxicity in Listeria monocytogenes. Cornelis P, ed. *PLoS ONE*. 2012;7(2):e30928. doi:10.1371/journal.pone.0030928

43. Gahan CGM, Hill C. Gastrointestinal phase of *Listeria monocytogenes* infection. *Journal of Applied Microbiology*. 2005;98(6):1345-1353. doi:10.1111/j.1365-2672.2005.02559.x

44. Van Erpecum KJ, Wang DQH, Moschetta A, et al. Gallbladder histopathology during murine gallstone formation: relation to motility and concentrating function. *Journal of Lipid Research*. 2006;47(1):32-41. doi:10.1194/jlr.M500180-JLR200

45. Cain AK, Barquist L, Goodman AL, Paulsen IT, Parkhill J, Van Opijnen T. A decade of advances in transposon-insertion sequencing. *Nat Rev Genet*. 2020;21(9):526-540. doi:10.1038/s41576-020-0244-x

46. Van Opijnen T, Bodi KL, Camilli A. Tn-seq: high-throughput parallel sequencing for fitness and genetic interaction studies in microorganisms. *Nat Methods*. 2009;6(10):767-772. doi:10.1038/nmeth.1377

47. Valentino MD, Foulston L, Sadaka A, et al. Genes Contributing to Staphylococcus aureus Fitness in Abscess- and Infection-Related Ecologies. McDaniel LS, ed. *mBio*. 2014;5(5):e01729-14. doi:10.1128/mBio.01729-14

48. Shull LM, Camilli A. Transposon Sequencing of Vibrio cholerae in the Infant Rabbit Model of Cholera. In: Sikora AE, ed. *Vibrio Cholerae*. Vol 1839. Methods in Molecular Biology. Springer New York; 2018:103-116. doi:10.1007/978-1-4939-8685-9_10

49. Stamm CE, McFarland AP, Locke MN, et al. RECON gene disruption enhances host resistance to enable genome-wide evaluation of intracellular pathogen fitness during infection. Kline KA, ed. *mBio*. Published online June 28, 2024:e01332-24. doi:10.1128/mbio.01332-24

50. Stoll R, Goebel W. The major PEP-phosphotransferase systems (PTSs) for glucose, mannose and cellobiose of Listeria monocytogenes, and their significance for extra- and intracellular growth. *Microbiology*. 2010;156(4):1069-1083. doi:10.1099/mic.0.034934-0

51. Deutscher J, Francke C, Postma PW. How Phosphotransferase System-Related Protein Phosphorylation Regulates Carbohydrate Metabolism in Bacteria. *Microbiol Mol Biol Rev*. 2006;70(4):939-1031. doi:10.1128/MMBR.00024-06

52. Müller-Herbst S, Wüstner S, Mühlig A, et al. Identification of genes essential for anaerobic growth of Listeria monocytogenes. *Microbiology*. 2014;160(4):752-765. doi:10.1099/mic.0.075242-0

53. Freitag NE, Port GC, Miner MD. Listeria monocytogenes — from saprophyte to intracellular pathogen. *Nat Rev Microbiol*. 2009;7(9):623-628. doi:10.1038/nrmicro2171

54. Becattini S, Littmann ER, Carter RA, et al. Commensal microbes provide first line defense against *Listeria monocytogenes* infection. *Journal of Experimental Medicine*. 2017;214(7):1973-1989. doi:10.1084/jem.20170495

55. Zemansky J, Kline BC, Woodward JJ, Leber JH, Marquis H, Portnoy DA. Development of a *mariner* -Based Transposon and Identification of *Listeria monocytogenes* Determinants, Including the Peptidyl-Prolyl Isomerase PrsA2, That Contribute to Its Hemolytic Phenotype. *J Bacteriol*. 2009;191(12):3950-3964. doi:10.1128/JB.00016-09

56. Faith NG, Kim JW, Azizoglu R, Kathariou S, Czuprynski C. Purine Biosynthesis Mutants (*purA* and *purB*) of Serotype 4b *Listeria monocytogenes* Are Severely Attenuated for Systemic Infection in Intragastrically Inoculated A/J Mice. *Foodborne Pathogens and Disease*. 2012;9(5):480-486. doi:10.1089/fpd.2011.1013

57. Reniere ML, Whiteley AT, Portnoy DA. An In Vivo Selection Identifies Listeria monocytogenes Genes Required to Sense the Intracellular Environment and Activate

Virulence Factor Expression. Brodsky IE, ed. *PLoS Pathog*. 2016;12(7):e1005741. doi:10.1371/journal.ppat.1005741

58. Marquis H, Bouwer HG, Hinrichs DJ, Portnoy DA. Intracytoplasmic growth and virulence of Listeria monocytogenes auxotrophic mutants. *Infect Immun*. 1993;61(9):3756-3760. doi:10.1128/iai.61.9.3756-3760.1993

59. Cotter PD, Gahan CGM, Hill C. Analysis of the role of the Listeria monocytogenes F0F1-ATPase operon in the acid tolerance response. *International Journal of Food Microbiology*. 2000;60(2-3):137-146. doi:10.1016/S0168-1605(00)00305-6

60. Mertins S, Joseph B, Goetz M, et al. Interference of Components of the Phosphoenolpyruvate Phosphotransferase System with the Central Virulence Gene Regulator PrfA of *Listeria monocytogenes*. *J Bacteriol*. 2007;189(2):473-490. doi:10.1128/JB.00972-06

61. Feng Y, Chang SK, Portnoy DA. The major role of *Listeria monocytogenes* folic acid metabolism during infection is the generation of N-formylmethionine. Freitag NE, ed. *mBio*. 2023;14(5):e01074-23. doi:10.1128/mbio.01074-23

62. Tang Q, Reniere ML. *Listeria monocytogenes* folate metabolism is required to generate N-formylmethionine during infection. Freitag NE, ed. *mBio*. 2023;14(5):e01385-23. doi:10.1128/mbio.01385-23

63. Kaplan Zeevi M, Shafir NS, Shaham S, et al. Listeria monocytogenes Multidrug Resistance Transporters and Cyclic Di-AMP, Which Contribute to Type I Interferon Induction, Play a Role in Cell Wall Stress. *Journal of Bacteriology*. 2013;195(23):5250-5261. doi:10.1128/JB.00794-13

64. Zaver SA, Pollock AJ, Boradia VM, Woodward JJ. A Luminescence-Based Coupled Enzyme Assay Enables High-Throughput Quantification of the Bacterial Second Messenger 3’3’-Cyclic-Di-AMP. *ChemBioChem*. 2021;22(6):1030-1041. doi:10.1002/cbic.202000667

65. Louie A, Bhandula V, Portnoy DA. Secretion of c-di-AMP by Listeria monocytogenes Leads to a STING-Dependent Antibacterial Response during Enterocolitis. Freitag NE, ed. *Infect Immun*. 2020;88(12):e00407-20. doi:10.1128/IAI.00407-20

66. Ishikawa H, Barber GN. STING is an endoplasmic reticulum adaptor that facilitates innate immune signalling. *Nature*. 2008;455(7213):674-678. doi:10.1038/nature07317

67. Brunette RL, Young JM, Whitley DG, Brodsky IE, Malik HS, Stetson DB. Extensive evolutionary and functional diversity among mammalian AIM2-like receptors. *Journal of Experimental Medicine*. 2012;209(11):1969-1983. doi:10.1084/jem.20121960

68. Sauer JD, Sotelo-Troha K, Von Moltke J, et al. The *N* -Ethyl- *N* -Nitrosourea-Induced *Goldenticket* Mouse Mutant Reveals an Essential Function of *Sting* in the *In Vivo* Interferon Response to *Listeria monocytogenes* and Cyclic Dinucleotides. Flynn JL, ed. *Infect Immun*. 2011;79(2):688-694. doi:10.1128/IAI.00999-10

69. Cesinger MR, Schwardt NH, Halsey CR, Thomason MK, Reniere ML. Investigating the Roles of Listeria monocytogenes Peroxidases in Growth and Virulence. *Microbiol Spectr*. 2021;9(1):e00440-21. doi:https://doi.org/10.1128/Spectrum

70. Ruhland BR, Reniere ML. Sense and sensor ability: redox-responsive regulators in Listeria monocytogenes. *Current Opinion in Microbiology*. 2019;47:20-25. doi:10.1016/j.mib.2018.10.006

71. Reniere ML, Whiteley AT, Hamilton KL, et al. Glutathione activates virulence gene expression of an intracellular pathogen. *Nature*. 2015;517(7533):170-173. doi:10.1038/nature14029

72. Mains DR, Eallonardo SJ, Freitag NE. Identification of Listeria monocytogenes Genes Contributing to Oxidative Stress Resistance under Conditions Relevant to Host Infection. Torres VJ, ed. *Infect Immun*. 2021;89(4):e00700-20. doi:10.1128/IAI.00700-20

73. Cesinger MR, Thomason MK, Edrozo MB, Halsey CR, Reniere ML. *Listeria monocytogenes* SpxA1 is a global regulator required to activate genes encoding catalase and heme biosynthesis enzymes for aerobic growth. *Mol Microbiol*. Published online April 22, 2020:mmi.14508. doi:10.1111/mmi.14508

74. Savelli B, Li Q, Webber M, et al. RedoxiBase: A database for ROS homeostasis regulated proteins. *Redox Biology*. 2019;26:101247. doi:10.1016/j.redox.2019.101247

75. Park S, You X, Imlay JA. Substantial DNA damage from submicromolar intracellular hydrogen peroxide detected in Hpx $^{-}$ mutants of *Escherichia coli*. *Proc Natl Acad Sci USA*. 2005;102(26):9317-9322. doi:10.1073/pnas.0502051102

76. Cosgrove K, Coutts G, Jonsson IM, et al. Catalase (KatA) and Alkyl Hydroperoxide Reductase (AhpC) Have Compensatory Roles in Peroxide Stress Resistance and Are Required for Survival, Persistence, and Nasal Colonization in *Staphylococcus aureus*. *J Bacteriol*. 2007;189(3):1025-1035. doi:10.1128/JB.01524-06

77. Olsen KN, Larsen MH, Gahan CGM, et al. The Dps-like protein Fri of Listeria monocytogenes promotes stress tolerance and intracellular multiplication in macrophage-like cells. *Microbiology*. 2005;151(3):925-933. doi:10.1099/mic.0.27552-0

78. Dussurget O, Dumas E, Archambaud C, et al. *Listeria monocytogenes* ferritin protects against multiple stresses and is required for virulence. *FEMS Microbiology Letters*. 2005;250(2):253-261. doi:10.1016/j.femsle.2005.07.015

79. Dons LE, Mosa A, Rottenberg ME, Rosenkrantz JT, Kristensson K, Olsen JE. Role of the *Listeria monocytogenes* 2-Cys peroxiredoxin homologue in protection against oxidative and nitrosative stress and in virulence. *Pathogens Disease*. 2014;70(1):70-74. doi:10.1111/2049-632X.12081

80. Kim KP, Hahm BK, Bhunia AK. The 2-Cys Peroxiredoxin-Deficient Listeria monocytogenes Displays Impaired Growth and Survival in the Presence of Hydrogen Peroxide In Vitro But Not in Mouse Organs. *Curr Microbiol*. 2007;54(5):382-387. doi:10.1007/s00284-006-0487-6

81. Milazzo L, Hofbauer S, Howes BD, et al. Insights into the Active Site of Coproheme Decarboxylase from *Listeria monocytogenes*. *Biochemistry*. 2018;57(13):2044-2057. doi:10.1021/acs.biochem.8b00186

82. Herskovits AA, Auerbuch V, Portnoy DA. Bacterial Ligands Generated in a Phagosome Are Targets of the Cytosolic Innate Immune System. Ausubel FM, ed. *PLoS Pathog*. 2007;3(3):e51. doi:10.1371/journal.ppat.0030051

83. Sun AN, Camilli A, Portnoy DA. Isolation of Listeria monocytogenes small-plaque mutants defective for intracellular growth and cell-to-cell spread. *Infect Immun*. 1990;58(11):3770-3778. doi:10.1128/iai.58.11.3770-3778.1990

84. Broden NJ, Flury S, King AN, Schroeder BW, Coe GD, Faulkner MJ. Insights into the Function of a Second, Nonclassical Ahp Peroxidase, AhpA, in Oxidative Stress Resistance in Bacillus subtilis. Henkin TM, ed. *J Bacteriol*. 2016;198(7):1044-1057. doi:10.1128/JB.00679-15

85. Proctor RA, Von Eiff C, Kahl BC, et al. Small colony variants: a pathogenic form of bacteria that facilitates persistent and recurrent infections. *Nat Rev Microbiol*. 2006;4(4):295-305. doi:10.1038/nrmicro1384

86. Hammer ND, Reniere ML, Cassat JE, et al. Two Heme-Dependent Terminal Oxidases Power Staphylococcus aureus Organ-Specific Colonization of the Vertebrate Host. Gilmore MS, ed. *mBio*. 2013;4(4):e00241-13. doi:10.1128/mBio.00241-13

87. Corbett D, Goldrick M, Fernandes VE, et al. Listeria monocytogenes Has Both Cytochrome *bd* -Type and Cytochrome *aa* $_3$ -Type Terminal Oxidases, Which Allow Growth at Different Oxygen Levels, and Both Are Important in Infection. Freitag NE, ed. *Infect Immun*. 2017;85(11). doi:10.1128/IAI.00354-17

88. Su M, Cavallo S, Stefanini S, Chiancone E, Chasteen ND. The So-Called *Listeria innocua* Ferritin Is a Dps Protein. Iron Incorporation, Detoxification, and DNA Protection Properties. *Biochemistry*. 2005;44(15):5572-5578. doi:10.1021/bi0472705

89. Bozzi M, Mignogna G, Stefanini S, et al. A Novel Non-heme Iron-binding Ferritin Related to the DNA-binding Proteins of the Dps Family in Listeria innocua. *Journal of Biological Chemistry*. 1997;272(6):3259-3265. doi:10.1074/jbc.272.6.3259

90. Hebraud M, Guzzo J. The main cold shock protein of *Listeria monocytogenes* belongs to the family of ferritin-like proteins. *FEMS Microbiology Letters*. 2000;190(1):29-34. doi:10.1111/j.1574-6968.2000.tb09257.x

91. Mohamed W, Darji A, Domann E, Chiancone E, Chakraborty T. The ferritin-like protein Frm is a target for the humoral immune response to Listeria monocytogenes and is required for efficient bacterial survival. *Mol Genet Genomics*. 2006;275(4):344-353. doi:10.1007/s00438-005-0090-8

92. Mohamed W, Sethi S, Darji A, Mraheil MA, Hain T, Chakraborty T. Antibody Targeting the Ferritin-Like Protein Controls *Listeria* Infection. *Infect Immun*. 2010;78(7):3306-3314. doi:10.1128/IAI.00210-10

93. Polidoro M, De Biase D, Montagnini B, et al. The expression of the dodecameric ferritin in Listeria spp. is induced by iron limitation and stationary growth phase. *Gene*. 2002;296(1-2):121-128. doi:10.1016/S0378-1119(02)00839-9

94. Jongbloed JDH, Grieger U, Antelmann H, et al. Two minimal Tat translocases in *Bacillus*. *Molecular Microbiology*. 2004;54(5):1319-1325. doi:10.1111/j.1365-2958.2004.04341.x

95. Miethke M, Monteferrante CG, Marahiel MA, Van Dijl JM. The Bacillus subtilis EfeUOB transporter is essential for high-affinity acquisition of ferrous and ferric iron. *Biochimica et Biophysica Acta (BBA) - Molecular Cell Research*. 2013;1833(10):2267-2278. doi:10.1016/j.bbamcr.2013.05.027

96. Ledala N, Sengupta M, Muthaiyan A, Wilkinson BJ, Jayaswal RK. Transcriptomic Response of *Listeria monocytogenes* to Iron Limitation and *fur* Mutation. *Appl Environ Microbiol*. 2010;76(2):406-416. doi:10.1128/AEM.01389-09

97. Dos Santos PT, Larsen PT, Menendez-Gil P, Lillebæk EMS, Kallipolitis BH. Listeria monocytogenes Relies on the Heme-Regulated Transporter hrtAB to Resist Heme Toxicity and Uses Heme as a Signal to Induce Transcription of lmo1634, Encoding Listeria Adhesion Protein. *Front Microbiol*. 2018;9:3090. doi:10.3389/fmicb.2018.03090

98. McLaughlin HP, Hill C, Gahan CG. The impact of iron on Listeria monocytogenes; inside and outside the host. *Current Opinion in Biotechnology*. 2011;22(2):194-199. doi:10.1016/j.copbio.2010.10.005

99. Jin B, Newton SMC, Shao Y, Jiang X, Charbit A, Klebba PE. Iron acquisition systems for ferric hydroxamates, haemin and haemoglobin in *Listeria monocytogenes*. *Molecular Microbiology*. 2006;59(4):1185-1198. doi:10.1111/j.1365-2958.2005.05015.x

100. Tiwari KB, Birlingmair J, Wilkinson BJ, Jayaswal RK. Role of the twin-arginine translocase (tat) system in iron uptake in Listeria monocytogenes. *Microbiology*. 2015;161(2):264-271. doi:10.1099/mic.0.083642-0

101. Xiao Q, Jiang X, Moore KJ, et al. Sortase independent and dependent systems for acquisition of haem and haemoglobin in *Listeria monocytogenes*. *Molecular Microbiology*. 2011;80(6):1581-1597. doi:10.1111/j.1365-2958.2011.07667.x

102. Pi H, Patel SJ, Argüello JM, Helmann JD. The *Listeria monocytogenes* Fur-regulated virulence protein FrvA is an Fe(II) efflux P_{1B4} -type ATPase: *Listeria monocytogenes* FrvA mediates ferrous iron efflux. *Molecular Microbiology*. 2016;100(6):1066-1079. doi:10.1111/mmi.13368

103. Borezée E, Pellegrini E, Beretti JL, Berche P. SvpA, a novel surface virulence-associated protein required for intracellular survival of Listeria monocytogenes. *Microbiology*. 2001;147(11):2913-2923. doi:10.1099/00221287-147-11-2913

104. Newton SMC, Klebba PE, Raynaud C, et al. The *svpA-srtB* locus of *Listeria monocytogenes:* Fur-mediated iron regulation and effect on virulence. *Molecular Microbiology*. 2005;55(3):927-940. doi:10.1111/j.1365-2958.2004.04436.x

105. Whiteley AT, Garelis NE, Peterson BN, et al. c-di-AMP modulates Listeria monocytogenes central metabolism to regulate growth, antibiotic resistance and osmoregulation. *Molecular Microbiology*. 2017;104(2):212-233. doi:10.1111/mmi.13622

106. Thompson CC, Carabeo RA. An Optimal Method of Iron Starvation of the Obligate Intracellular Pathogen, Chlamydia Trachomatis. *Front Microbio*. 2011;2. doi:10.3389/fmicb.2011.00020

107. Sauer JD, Herskovits AA, O'Riordan MXD. Metabolism of the Gram-Positive Bacterial Pathogen *Listeria monocytogenes*. Fischetti VA, Novick RP, Ferretti JJ, Portnoy DA, Braunstein M, Rood JI, eds. *Microbiol Spectr*. 2019;7(4). doi:10.1128/microbiolspec.GPP3-0066-2019

108. Chico-Calero I, Suárez M, González-Zorn B, et al. Hpt, a bacterial homolog of the microsomal glucose- 6-phosphate translocase, mediates rapid intracellular proliferation in *Listeria*. *Proc Natl Acad Sci USA*. 2002;99(1):431-436. doi:10.1073/pnas.012363899

109. Joseph B, Przybilla K, Stühler C, et al. Identification of *Listeria monocytogenes* Genes Contributing to Intracellular Replication by Expression Profiling and Mutant Screening. *J Bacteriol*. 2006;188(2):556-568. doi:10.1128/JB.188.2.556-568.2006

110. Aké FMD, Joyet P, Deutscher J, Milohanic E. Mutational analysis of glucose transport regulation and glucose-mediated virulence gene repression in *Listeria monocytogenes*. *Molecular Microbiology*. 2011;81(1):274-293. doi:10.1111/j.1365-2958.2011.07692.x

111. Bishop DK, Hinrichs DJ. Adoptive transfer of immunity to Listeria monocytogenes. The influence of in vitro stimulation on lymphocyte subset requirements. *J Immunol*. 1987;139(6):2005-2009.

112. Bécavin C, Bouchier C, Lechat P, et al. Comparison of Widely Used Listeria monocytogenes Strains EGD, 10403S, and EGD-e Highlights Genomic Variations Underlying Differences in Pathogenicity. *MBio*. 2014;5(2):e00969-14. doi:10.1128/mBio.00969-14

113. Simon R, Priefer U, Puhler A. A broad host range mobilization system for in vivo genetic engineering: Transposon mutagenesis in Gram negative bacteria. *Bio/Technology*. 1983;1:784-791. doi:doi.org/10.1038/nbt1183-784

114. Portnoy DA, Jacks PS, Hinrichs DJ. Role of hemolysin for the intracellular growth of Listeria monocytogenes. *J Exp Med*. 1988;167(4):1459-1471.

115. Camilli A, Tilney LG, Portnoy DA. Dual roles of *plcA* in *Listeria monocytogenes* pathogenesis. *Molecular Microbiology*. 1993;8(1):143-157. doi:10.1111/j.1365-2958.1993.tb01211.x

116. Argov T, Rabinovich L, Sigal N, Herskovits AA. An Effective Counterselection System for Listeria monocytogenes and Its Use To Characterize the Monocin Genomic Region of Strain 10403S. Nojiri H, ed. *Appl Environ Microbiol*. 2017;83(6):e02927-16. doi:10.1128/AEM.02927-16

117. Lauer P, Chow MYN, Loessner MJ, Portnoy DA, Calendar R. Construction, Characterization, and Use of Two *Listeria monocytogenes* Site-Specific Phage Integration Vectors. *J Bacteriol*. 2002;184(15):4177-4186. doi:10.1128/JB.184.15.4177-4186.2002

118. Schneider CA, Rasband WS, Eliceiri KW. NIH Image to ImageJ: 25 years of image analysis. *Nat Methods*. 2012;9(7):671-675. doi:10.1038/nmeth.2089

119. Bécavin C, Bouchier C, Lechat P, et al. Comparison of Widely Used Listeria monocytogenes Strains EGD, 10403S, and EGD-e Highlights Genomic Differences Underlying Variations in Pathogenicity. Casadevall A, ed. *mBio*. 2014;5(2):e00969-14. doi:10.1128/mBio.00969-14

120. Moreira AC, Neves JV, Silva T, Oliveira P, Gomes MS, Rodrigues PN. Hepcidin-(In)dependent Mechanisms of Iron Metabolism Regulation during Infection by Listeria and Salmonella. Freitag NE, ed. *Infect Immun*. 2017;85(9):e00353-17. doi:10.1128/IAI.00353-17